Current Conveyor-based Universal Filter and Oscillator

by

Mohammed Ali Mohammed Al-Gahtani

A Thesis Presented to the

FACULTY OF THE COLLEGE OF GRADUATE STUDIES

KING FAHD UNIVERSITY OF PETROLEUM & MINERALS

DHAHRAN, SAUDI ARABIA

In Partial Fulfillment of the
Requirements for the Degree of

MASTER OF SCIENCE

In

ELECTRICAL ENGINEERING

March, 1997

INFORMATION TO USERS

Current Conveyor-based Universal
Filter and Oscillator

BY

MOHAMMED ALI MOHAMMED AL-GAHTANI

A Thesis Presented to the

FACULTY OF THE COLLEGE OF GRADUATE STUDIES

KING FAHD UNIVERSITY OF PETROLEUM & MINERALS

DHAHRAN, SAUDI ARABIA

In Partial Fulfillment of the
Requirements for the Degree of

MASTER OF SCIENCE
In

ELECTRICAL ENGINEERING

March 1997

Current Conveyor-based Universal

Filter and Oscillator

BY

MOHAMMED ALI MOHAMMED AL-GAHTANI

A Thesis Presented to the

COLLEGE OF GRADUATE STUDIES

KING FAHD UNIVERSITY OF PETROLEUM & MINERALS

Dhahran, Saudi Arabia

In Partial Fulfillment of the

Requirements for the Degree of

MASTER OF SCIENCE

In

ELECTRICAL ENGINEERING

March 1997

UMI Number: 1385306

UMI
300 North Zeeb Road
Ann Arbor, MI 48103
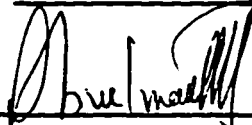
KING FAHD UNIVERSITY OF PETROLEUM AND MINERALS

DHAHRAN, SAUDI ARABIA
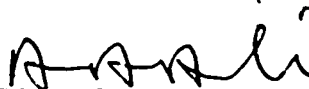
COLLEGE OF GRADUATE STUDIES

This thesis written by MOHAMMED ALI MOHAMMED AL-GAHTANI under the direction of his Thesis Advisor and approved by his Thesis Committee, has been presented to and accepted by the Dean of the College of Graduate Studies, in partial fulfillment of the requirements for the degree of MASTER OF SCIENCE IN ELECTRICAL ENGINEERING.

Thesis Committee

_____

Dr. M.T.Abuelma'atti (Advisor)

_____

Dr. Abdul-Rahman Al-Ali (Member)

_____

Dr. Zeini J. Al- Satti (Member)

_____

Dr. Yahya Chedly (Member)

Dr.Samir A. Al-Baiyat

Department Chairman

Dr. Abdullah Al-Shehri

Dean, College of Graduate Studies

Date: 31 March 1997

i

To my parents, who learned my how to give

Acknowledgment

CONTENTS

List of Figures

List of Table

Abstract

Name: Mohammed Ali Al-Gahtani

Title: Current Conveyor-based Universal Filter and Oscillator

Major Field: Electrical Engineering

Date of Degree: March, 1997

In this thesis, the second generation current conveyor (CCII) is used in realizing new active-RC, active-R and active-C multiphase sinusoidal oscillators (MPSOs) and unity gain cell-based universal filters. Also, taking advantage of the parasitic resistance R_x which appears at the port X of the CCII, a new programmable active-C current-mode universal filter is presented. In order to be compatible with integration requirements, 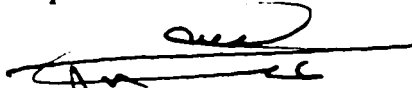these circuits use minimum number of active and passive elements, enjoy independent control of the critical circuit parameters, use grounded capacitors and enjoy low active and passive sensitivities. The effects of parasitics, voltage and current tracking errors of the CCII, on the circuit parameters are discussed. Extending the use of current conveyor to nonlinear applications is investigated and a simple current-mode analog multiplier/divider circuit using only two CCCII is presented. Comparisons between all of the proposed circuits and the previously published circuits are included.

Master of Science Degree

King Fahd University of Petroleum and Minerals

Dhahran, Saudi Arabia

March,1997

خلاصة الرسالة

الاسم: محمد علي محمد آل راشد القحطاني

عنوان الرسالة: مولدات للذبذبة و مرشحات باستخدام ناقل التيار

التخصص: هندسة كهربائية

تاريخ الدرجة: مارس ١٩٩٧م

في هذه الأطروحة تم مناقشه عدد من الدوائر الإلكترونية الجديدة، حيث أُستخدم ناقل التيار في تصميم مولدات للذبذبة متعددة الأطوار وفي تصميم مرشحات متعددة الاستخدامات. كذلك تم تطوير المقاومة غير المرغوب فيها – الموجودة عند مدخل ناقل التيار– في تصميم جديد لمرشح مبرمج. كما تم استخدام ناقل التيار في تصميم الدوائر غير الخطية. ومن أجل تخفيق المتطلبات اللازمه لتصنيع هذه الدوائر على صورة دوائر متكاملة فقد روعي تحقيق الشروط الآتية : استخدام أقل عدد من المقاومات والمكثفات، كذلك عدم اعتماد الخصائص الأساسية للدوائر على بعضها البعض. كما نوقش تأثير الخصائص غير المثالية لناقل التيار على الدوائر المقترحة. وباستخدام نموذج غير مثالي تم الحصول على نتائج أفضل. كم تم المقارنة بين الدوائر المطروحة وما قد صمم من قبل في هذا المجال.

Chapter 1

Introduction

In this introduction, first a survey of the current conveyor and the related devices will be presented. Secondly, a literature survey of the applications of current conveyor, and related devices, in designing oscillators and filters will be presented.

1.1 Current Conveyor

At present there is a growing interest in using current conveyors for designing analog signal processing circuits. This is attributed to the larger bandwidths and wider dynamic ranges obtainable compared to the classical operational amplifier based circuits. The current conveyor was originally conceived by Smith and

Sedra[1] who presented the first-generation conveyor and subsequently the second-generation conveyor [2]. The current conveyor is a three-terminal device with terminals labeled X , Y and Z , as shown in Fig. 1.1.

The general current conveyor can be represented by the following matrix:

$$\begin{pmatrix} i_y \\ v_x \\ i_z \end{pmatrix} = \begin{pmatrix} 0 & a & 0 \\ 1 & 0 & 0 \\ 0 & b & 0 \end{pmatrix} \begin{pmatrix} v_y \\ i_x \\ v_z \end{pmatrix} \tag{1.1}$$

When a=1 the first-generation current conveyor (commonly denoted CCI) is obtained. For a=0 we obtain the second-generation current conveyor (commonly denoted CCII). For a= -1 we obtain the third-generation current conveyor (commonly denoted by CCIII) [3].

Usually, b=±1. The sign of the b parameter determines the conveyor current-transfer polarity. Positive b indicates that the CC has a positive current-transfer ratio and is denoted by CCI+, CCII+ or CCIII+ while negative b means that it has a negative current-transfer ratio and is denoted by CCI-, CCII- or CCIII-.
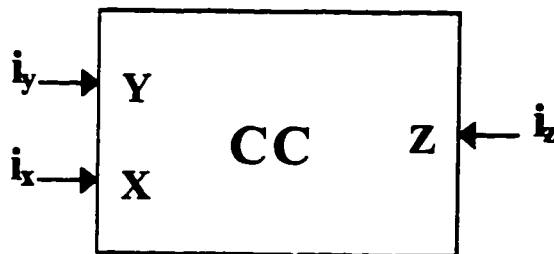
Fig.1.1 Electrical Symbol of the Current Conveyor

1.1.1 Current conveyor implementation using power supply current sensing technique

Earlier designs of current conveyors suffered from an excessive number of operational amplifiers, tightly matched resistances and very low bandwidths [4]. Operational transconductance amplifiers have also been used, but again with poor bandwidths and output capability even into moderately low load [5].

Meanwhile, developments had been taking place in current mirror design that would eventually prove to be useful for current conveyors. The traditional two transistor current mirror circuit exhibited two weaknesses; poor accuracy beyond approximately 1mA and a strong dependence of output current on output voltage. The addition of a third transistor in the output side of the mirror assisted in buffering the primary pair against output voltage changes, resulting in improved performance. Finally, errors in the current transfer ratio over a wide range of current were minimized by the inclusion of a fourth transistor in the input side of the mirror, as shown in Fig. 1.2. This four transistor version of the current mirror which is named as Wilson current mirror had become the accepted building block in precision application. The symbol most often used to denote a current mirror (no matter how many transistors are used) is shown in Fig. 1.2, with the arrow indicating both the input terminal and mirror polarity [6].

Combining the improvements in current mirror formulations with voltage operational amplifier (VOA), supply current sensing technique resulted in one of the

most successful current conveyor designs where current mirrors are used to sense the output current of the VOA via its power supply rails [7].

Fig. 1.3(a), illustrates the principle of operational amplifier (VOA)-based current sensing in conjunction with current mirrors (modified Wilson current mirrors) used in the design of new CCII+ conveyors. Input Y is short-circuit stable voltage input of very high impedance that draws only the VOA bias current and input X port reflects the voltage at Y ($V_x = V_y$) and performs as an open-circuit stable current terminal .

Assuming unity transfer current ratio for the two current mirrors of Fig.1.3(a), nodal analysis gives

$$I_1 + i_X = I_2$$

(1.2)

$$I_1 + i_Z = I_2$$

(1.3)

It results from the above two equations that ($i_x = i_z$). Also, it is obvious that ($V_x = V_y$) and ($i_y = 0$). Thus this circuit is performing the CCII+ function. To produce CCII- conveyor requires that the phase relationship between i_x and i_z be inverted. This can most effectively be achieved by the addition of a second pair of current mirrors crosscoupled to produce the current inversion, as shown in Fig 1.3(b).

Fig 1.2 Four-transistor current mirror and symbol
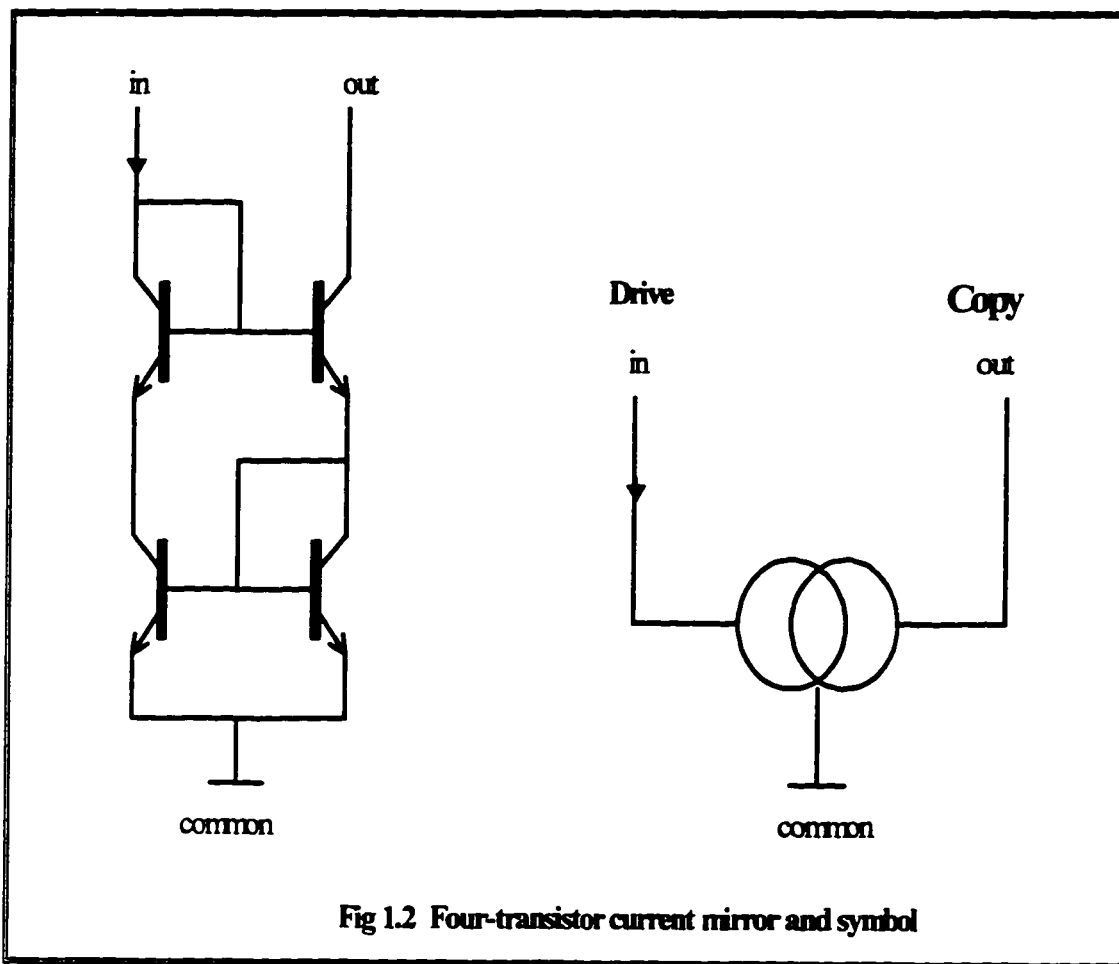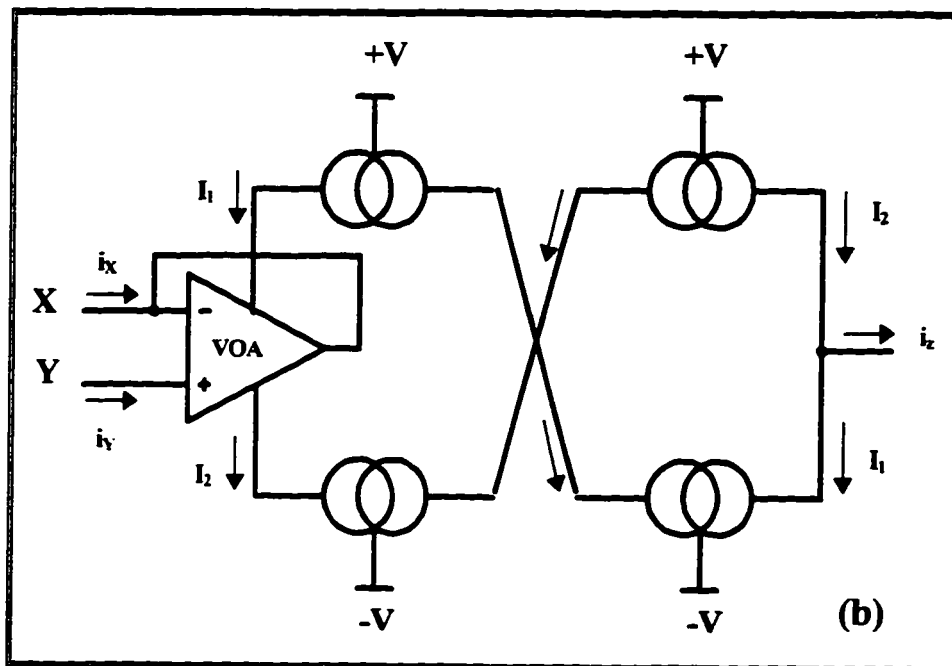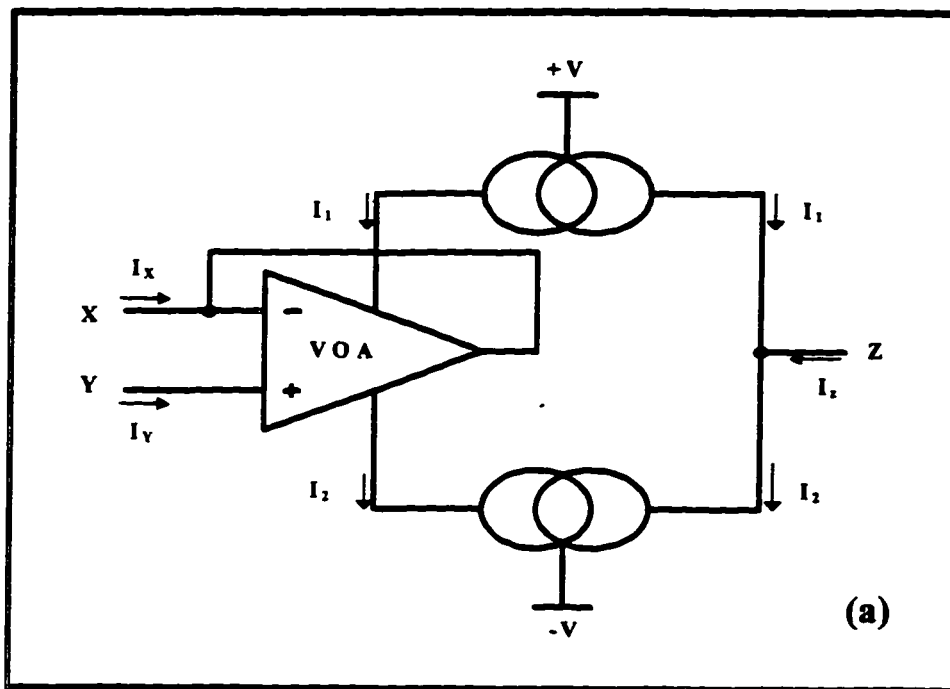
Fig 1.3 Current Conveyor Implementations using Power Supply
current sensing technique

(a)CCII+

(b)CCII-

1.1.2 Translinear current conveyors implementation

An important and expanding branch of analog circuits is the translinear group which was introduced by Gilbert [8]. Their primary function arises from the exploitation of the precise proportionality of transconductance to collector current in bipolar transistors so as to result in fundamentally exact, temperature-insensitive behaviour. Translinear implementations allow the design of high-performance circuits that exhibit both extended band-widths and high thermal stability[8-14]. Of particular interest here is the translinear mixed loop in Fig. 1.4(a) which comprises two PNP and two NPN transistors. This cell today appears unsurpassed for high-speed current-mode applications as it can be driven directly by currents with bipolar values and enables a virtual ground to be obtained without requiring feedback. Therefore, it is commonly used as the input stage of many high-performance analog functions such as current conveyors [9].

Assuming that the following standard translinear conditions are satisfied [12] :

(a) emitter areas of transistors of the same type are equal and all at the same temperature

(b) transistors are forward-biased so that each base-emitter voltage is high in comparison with V_T.($V_T = 26mv$ at 300 k being the thermal voltage)

(c) all the static current gains β are high in comparison with unity

Then the basic circuit, in Fig 1.4(b), is commonly described by the following general equation :

$$I_1 I_3 = I_2 I_4 \tag{1.4}$$

Also assuming unity transfer current ratio for the two current mirrors, nodal analysis gives

$$I_3 = I_1 + i_y \tag{1.5}$$

$$I_4 = i_2 + i_x = I_2 + i_z \tag{1.6}$$

When the DC bias current I_1 and I_3 are the same($I_1 = I_3 = I_o$), it results from equation (1.5) that $i_y =0$. In fact, for peak to peak input currents smaller than the bias current ($i_x << I_1 =I_3$), the input translinear loop also imposes $V_x=V_y$. From (1.6) it follows that $i_x = i_z$. Thus the circuit of Fig.1.4(b) is capable of performing the CCII+ function. Also, we can produce CCII with more than one output by connecting more than one current mirror pair in parallel as shown in Fig. 1.4(c). To produce CCII- conveyor requires that the phase relationship between i_x and i_z be inverted. This can most effectively be achieved by the addition of a second pair of current mirrors crosscoupled to produce the current inversion, as shown in Fig 1.4(d).

In fact, the current conveyor is not ideal. It is suffering from voltage and current tracking errors. The voltage tracking error implies that V_x is not exactly equal to V_y. And the current tracking error implies that i_x is not exactly equal to i_z for CCII or i_z and i_y for CCI.

An integrated circuit implementing a current conveyor is now commercially available AD844. It contains a CCII+ with built in voltage follower. Fig.1.5 shows

the schematic diagram of the AD844. Q1-Q4 constitute the translinear input cell,

Q5-Q9 and Q10-Q14 constitute two current mirrors to mirror I_2 and I_4 respectively.

Q15-Q18 constitute a buffer in which Q15 and Q16 form low output impedance and

Q17 and Q18 form emitter followers, thus providing the circuit with high input

resistance and provide V_{be} compensation for Q15 and Q16 respectively to have

$V_z = V_w$.
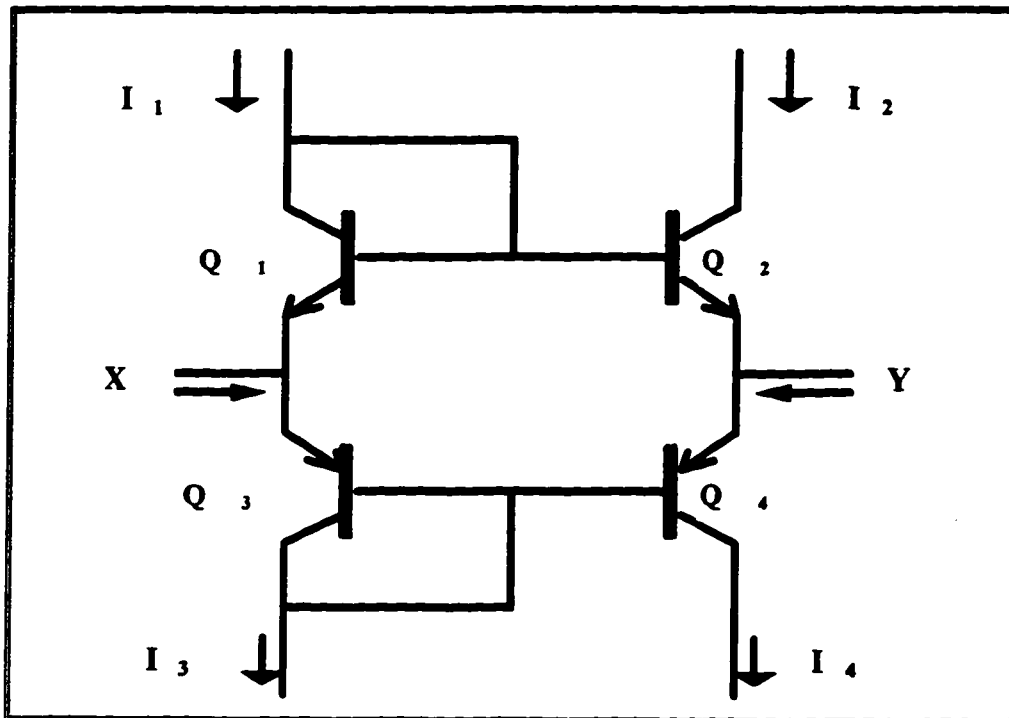
Fig.1.4(a) Elementary translinear mixed loop Implemented from four transistors
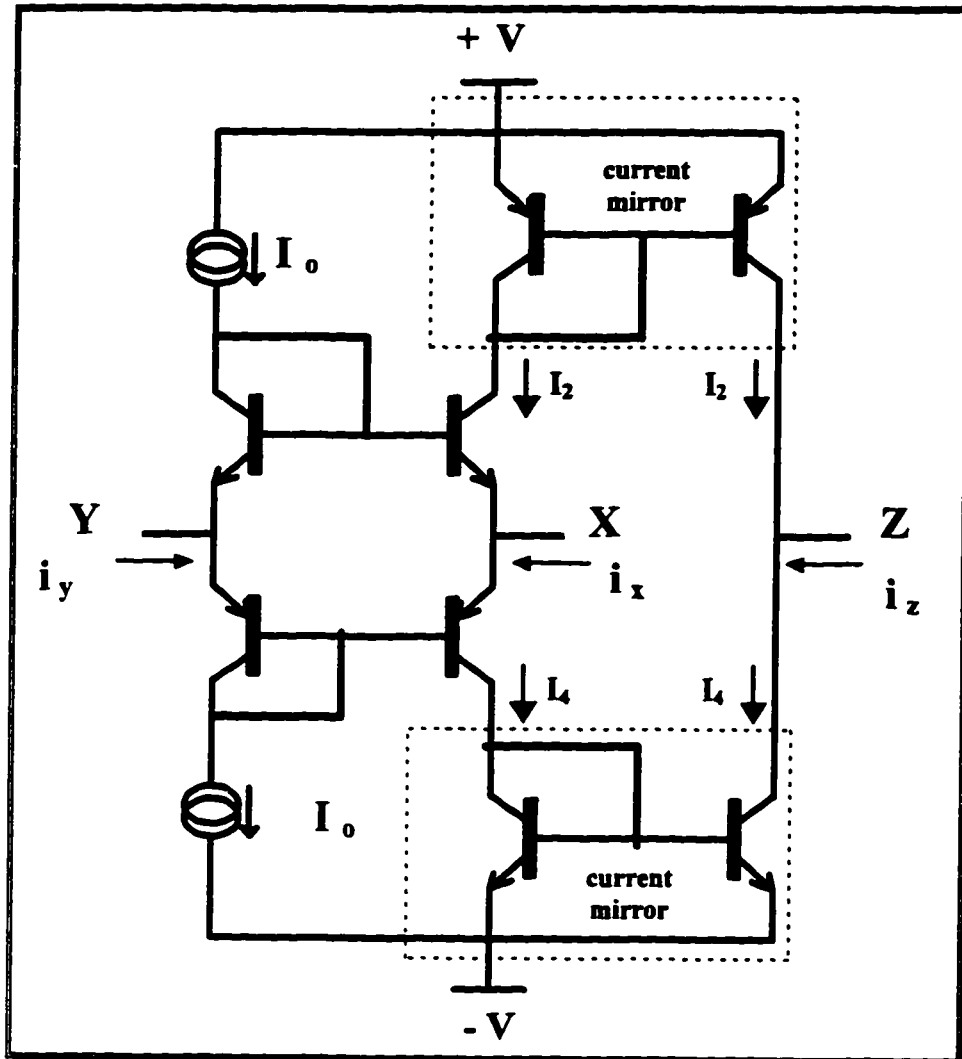
Fig1.4(b) Translinear Current Conveyor Implementations of CCII+
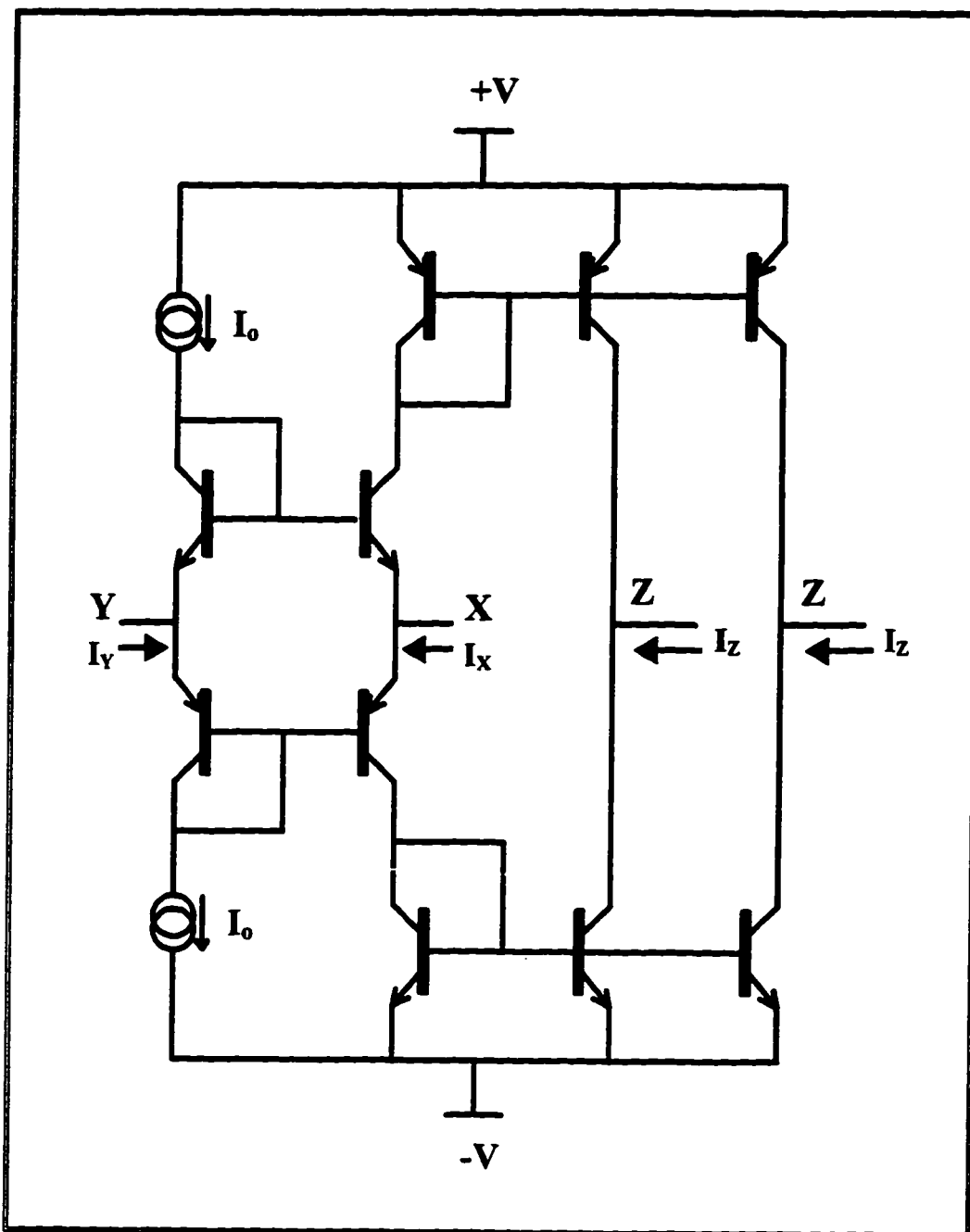
Fig1.4(c) Translinear CCII with two output
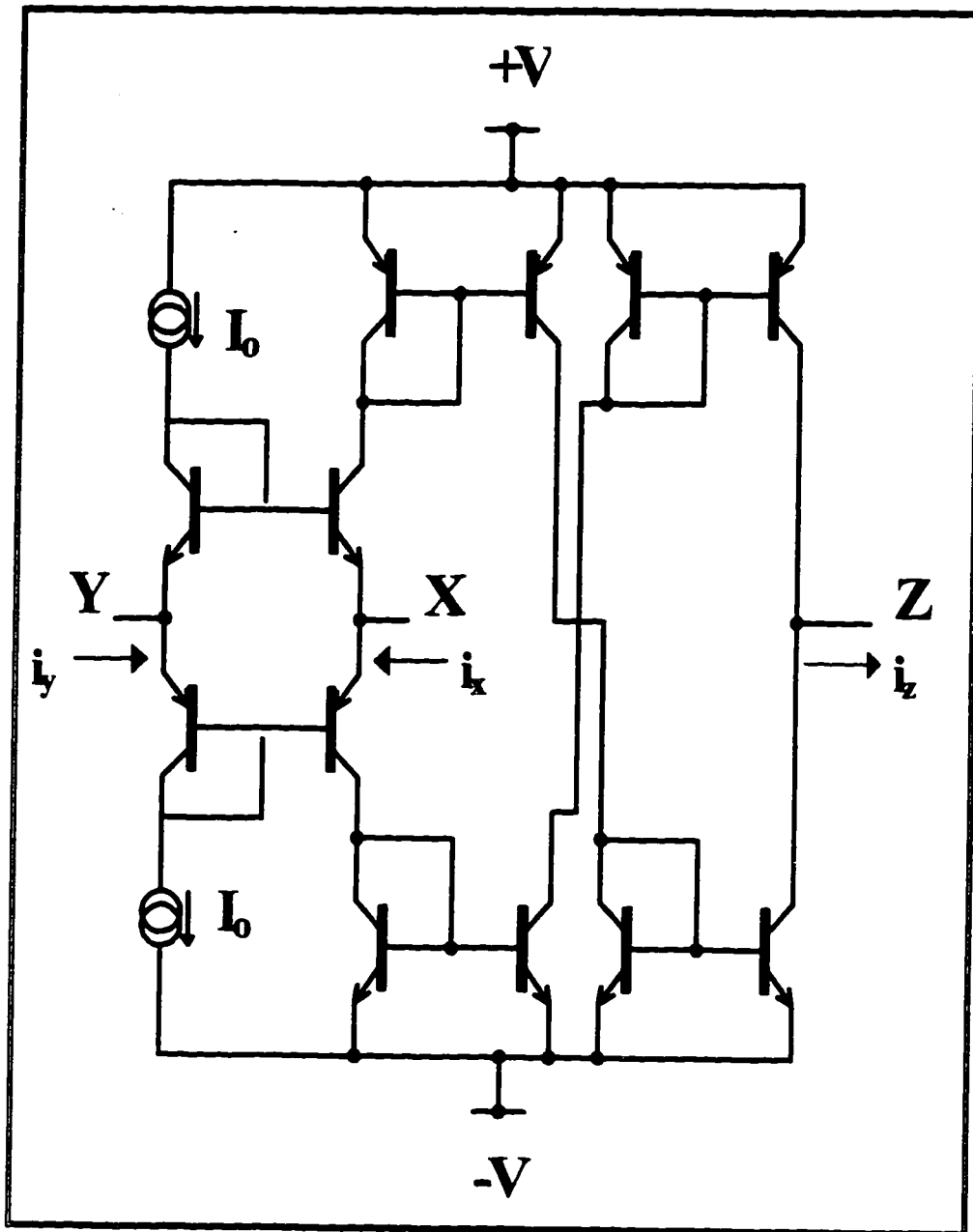
Fig1.4(d) Translinear Current Conveyor Implementations of CCII-
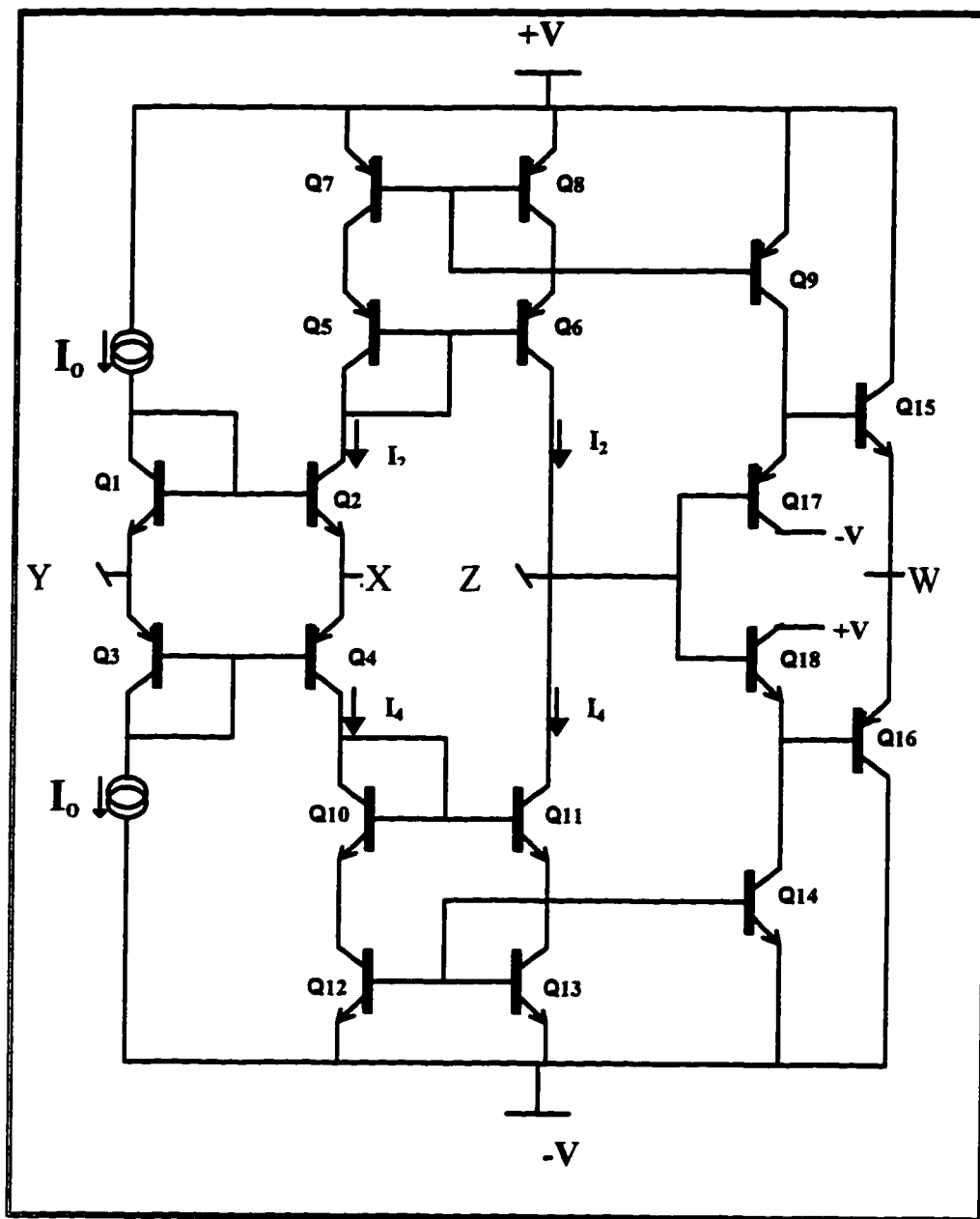
Fig. 1.5 Simplified Schematic of commercially available CCII+ AD844

1.1.3 Conversion between first-, second- and third-generation conveyors

An obvious generalization of the conveyor concept is the introduction of multiple output conveyors, as shown in Fig. 1.6. In this way the positive and negative conveyors are combined in a single device with a differential current output. From this extension of the current conveyor definition, conversion between CCIs, CCIIs and CCIIIs is easy by observing that, the difference in Y-input current in a CCI and CCIII compared with a CCII, is Iz with two different polarity. Thus, the Y-input current of the CCI and CCIII is achieved by connecting a CCII Y-input to a positive or a negative Z-output respectively. Similarly, a CCII Y-input can be obtained by connecting a CCI Y-input to a negative Z-output or a CCIII Y-input to a positive Z-output [15].

These transformation are shown in Fig.1.7 and Fig.1.8 . It is obvious that a single device implementing all of the fundamental current conveyor types could be a CCII with two positive Z-output and two negative Z-output.
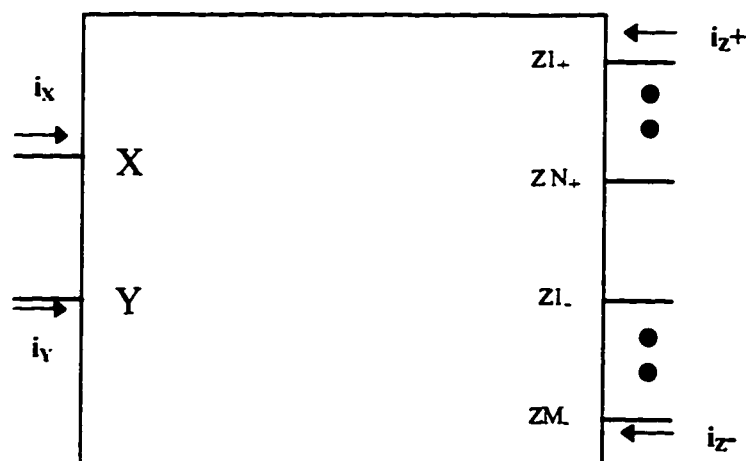
Fig. 1.6 Multiple-output current conveyor

16
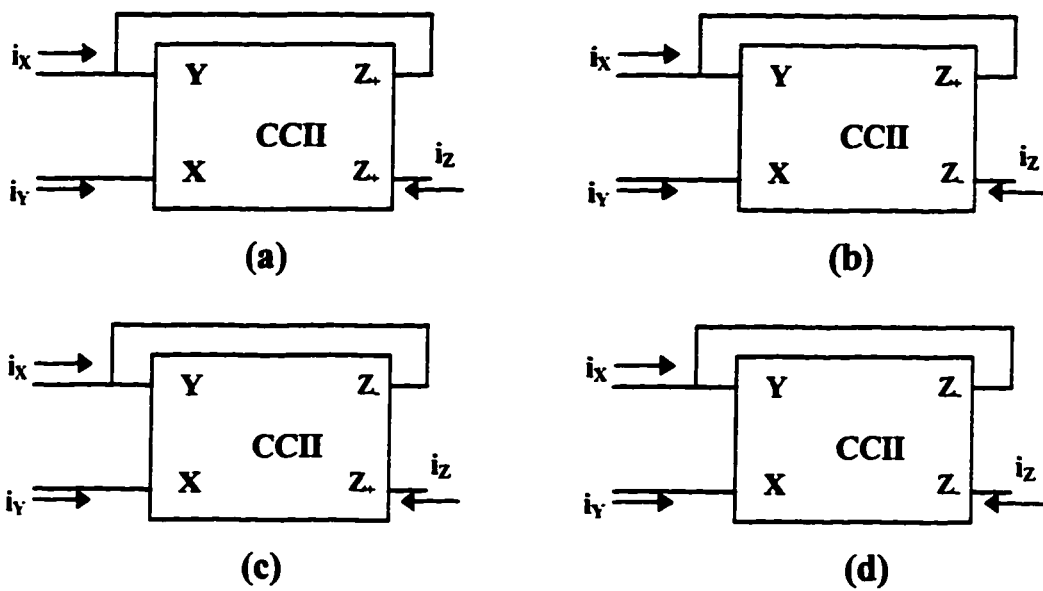
Fig 1.7 Conversions from CCII to CCI and CCIII
(a) CCI+ configured from CCII
(b) CCI- configured from CCII
(c) CCIII+ configured from CCII
(d) CCIII- configured from CCII
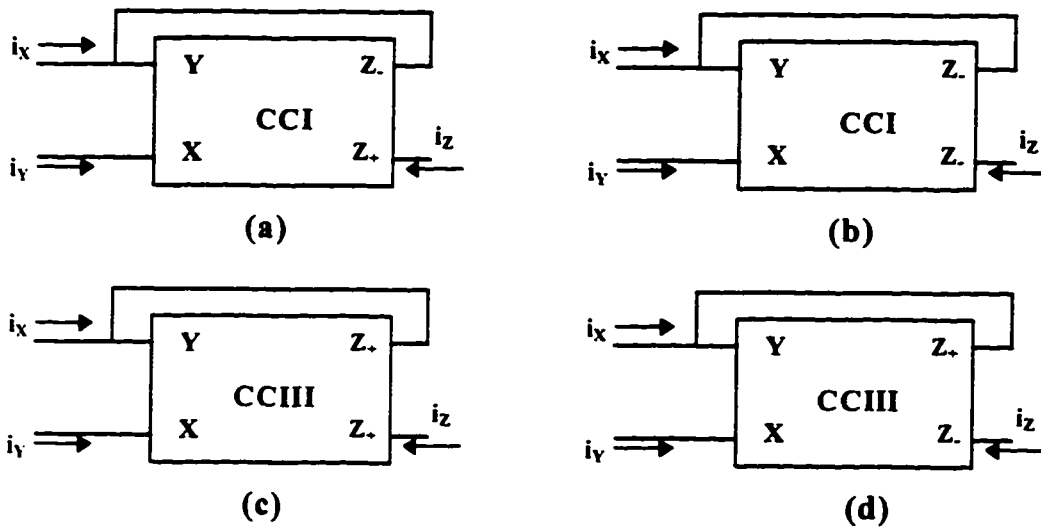
Fig 1.8 Conversions from CCI and CCIII to CCII
(a) CCII+ configured from CCI
(b) CCII- configured from CCI
(c) CCII+ configured from CCIII
(d) CCII- configured from CCIII

1.1.4 Current follower implementation

A current follower (CF) is the antithesis of a voltage follower. It has extremely low (ideally zero) input impedance, extremely high (ideally infinite) output impedance and unity current gain [16-18]. The CF is a two-port network X and Z, where i_x is equal to i_z; see Fig. 1.9. The CF can be obtained by grounding the Y terminal of a current conveyor. CF can be represented by the following matrix:

$$\begin{pmatrix} i_X = \pm i_Z \\ V_X = 0 \end{pmatrix}$$

(1.7)

Where the plus and minus signs of the current transfer ratio denote CF+ and CF-.
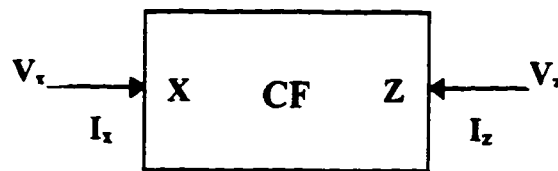
Fig.1.9 Electrical Symbole of a Current Follower

1.1.5 Current Controlled Conveyor

When the input cell of CCII is implemented from mixed translinear loop, it has the disadvantage of presenting a parasitic resistance on port X (around 50 Ω in commercially available CCII+ AD844). It is possible to take advantage of this parasitic resistance because its value depends on the bias current I_0 of the CCII. This property is used in the realization of a current controlled conveyor CCCII as

shown in Fig.1.10(a), which has therefore its serial resistance on port X controlled by the bias current I_o [19-20].
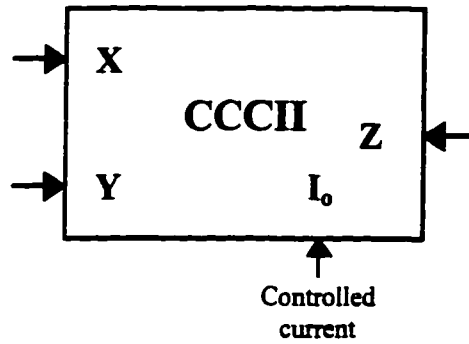
Fig.1.10(a) Electrical Symbol of the CCCII

The schematic implementation of the second generation current controlled current conveyor with a positive current transfer from X to Z CCCII+ is shown Fig 1.10(b). The notations of the input-output ports: X , Y , Z are those generally used for current conveyors. The matrix-relationship which is generally written for the CCII+ will also be valid for the CCCII+, by considering the intrinsic point X_i of the CCCII+ as shown in Fig. 1.10(c). Thus equation (1.1) becomes

$$\begin{pmatrix} i_y \\ v_{Xi} \\ i_z \end{pmatrix} = \begin{pmatrix} 0 & 0 & 0 \\ 1 & 0 & 0 \\ 0 & 1 & 0 \end{pmatrix} \begin{pmatrix} v_y \\ i_x \\ v_z \end{pmatrix} \tag{1.8}$$

This matrix-relationship can also be rewritten using conventional variables as shown in Fig. 1.10(a), also valid for the CCCII+ taking into account its intrinsic resistance R_x

$$\begin{pmatrix} i_y \\ v_X \\ i_Z \end{pmatrix} = \begin{pmatrix} 0 & 0 & 0 \\ 1 & R_x & 0 \\ 0 & 1 & 0 \end{pmatrix} \begin{pmatrix} v_Y \\ i_x \\ v_Z \end{pmatrix} \tag{1.9}$$

Considering the schematic form of the CCCII+ in Fig 1.10 (b) and assuming unity transfer current ratio for the two current mirrors, the relationship between R_x and the bias current I_0 can be obtained as follows.

$$V_{XY}(t) = -V_T \ln\frac{I_2(t)}{I_o} \Rightarrow I_2(t) = I_o \exp(-\frac{V_{XY}}{V_T})$$

$$V_{XY}(t) = V_T \ln\frac{I_4(t)}{I_o} \Rightarrow I_4(t) = I_o \exp(\frac{V_{XY}}{V_T})$$

$$i_X = I_4 - I_2 = I_o[\exp(\frac{V_{XY}}{V_T}) - \exp(-\frac{V_{XY}}{V_T})]$$

$$i_X = 2I_o \sinh(\frac{V_{XY}}{V_T})$$

$$\tag{1.10}$$

For $i_X \ll I_o$

$$V_{XY} = \frac{V_T}{2I_o} i_X(t) \Rightarrow V_{XY} = R_X \times i_X$$

$$R_X = \frac{V_T}{2I_o}$$

$$\tag{1.11}$$

As a general rule, a current controlled conveyor CCCII is a translinear CCII to which the possibility of modifying the value of the DC bias current I_0 will confer additional properties. All the other characteristics of the CCIIs are preserved.

In order to underline the advantages of the use of the controlled conveyors described here, we will compare its performance with the conventional bipolar operational transconductance amplifier (OTA) shown in Fig. 1.10(d). For OTA the value of $gm=I_0/(2V_T)$. Comparing this value with $1/R_x$ deduced from (1.11), it can be

seen that for the same value of I_o the transconductance of the bipolar OTA will be four times less than that of the CCCII. Thus, for the same transconductance the power consumption of the bipolar OTA will be about three time greater than with the CCCII. Second, with very high values for the collector currents of the transistors, the maximum usable frequency of the OTA will be reached sooner. This consequently indicates that the frequency performance of circuits with controlled conveyors will be much better than that for OTA implementations.[20]
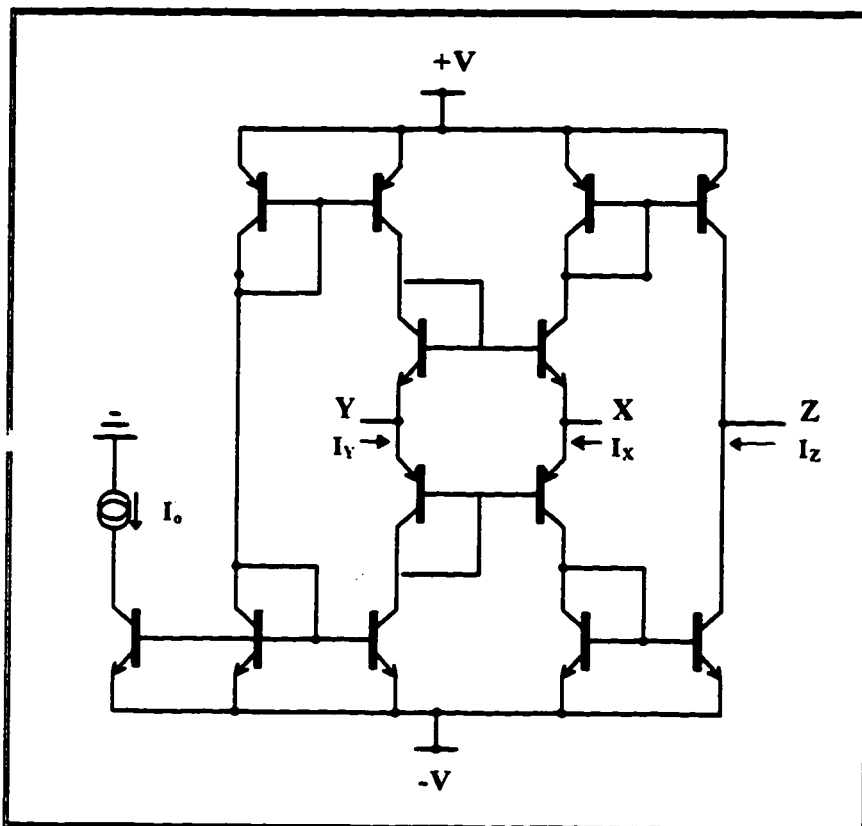
Fig 1.10(b) Current Controlled Conveyor Implementations
CCCII+
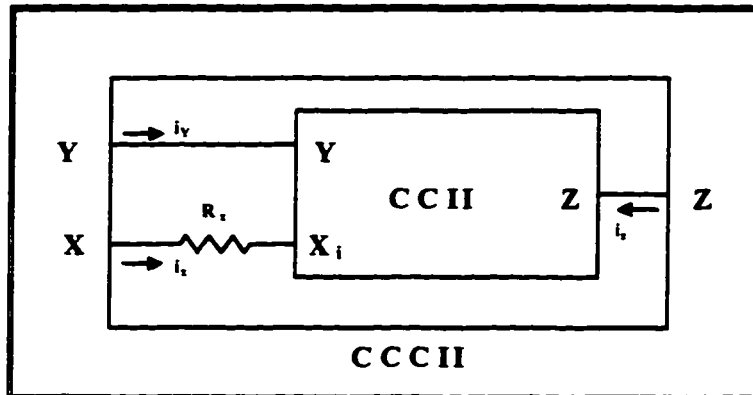
**Fig1.10(c)   The relation between the ideal CCII
and the CCCII**
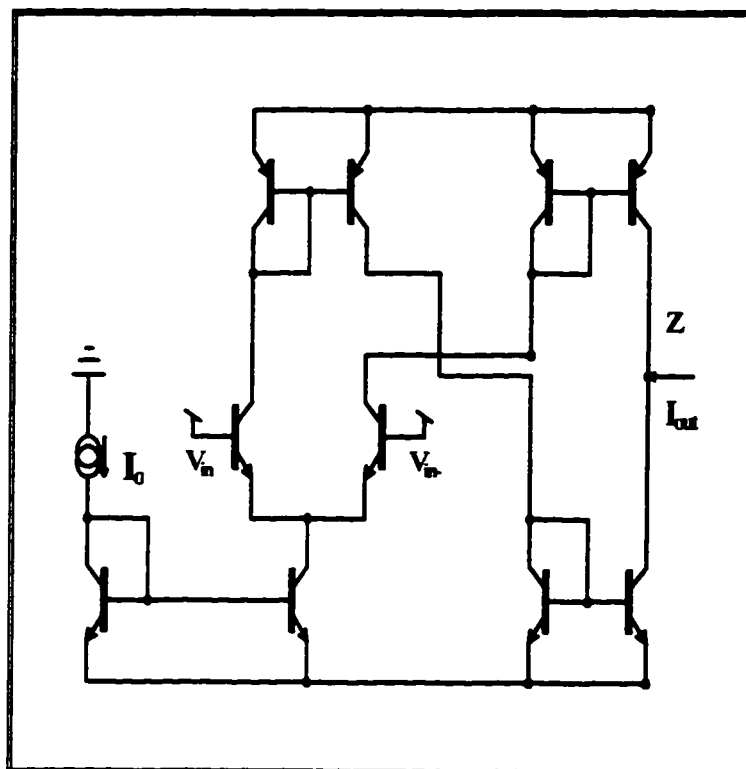
**Fig.1.10 (d) Conventional bipolar implementation
of the operational transconductance amplifier
(OTA)**

1.2 Literature Review

The current conveyor is now widely used for the implementation of high performance electronic functions operating in the current-mode as well as in the voltage-mode because it features a very high bandwidth, and of more importance this bandwidth is substantially independent of the closed loop gain setting. This part of the thesis is set out to survey the feasibility of developing multiphase sinusoidal oscillators MPSOs using second-generation current conveyors CCIIs, the feasibility of developing universal filters based on current and voltage followers which can be deduced from CCII by grounding the Y terminal, the feasibility of taking advantage of the parasitic resistance R_x, which appears when the input cell of CCII is implemented from mixed translinear loop CCCII, in developing new programmable active-C current-mode universal filters and the feasibility of extending the use of current conveyors to nonlinear applications.

1.2.1 Multiphase sinusoidal oscillators

Multiphase sinusoidal oscillators find a wide range of applications in communications, signal processing and power electronics. Several multiphase sinusoidal oscillator structures based on different design techniques are available in the literature [21-32]. Multiphase sinusoidal oscillators circuits proposed in references[21-25] suffer from complex structures and use of large number of active and passive components. The simple structure operational transconductance amplifier-based realization [26] suffer from limited output voltage swing, the inter-

dependence of the basic parameters of the MPSOs and from the temperature sensitivity. Although the voltage operational amplifier-based realization [27,28], current conveyor-based realization [29-30], current feedback operational amplifier-based realization [31] and current-follower-based realization [32] possess better performance, they lack the electronic tunabilty and suffer from the inter-dependence of the frequency of oscillation and condition of oscillation. Finally, most of these circuits can realize odd-phase signals only.

1.2.2 Universal filter based on unity gain cells

Recently, there has been a growing interest in designing current-mode and voltage-mode continuous-time filters using unity gain current mirrors and/or voltage followers [33-36]. This is attributed to their low power dissipation and high frequency of operation. While [33-35] report several specific application filters, Celma, Sabadell and Martinez [36] report a universal filter structure which can implement all the basic second-order filter functions (lowpass, highpass, bandpass, notch and allpass). These five filters, however, can not be simultaneously realized as it is necessary to change the circuit topology to achieve a specific filter function.

1.2.3 Active-C programmable Current-Mode Filter Using The CCCII

Universal active-C programmable filter which use active devices and capacitors only to realize all the basic second order filter responses (lowpass, highpass, bandpass, notch and allpass) received wide attention due to integratability and

programmability. Using OTA to implement these types of filters is one of the most successful methods due to its simplicity [37-41]. However, they have some problems with dynamic range and at high frequencies of operation. On the other hand, current-mode current-conveyor based filters can offer wider signal bandwidths, greater linearity and wider dynamic ranges of operation [42-54]. However, they lack programmability. While programmability can be achieved by combining current conveyor and OTAs [54], the recently introduced second-generation current controlled conveyor (CCCII) [19,20] allows current conveyor applications to be extended to the domain of electronically programmable functions. Using CCCIIs, a current-mode band pass filter was reported by Fabre et al, [19] and a voltage-mode bandpass filter was reported by Fabre et al, [20]. No attempt has been reported, so far, to present universal second-order filters using CCCIIs.

1.2.4 A Current-Mode Current-Controlled current-conveyor-Based Analog Multiplier/Divider

Analog multipliers and dividers are widely used in telecommunications, control, instrumentation and signal processing. The application of the second-generation current conveyor in realizing voltage-mode multiplier and divider circuits has been demonstrated [55-57]. These circuits invariably use MOS transistors. In order to avoid the effect of the nonlinearities of the MOS transistors, it is essential to ensure the operation of the MOS transistors in the linear region. This requires some operation constraints [55-57]. The application of the second-generation current

conveyor in realizing current-mode multiplier and divider circuits has not been introduced yet. Also, the use of the recently introduced second-generation current controlled conveyor (CCCII) for implementing nonlinear signal processing circuit has not been reported yet.

From all of the above literature survey, it appears, that there is a need to investigate the feasibility of using second generation current conveyors in developing the following :

1. generalized simple structure MPSOs which can realize either odd or even-phase signals and enjoy the use of grounded resistors and the independent control of the frequency and the condition of oscillation. This would be attractive for monolithic integration and pave the way of electronic tunability.

2. universal filters using unity gain cells which can realize lowpass, bandpass, highpass, notch and allpass responses without changing the circuit topology and enjoy the independent tuning of the natural frequency (ω_o), the bandwidth (ω_o/Q_o) and the gains of all of the responses.

3. programmable universal filter using CCCIIs and capacitors only (no externally connected resistors) which can realize lowpass, bandpass, highpass, notch and allpass responses and enjoy the independent current control of the parameters ω_o, ω_o/Q_o and the gains of all of the responses.

All of the new circuits should enjoy the following features :

a. use of the minimum number of active and passive elements,

b. employment of grounded capacitors which pave the way for high frequency operation and this would be attractive for monolithic integration,

and

c. low active and passive sensitivities.

Moreover, there is a need to investigate the feasibility of using CCCII in developing current-mode multipliers and dividers without using any external passive elements or MOS transistors.

Chapter 2

Multiphase sinusoidal oscillators

2.1 Introduction

Because of the potential applications in communications, signal processing and power electronics, multiphase oscillators have been receiving significant attention. Several multiphase sinusoidal oscillator structures based on different design techniques are available in the literature [21-32]. While the oscillator circuits proposed in references[21-25] exhibit good performance, they suffer from complex structures and use of large number of active and passive components. The simple structure operational transconductance amplifier-based realization [26] enjoys

electronic tunability but suffer from limited output voltage swing, the inter-dependence of the basic parameters of the MPSOs and from the temperature sensitivity. Although the active-R realization using the voltage mode operational amplifier [27,28] enjoys simple structure it lacks electronic tunability and it uses floating passive elements. The basic second-generation current-conveyor based structures [29-30] possess better performance in bandwidth, linearity and dynamic range than previous MPSOs. It uses a single current conveyor per phase. However, to achieve electronic tunability a JFET and three current-conveyors are required for each phase[30]. The current feedback operational amplifier-based realization [31] is simple. It exploits the internal pole of the amplifier to advantage and can operate at relatively high frequencies. However, it requires a current feedback operational amplifier with accessible compensation terminal. It lacks the electronic tunabilty and suffers from the inter-dependence of the frequency of oscillation and condition of oscillation and the use of floating passive elements. The current-follower based structure [32] suffer from complexity and use of large number of active and passive components, it requires two current followers with variable gain, one floating resistor and one floating capacitor for each phase and does not enjoy electronic tunability. Most of these circuits can realize odd-phase signals only .

In this chapter, three multiphase sinusoidal oscillators (MPSOs) realizations will be presented. These oscillators can produce (n) signals (n being even or odd) equally spaced in phase and enjoy independent control of the frequency and the condition of oscillation. The first one is an active-RC realization with grounded resistors and

capacitors. The second one is an active-R realization with grounded resistors. The last one is an active-C realization with grounded capacitors. Comparison between the proposed oscillators and previously published realizations will be performed.

2.2 Active-RC Multiphase Oscillator

A new simple active-RC multiphase sinusoidal oscillator will be presented. The proposed MPSO uses the CCIIs with grounded resistors and capacitors which makes it suitable for high frequency oscillation and monolithic IC fabrication. It enjoys the independent control of the frequency and the condition of oscillation, low sensitivity performance and possible electronic tunability. The proposed active-RC MPSO has two schemes, one can realize even or odd number of phases while the other one can realize odd number of phases only.

2.2.1 Even/odd-phase sinusoidal oscillator

The generalized scheme for even/odd-phase sinusoidal oscillators is shown in Fig.2.1. The n-th stage is an inverting, first-order high-pass section. All the other basic building blocks for this scheme are identical, non-inverting, first-order high-pass sections. Each of these are characterized by the voltage transfer function:

$$T(s) = \frac{sa}{s+b} \tag{2.1}$$
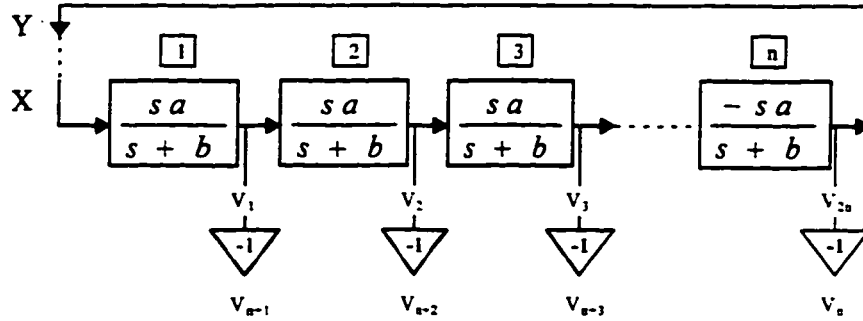
Fig. 2.1 Basic scheme for even/odd-phase sinusoidal oscillators

where a is the gain and b is the pole frequency. The loop-gain between the points X and Y can be expressed for (n) sections by

$$L(s) = -(\frac{sa}{s+b})^n \qquad (2.2)$$

For this scheme to produce and sustain sinusoidal oscillation, the loop gain must be equal to unity. Thus, the characteristic equation of the scheme of Fig. 2.1 can be expressed as:

$$-(\frac{sa}{s+b})^n_{s=j\omega_o} = 1 \qquad (2.3)$$

$$(j\omega_o + b)^n + (j\omega_0 a)^n = 0 \qquad (2.4)$$

From (2.4) the condition of the magnitude can be expressed as

$$\omega_o^2 + b^2 = a^2 \omega_o^2 \qquad (2.5)$$

and the condition of the phase can be expressed as

$$90 - \frac{180}{n} = \arctan(\frac{\omega_o}{b})$$ (2.6)

Using (2.5) and (2.6) the frequency and the condition of oscillation for different values of n can be calculated. Sample results are shown in Table 2.1.

No. of building blocks (n)	No. of phases	Condition of oscillation	Frequency of oscillation (ω_o)
3	3,6	a=2	0.5774b
4	4,8	a=1.414	b
5	5,10	a=1.237	1.374b
6	6,12	a=1.154	1.733b
7	7,14	a=1.11	2.07b
8	8,16	a=1.082	2.415b

Table 2.1. Frequency and condition of oscillation of even/odd-phase sinusoidal oscillators.

Fig. 2.2 shows a possible realization for the proposed even/odd-phase MPSOs using the dual output second-generation current-conveyor. Each phase requires a first-order high-pass section consisting of a dual output CCII, three grounded capacitors and one grounded resistor. The use of dual output CCIIs provides an outptut with 180 degree phase shift from the phase of the previous output such that there are (2n) phase output signals. Therefore, the circuit of Fig. 2.2 can realize n- or 2n-phase sinusoidal oscillator for n>2. Assuming identical current conveyors and using the standard notation, the dual-output current-conveyor can be characterized by $i_{zt} =$

$\pm\beta i_x$, $i_y = 0$, $v_x = \alpha v_y$, where $\alpha = 1-\varepsilon$, $|\varepsilon| \ll 1$ **represents the voltage tracking error and**

$\beta = 1-\delta$, $|\delta| \ll 1$ **represents the current tracking error. Routine analysis shows that the**

transfer function of a single stage of the circuit of Fig. 2.2 can be expressed as

$$T(s) = \frac{s\alpha\beta(C_1 / C)}{s + 1/(RC)} \tag{2.7}$$

From (2.1) and (2.7), we can see that

$$a = \alpha\beta C_1 / C \tag{2.8a}$$

$$b = 1/(CR) \tag{2.8b}$$

From (2.5), (2.6) and (2.8), the frequency of oscillation can be expressed as

$$\omega_0 = \frac{1}{RC} \tan(90 - \frac{180}{n}) \tag{2.9}$$

and the condition of oscillation can be expressed as

$$(\alpha\beta \frac{C_1}{C})^2 = \frac{\tan^2(90 - \frac{180}{n}) + 1}{\tan^2(90 - \frac{180}{n})} \tag{2.10}$$

From (2.9) and (2.10), we can see that the frequency of oscillation can be adjusted

by tuning the grounded resistor R without disturbing the condition of oscillation

which can be adjusted by tuning the grounded capacitor C_1 without disturbing the

frequency of oscillation. Also, we can see that while the frequency of oscillation of

the MPSOs will not be affected by the current and voltage tracking errors of the current conveyors, the condition of oscillation will be slightly affected.
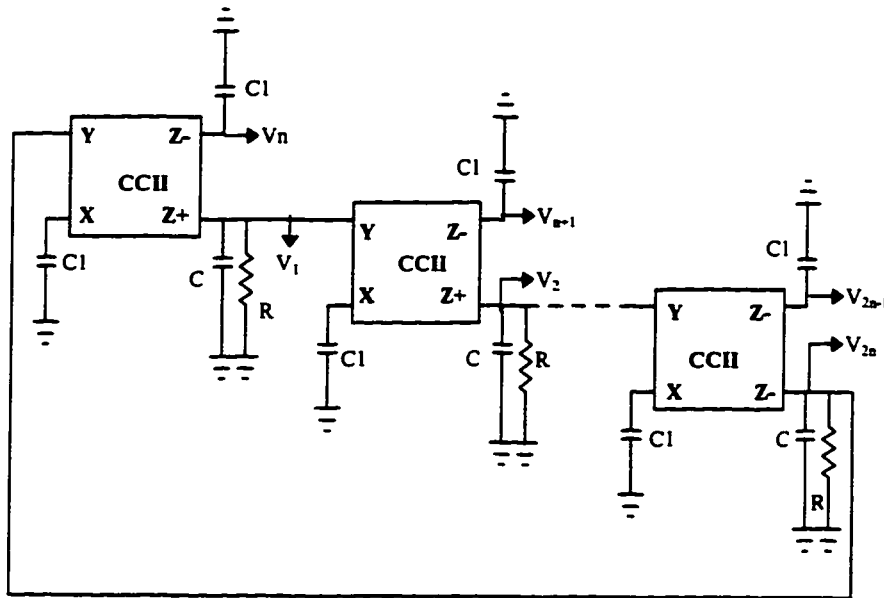
Fig 2.2 Generalized circuit for realizing an even/odd-phase multiphase oscillator.

2.2.2. Odd-phase sinusoidal oscillator

The generalized scheme for odd-phase (n) sinusoidal oscillators is shown in Fig.2.3. The basic building blocks for this scheme are identical, inverting, first-order high-pass sections. Each of these are characterized by the voltage transfer function:

$$T(s) = \frac{sa}{s+b}$$
(2.11)
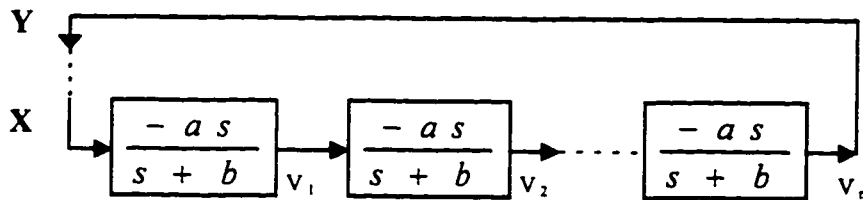
Fig 2.3 Basic scheme for odd-phase sinusoidal oscillators

where a is the gain and b is the pole frequency. The loop-gain between the points X and Y can be expressed for n (odd integer) sections by

$$L(s) = (-\frac{sa}{s+b})^n \qquad (2.12)$$

If the loop gain is unity, this scheme can be set to provide and sustain sinusoidal oscillation. Thus, the characteristic equation of the scheme of Fig. 2.3 can be expressed as

$$(-\frac{sa}{s+b})^n_{s=j\omega_o} = 1 \qquad (2.13)$$

$$(j\omega_o + b)^n + (-1)^{n+1}(j\omega_0 a)^n = 0 \qquad (2.14)$$

From (2.14) the condition of the magnitude can be expressed as

$$\omega_o^2 + b^2 = a^2 \omega_o^2 \qquad (2.15)$$

and the condition of the phase can be expressed as

$$90 - \frac{180}{n} = \arctan(\frac{\omega_o}{b}) \qquad (2.16)$$

Using (2.15) and (2.16) the frequency and the condition of oscillation for different values of n can be calculated. Sample results are shown in Table 2.2.

No. of phase (n)	Condition of oscillation	Frequency of oscillation (ω_o)
3	a=2	0.5774b
5	a=1.237	1.374b
7	a=1.11	2.07b

Table 2.2. Frequency and condition of oscillation of odd-phase sinusoidal oscillators.

Fig. 2.4 shows a possible realization for the proposed odd-phase oscillator using the second-generation current-conveyor. Each phase requires a first-order high-pass section consisting of a CCII-, two grounded capacitors and one grounded resistor. Assuming identical current conveyors and using the standard notation, the CCII-can be characterized by $i_z = -\beta i_x$, $i_y = 0$, $v_x = \alpha v_y$, where $\alpha = 1-\varepsilon$, $|\varepsilon| \ll 1$ represents the voltage tracking error and $\beta = 1-\delta$, $|\delta| \ll 1$ represents the current tracking error. Routine analysis show that the transfer function of a single stage of the circuit of Fig. 2.4 can be expressed as

$$T(s) = \frac{s\alpha\beta\dfrac{C_1}{C}}{s + \dfrac{1}{RC}} \tag{2.17}$$

From (2.11) and (2.17), we can see that

$a = \alpha\beta C_1/C$

$$\tag{2.18a}$$

$b = 1/(CR)$

$$\tag{2.18b}$$

From (2.15), (2.16) and (2.18), the frequency of oscillation can be expressed as

$$\omega_0 = \frac{1}{RC} \tan(90 - \frac{180}{n})$$

(2.19)

and the condition of oscillation can be expressed as

$$(\alpha\beta\frac{C_1}{C})^2 = \frac{\tan^2(90 - \frac{180}{n}) + 1}{\tan^2(90 - \frac{180}{n})}$$

(2.20)

From (2.19) and (2.20), we can see that the frequency of oscillation can be adjusted by tuning the grounded resistor R without disturbing the condition of oscillation which can be adjusted by tuning the grounded capacitor C_1 without disturbing the frequency of oscillation. Also, we can see that while the frequency of oscillation of the MPSOs will not be affected by the current and voltage tracking errors of the current conveyors, the condition of oscillation will be slightly affected.
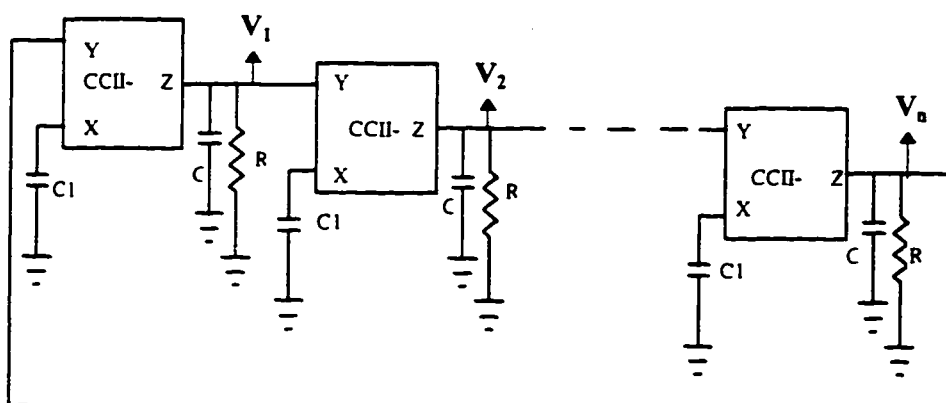
Fig 2.4 Generalized circuit for realizing an odd-phase oscillator

2.2.3 Sensitivity Analysis

Sensitivity study forms an important index of the performance of any active network. The sensitivity of a parameter F to an element of variation x_i can be expressed as

$$S_{x_i}^{F} = S(F;x_i) = \frac{x_i}{F}\frac{\delta F}{\delta x_i} \qquad (2.21)$$

For oscillators, the frequency of oscillation (ω_o) is the parameter of major interest. It is easy to show that the active and passive sensitivities of the frequency of oscillation for Fig. 2.2 and Fig. 2.4 are given by

$$S_R^{\omega_o} = S_C^{\omega_o} = -1 \qquad (2.22)$$

$$S_{C_1}^{\omega_o} = S_{\alpha}^{\omega_o} = S_{\beta}^{\omega_o} = 0 \qquad (2.23)$$

Thus the proposed circuits enjoy low active and passive ω_o-sensitivities

2.2.4 Simulation Result and Discussion

The three-phase and the six-phase sinusoidal oscillators shown in Fig 2.5 (a) and (b) were obtained from Fig.2.2 and Fig2.4. To investigate the workability of these oscillators, both circuits were simulated using Pspice circuit simulation program. Although there are several ways to simulate the current-conveyors required, the simulation was performed using the modified version, shown in Fig. 2.5(c), of the

model proposed by Svoboda[55] because, it can represent the most important sources of nonidealities of CCII. The Kernel of the work presented here is independent of the particular simulation selected. The start of the oscillation is caused by a fast decaying sinusoidal function. To demonstrate that the oscillations are self-starting, the voltage across the capacitors was initialized at zero. To provide a simple method for amplitude control, an antiparallel Zener-diode pair, with $V_z=5V$, was connected between terminals Y and the ground for each current-conveyor. Fig.2.6 (a) and (b) show the simulated oscillations obtained from the circuits of Fig. 2.5 (a) and (b) for three-phase and six-phase oscillations with $R=1k\Omega$, $C=1nF$ and $C_1=2.1nF$.

The results obtained in (2.8) and (2.18) take into consideration the current and voltage tracking errors of the current conveyor. To study in-depth the effect of current conveyor non-idealities on the performance of the circuits of Fig.2.5 (a) and (b), we have to use the nonideal model of the current conveyor in the circuit of Fig.2.5(c). Of particular interest here is the effect of the finite pole represented by (R_Z and C_Z). We can add them in parallel with (R and C). Also, we can add R_y in parallel with R. Thus the frequency of oscillation can be expressed as

$$\omega_o = \frac{1}{(R\,/\,/R_z\,/\,/R_y)(C+C_z)}\tan(90-\frac{180}{n})$$

(2.24)

and the condition of oscillation can be expressed as

$$\left(\alpha\beta \frac{C_1}{C + C_z}\right)^2 = \frac{\tan^2(90 - \frac{180}{n}) + 1}{\tan^2(90 - \frac{180}{n})} \tag{2.25}$$

Fig.2.6(c) shows the theoretical results obtained from (2.24) and the simulation results of the frequency of oscillation at different values of R with (R_z=3MΩ, R_y=10MΩ R_x=50Ω C=1nF and C_1=2.1nF). The simulation results deviate from the theoretical results by an error less than 6%.

The parasitic resistance R_x at port X, of the current-conveyor, may lead to incorrect transfer functions when a capacitor is connected to port X. To minimize these errors, current conveyor realizations of Fig.1.3 built around unity-gain amplifiers and using the power-supply current-sensing technique [3] would be more appropriate as they have lower parasitic resistance at port X compared to current-conveyor realizations using the mixed translinear loop[8]. To show the effect of R_x on the frequency and condition of oscillation, Table 2.3 shows the deviation of the simulated frequency and condition of oscillation from the results obtained using (2.24), for different values of R_x with R=1kΩ, R_z=3MΩ, R_y=10MΩ, C=1nF and C_z=4.5pF. Thus for small percentage of error, R_x should be small.

Rx	Condition of oscillation	% error in frequency of oscillation
100Ω	$C_1=12C$	21%
80Ω	$C_1=4.8C$	11.3%
60Ω	$C_1=2.2C$	7.1%
40Ω	$C_1=2.1C$	4.1%
20Ω	$C_1=2.02C$	1.9%
10Ω	$C_1=2C$	0.7%
5Ω	$C_1=2C$	0.5%

Table 2.3 The deviation of the simulated frequency and condition of oscillation from the results obtained using (2.24), for different values of R_x

Since, the frequency of oscillation can be adjusted by tuning the grounded resistor R without disturbing the condition of oscillation, then obtaining a voltage controlled multiphase oscillator is feasible by replacing the resistor R by a JFET.

To show the merits and demerits of this MPSOs, Table 2.4 shows a comparison between the proposed MPSOs and the most recently published MPSOs. Comparison shows that the proposed MPSOs and the MPSOs published in [28] are able to produce even or odd numbers of phases while the MPSOs published in 1992 [26] and 1995 [31] can produce odd number of phases only. Moreover, the proposed MPSOs use less number of active devices and grounded passive elements than what has been reported in 1995 [29]. The big advantage of the proposed MPSOs over the

previously published MPSOs is the ability of controlling ω_0 without changing the condition of oscillation through grounded resistor while the other can't do that.

	MPSOs using OTA[26] 1992	MPSOs using CFA [31] 1995	MPSOs using CCII [29] 1995	Proposed active-RC MPSOs
No. of active devices for (2n) EVEN-MPSOs	----------	----------	(2n)	(n)
No. of passive elements for (n) EVEN-MPSOs	----------	----------	(5n)	(4n)
No. of Active Devices for (n) ODD-MPSOs	(2n)	(n)	(n)	(n)
No. of passive elements for (n) ODD-MPSOs	(n)	(2n) (n) of them floating	(3n)	(3n)
The ability of controlling ω_0 without changing the condition of oscillation through grounded resistor or through gm of the OTA	No	No	No	Yes

Table 2.4 Comparison between the latest MPSOs and the proposed one
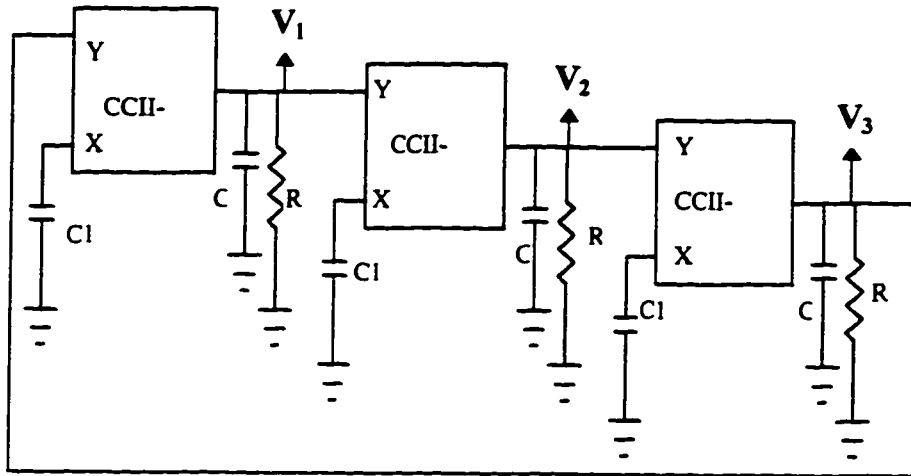
Fig 2.5 (a) Three-phase sinusoidal oscillator
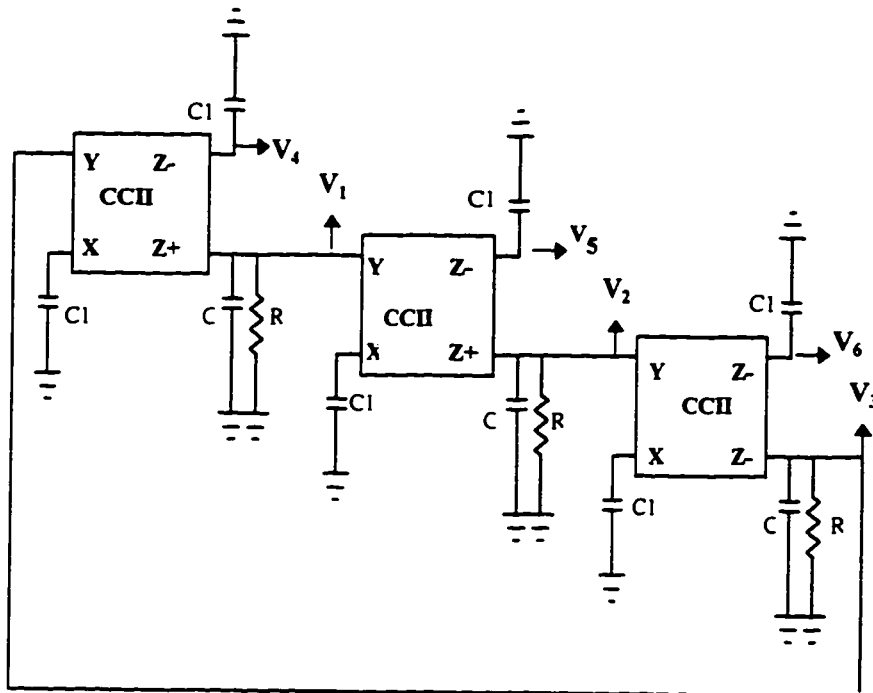
Fig 2.5 (b) Six-phase sinusoidal oscillator
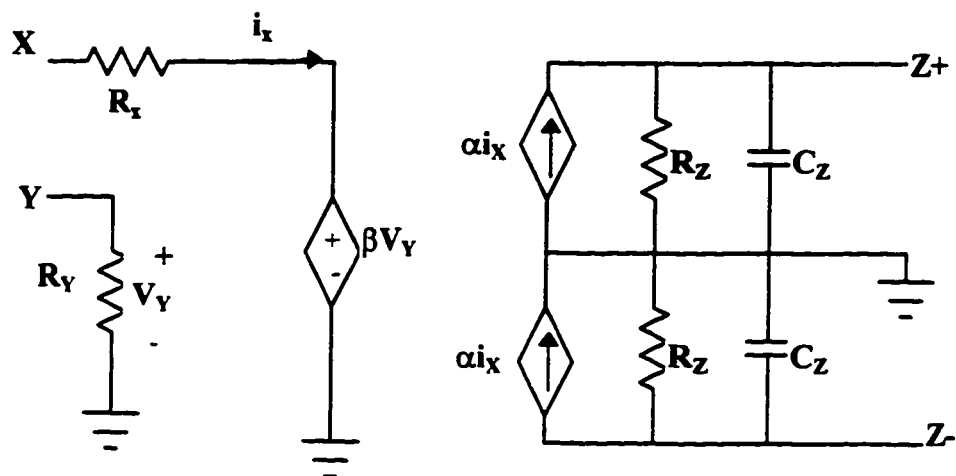
Fig.2.5(c) Amodified version of Svoboda model for the modelling of the dual-output current conveyor R_x=50Ω, R_Y=10MΩ, R_Z=3MΩ, C_Z=4.5pF
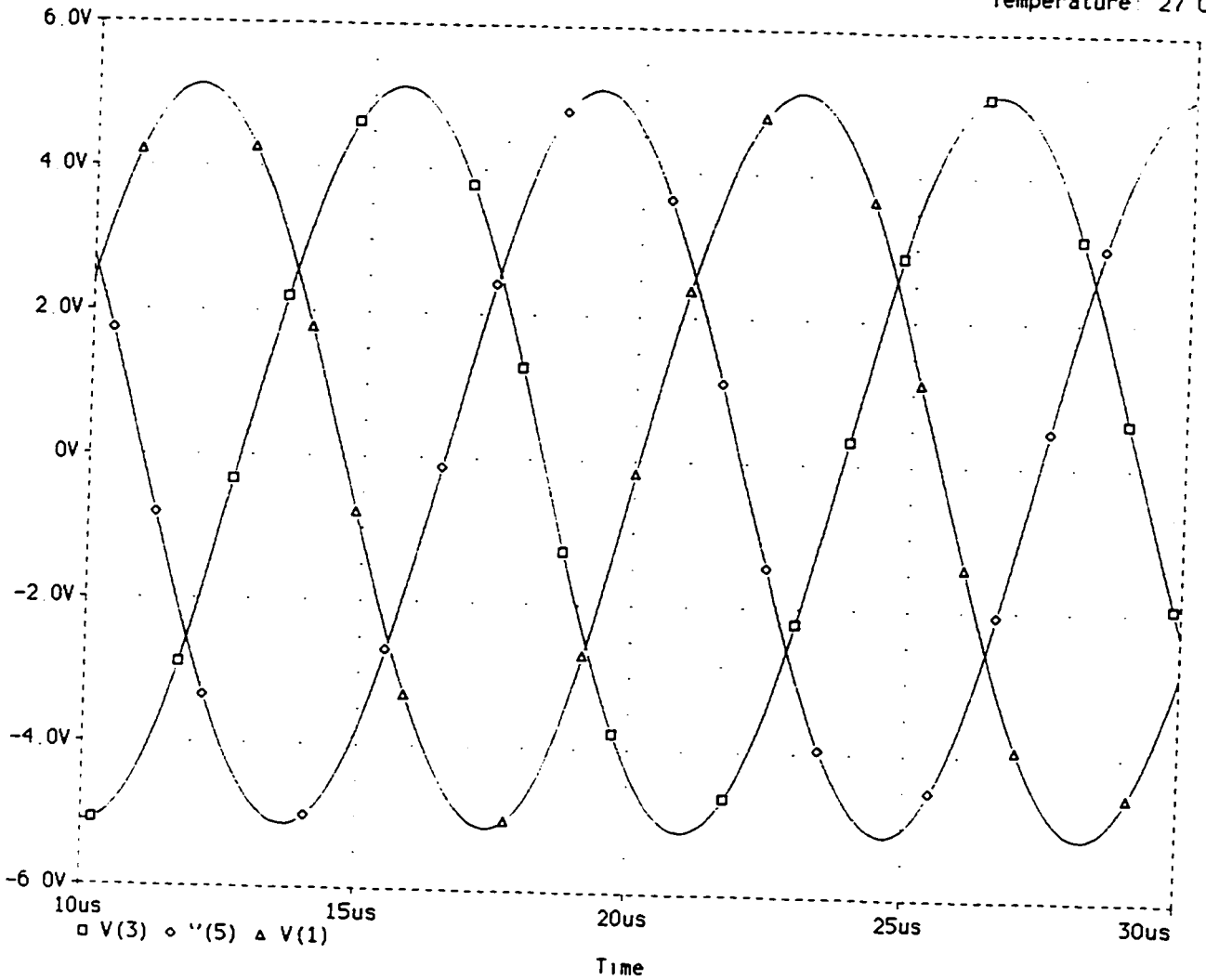
Fig 2.6 (a) Three-phase output obtained from
2.5(a) with
R=1kΩ, C=1nF,C₁=2.1nF

SIX PHASE OSCILLATOR

Temperature: 27.0

□ V(3) ◇ V(5) △ V(1) ▽ V(8) ○ V(9) + V(10)

Time
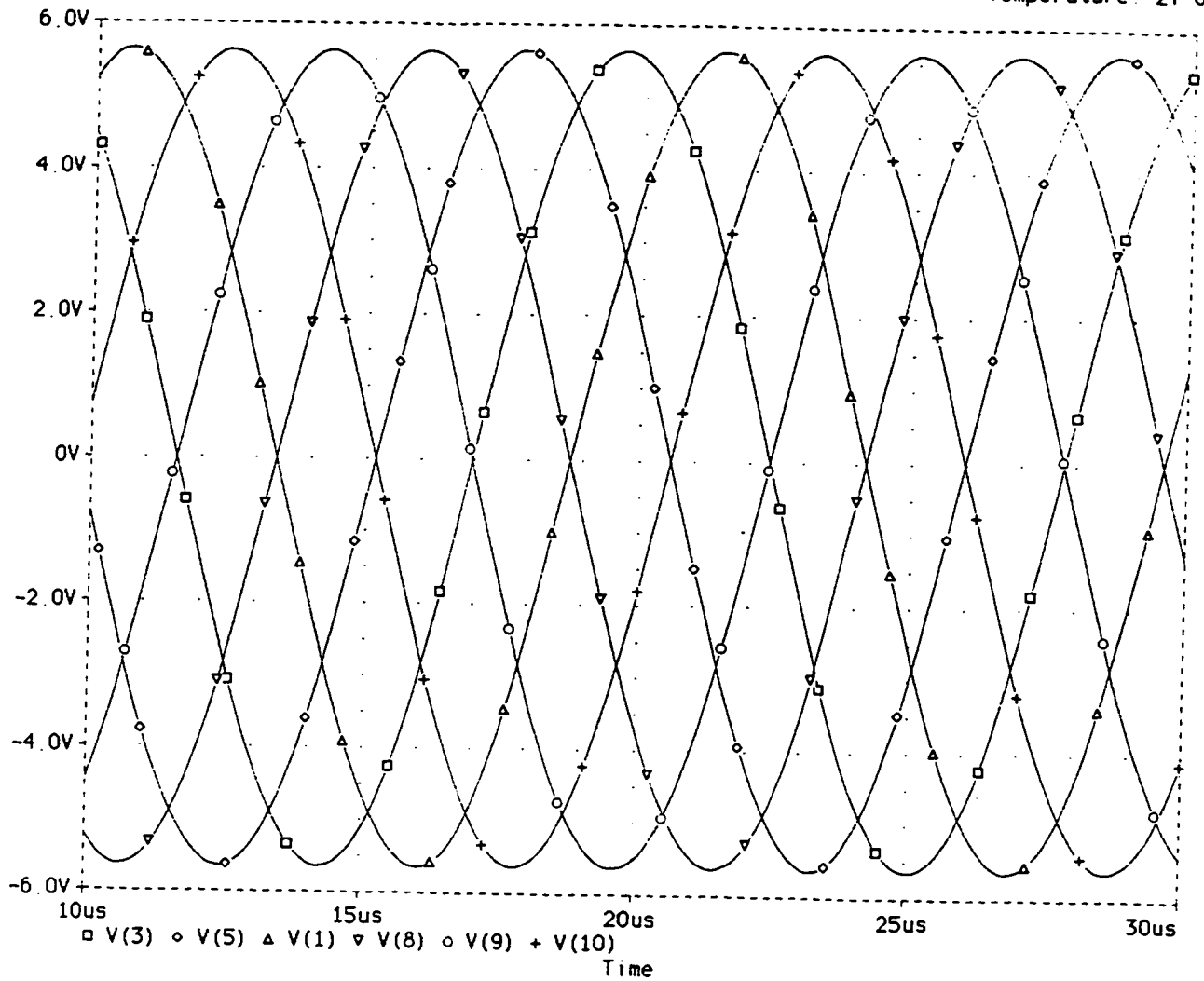
**Fig 2.6 (b) Six-phase output obtained from
2.5(b) with
R=1kΩ, C=1nF,C_1=2.1nF**
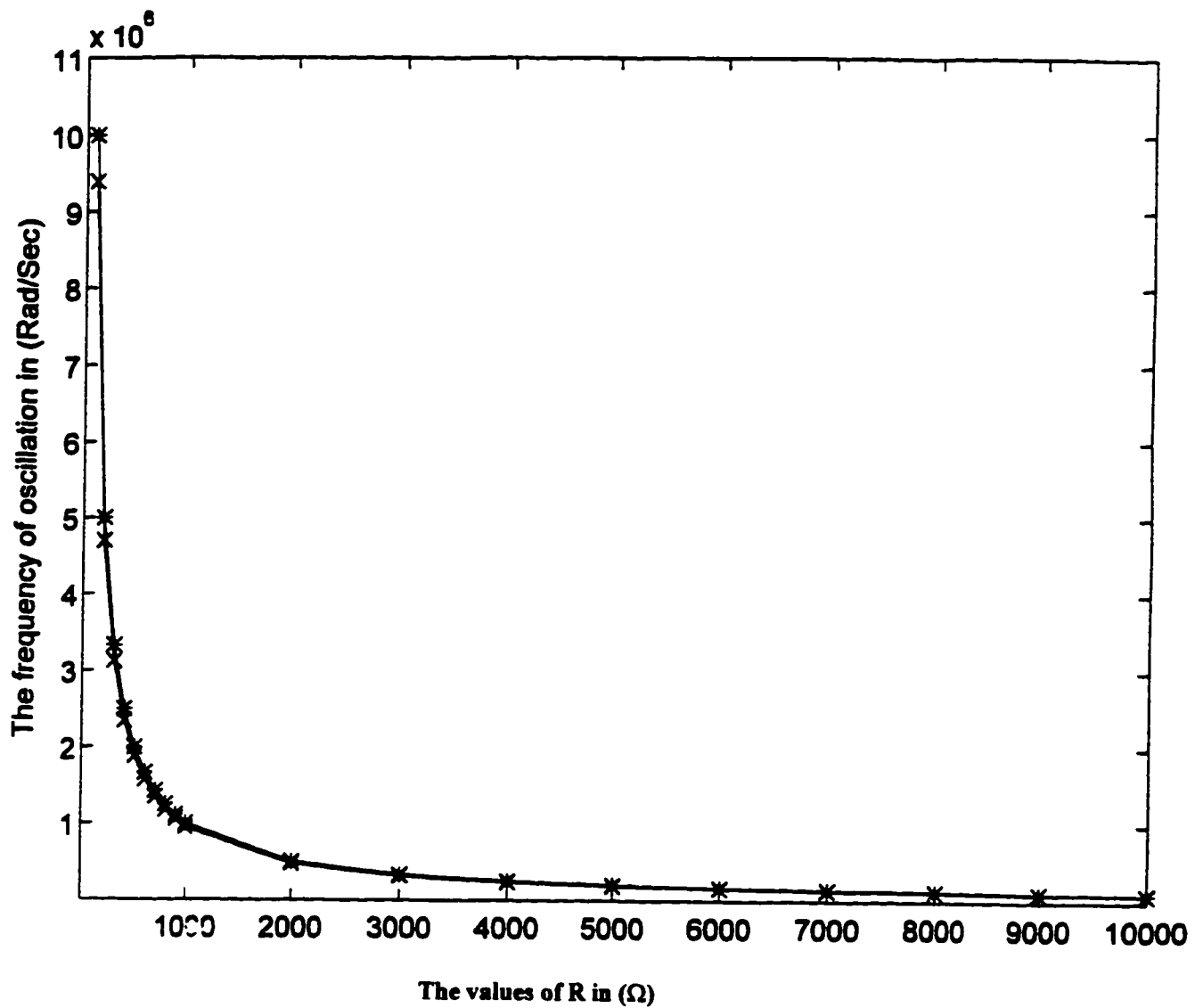
* The theoretical results obtained from (2.24)
x The simulation results

Fig 2.6 (c) The frequency of oscillation (ω_o) in
(rad/second) vs.
the values of R in(Ω)
with
C=1nF and C_1=2.1nF

2.3 Active-R Multiphase Oscillator

A new simple active-R multiphase sinusoidal oscillator will be presented. The proposed MPSO exploits the internal pole of the CCII to advantage. The use of grounded resistors makes it suitable for high frequency oscillation and monolithic IC fabrication. It enjoys the independent control of the frequency and the condition of oscillation, low sensitivity performance and possible electronic tunability. The proposed active-R MPSO has two schemes, one can realize even or odd number of phases while the other can realize odd number of phases only.

2.3.1 Even/odd-phase sinusoidal oscillator

The generalized scheme for even/odd-phase sinusoidal oscillators is shown in Fig. 2.7. The last stage is an inverting first-order low-pass section, while the other basic building blocks for this scheme are identical, non-inverting, first-order low-pass sections. Each of these are characterized by the voltage transfer function:

$$T(s) = \frac{a}{s+b}$$ (2.26)
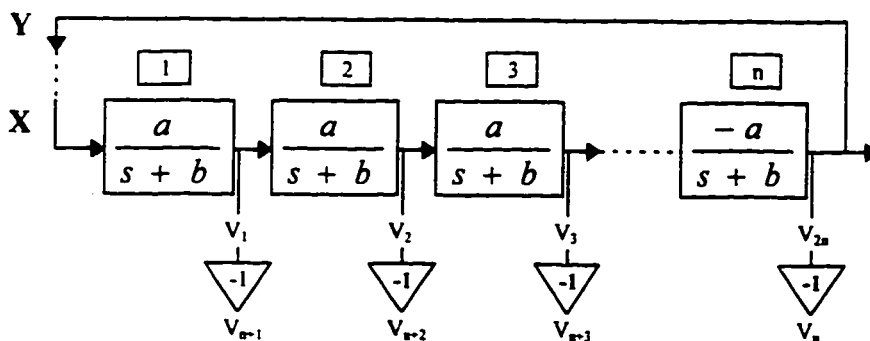
Fig 2.7 Basic scheme for even/odd-phase sinusoidal oscillators.

where a is the gain and b is the pole frequency. The loop-gain between the points X and Y can be expressed for (n) sections by

$$L(s) = -(\frac{a}{s+b})^n \qquad (2.27)$$

For this scheme to produce and sustain sinusoidal oscillation, the loop gain must be equal to unity. Thus, the characteristic equation of the scheme of Fig. 2.7 can be expressed as

$$-(\frac{a}{s+b})^n_{s=j\omega_o} = 1 \qquad (2.28)$$

$$(j\omega_o + b)^n + a^n = 0 \qquad (2.29)$$

From (2.29) the condition of the magnitude can be expressed as

$$\omega_o^2 + b^2 = a^2 \qquad (2.30)$$

and the condition of the phase can be expressed as

$$\frac{180}{n} = \arctan(\frac{\omega_o}{b}) \qquad (2.31)$$

Fig. 2.8 shows a possible realization for the proposed even/odd-phase oscillator using the current conveyors (CCIIs). Each phase requires a first-order lowpass section consisting of a CCII and two grounded resistors. The use of multiple output CCII provides an inverted version of the output. Thus, for (n) building blocks there

are 2n-phase sinusoidal oscillator. Therefore, the circuit in Fig. 2.8 can realize n- or

2n-phase sinusoidal oscillator for n>2. Assuming identical CCII and using the

modified version, shown in Fig.2.5 (c), of the CCII model proposed by Svoboda[55],

routine analysis show that the transfer function of a single stage of the circuit of Fig.

2.8 can be expressed as

$$T(s) = \frac{\dfrac{\alpha\beta}{C_z(R_1 + R_x)}}{s + \dfrac{1}{C_z(R_y\,//\,R_z\,//\,R_2)}}$$

(2.32)

From (2.26) and (2.32), we can see that

a $= \alpha\beta/(C_z(R_1+R_x))$

(2.33a)

b$=1/(C_z(R_y//R_z//R_2))$

(2.33b)

From (2.30), (2.31) and (2.33), the frequency of oscillation can be expressed as

$$\omega_o = \frac{1}{C_z(R_y\,//\,R_z\,//\,R_2)}(\tan\frac{180}{n})$$

(2.34)

and the condition of oscillation can be expressed as

$$\alpha\beta(R_2\,//\,R_z\,//\,R_y) = (R_1 + R_x)\sqrt{((\tan\frac{180}{n})^2 + 1)}$$

(2.35)

Using (2.34) and (2.35) the frequency and the condition of oscillation for different

values of n can be calculated. Sample results are shown in Table 2.5.

No. of building blocks (n)	No. of phases	Condition of oscillation	Frequency of oscillation (ω_o)
3	3,6	$\alpha\beta(R_z//R_y //R_2) = 2(R_1+Rx)$	$1.732/(Cz(R_y//R_z//R_2))$
4	4,8	$\alpha\beta(R_z//R_y //R_2) = 1.414(R_1+Rx)$	$1/(Cz(R_y//R_z//R_2))$
5	5,10	$\alpha\beta(R_z//R_y //R_2) = 1.237(R_1+Rx)$	$0.728/(Cz(R_y//R_z//R_2))$
6	6,12	$\alpha\beta(R_z//R_y //R_2) = 1.154(R_1+Rx)$	$0.577/(Cz(R_y//R_z//R_2))$
7	7,14	$\alpha\beta(R_z//R_y //R_2) = 1.11(R_1+Rx)$	$0.482/(Cz(R_y//R_z//R_2))$
8	8,16	$\alpha\beta(R_z//R_y //R_2) = 1.082(R_1+Rx)$	$0.414/(Cz(R_y//R_z//R_2))$

Table 2.5 Frequency and condition of oscillation of even/odd-phase
sinusoidal oscillators.

From (2.34) and (2.35) we can see that the frequency of oscillation can be adjusted

by tuning the total parasitic grounded capacitor without disturbing the condition of

oscillation which can be adjusted by tuning the grounded resistor R_1 without

disturbing the frequency of oscillation.
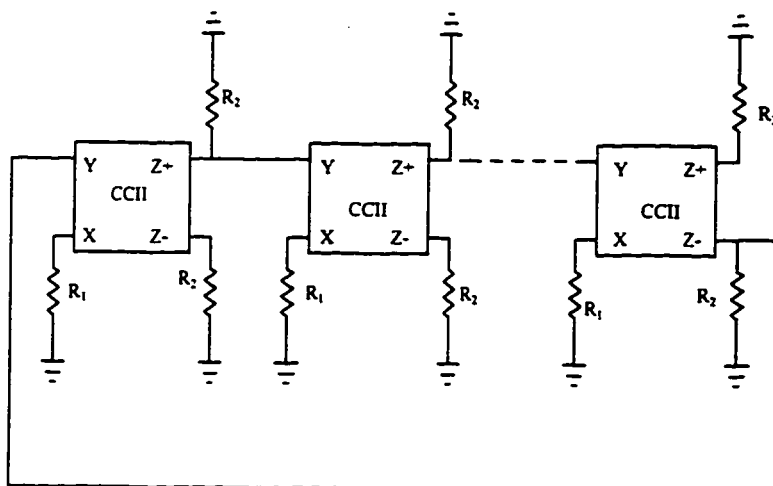
Fig 2.8 Generalized circuit for realizing an even/odd-phase
MPSOs

2.3.2 Odd-phase sinusoidal oscillator

The generalized scheme for odd-phase (n) sinusoidal oscillators is shown in Fig.2.9. The basic building blocks for this scheme are identical, inverting, first-order low-pass sections. Each of these are characterized by the voltage transfer function:

$$T(s) = \frac{a}{s+b} \qquad (2.36)$$
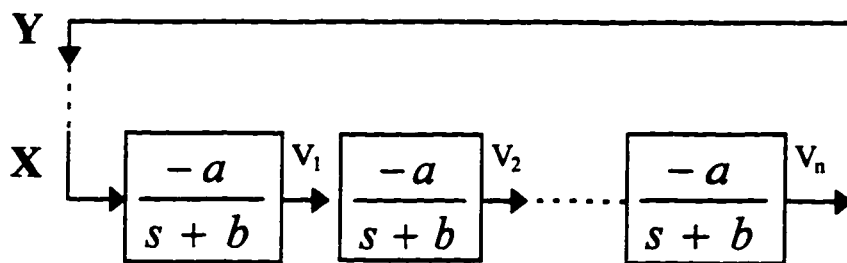
Fig 2.9 Basic scheme for odd-phase sinusoidal oscillators

where a is the gain and b is the pole frequency. The loop-gain between the points X and Y can be expressed for (n) odd sections by

$$L(s) = (-\frac{a}{s+b})^n \qquad (2.37)$$

If the loop gain is unity, this scheme can be set to provide and sustain sinusoidal oscillation. Thus, the characteristic equation of the scheme of Fig. 2.9 can be expressed as

$$(-\frac{a}{s+b})^n_{s=j\omega_o} = 1 \qquad (2.38)$$

$$(j\omega_o + b)^n + a^n = 0 \tag{2.39}$$

From (2.38) and (2.39) the condition of the magnitude can be expressed as

$$\omega_o^2 + b^2 = a^2 \tag{2.40}$$

and the condition of the phase can be expressed as

$$\frac{180}{n} = \arctan(\frac{\omega_o}{b}) \tag{2.41}$$

Fig 2.10 shows a possible realization of the proposed odd-phase MPSOs using the CCIIs. Each phase requires a first-order lowpass section consisting of a CCII and two grounded resistors. Assuming identical current conveyors and using the CCII model, proposed by Svoboda [55] and shown in Fig.2.5 (c), routine analysis show that the transfer function of a single stage of the circuit of Fig. 2.8 can be expressed as

$$T(s) = \frac{\dfrac{\alpha\beta}{C_z(R_1 + R_x)}}{s + \dfrac{1}{C_z(R_y // R_z // R_2)}} \tag{2.42}$$

From (2.36) and (2.42), we can see that

$$a = \alpha\beta/(C_z(R_1+R_x)) \tag{2.43a}$$

$b = 1/(C_z(R_y//R_z//R_2))$

(2.43b)

From (2.40), (2.41) and (2.43), the frequency of oscillation can be expressed as

$$\omega_0 = \frac{1}{C_z(R_y//R_z//R_2)}(\tan\frac{180}{n})$$

(2.44)

and the condition of oscillation can be expressed as

$$\alpha\beta(R_2//R_z//R_y) = (R_1 + R_x)\sqrt{((\tan\frac{180}{n})^2 + 1)}$$

(2.45)

Using (2.44) and (2.45) the frequency and the condition of oscillation for different values of n can be calculated. Sample results are shown in Table 2.6.

No. of phase (n)	Condition of oscillation	Frequency of oscillation (ω_0)
3	$\alpha\beta(R_z//R_y//R_2) = 2(R_1+R_x)$	$1.732/(C_z(R_y//R_z//R_2))$
5	$\alpha\beta(R_z//R_y //R_2) = 1.237(R_1+R_x)$	$0.728/(C_z(R_y//R_z//R_2))$
7	$\alpha\beta(R_z//R_y //R_2) = 1.11(R_1+R_x)$	$0.482/(C_z(R_y//R_z//R_2))$
9	$\alpha\beta(R_z//R_y //R_2) = 1.063(R_1+R_x)$	$0.364/(C_z(R_y//R_z//R_2))$

Table 2.6 Frequency and condition of oscillation of odd-phase sinusoidal oscillators.

From Table 2.6 it can be seen that the frequency of oscillation can be adjusted by tuning the total parasitic grounded capacitor without disturbing the condition of oscillation which can be adjusted by tuning the grounded resistor R_1 without disturbing the frequency of oscillation.
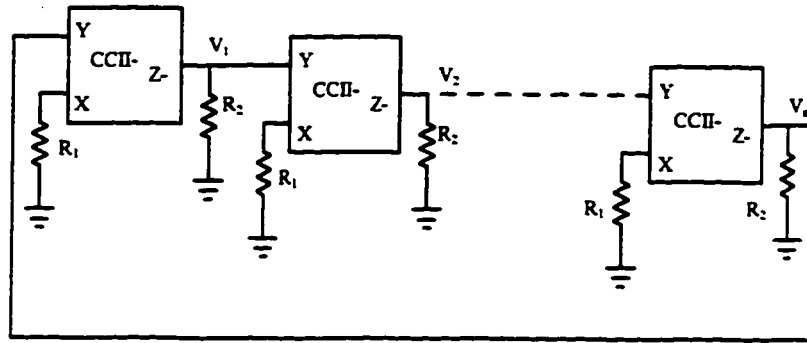
Fig 2.10 Generalized circuit for realizing an even-phase MPSOs

2.3.3 Sensitivity Analysis

From (2.21), (2.23), (2.34) and (2.44), it is easy to show that the active and passive sensitivities of the frequency of oscillation of Fig. 2.8 and Fig 2.10 are given by

$$S_{C_z}^{\omega_o} = -1, S_{R_2}^{\omega_o} = \frac{-1}{1 + R_2/(R_y//R_z)} \approx -1 \tag{2.46}$$

$$S_{(R_z//R_y)}^{\omega_o} = \frac{-1}{1+(R_z//R_y)/R_2} \approx 0, S_{R_1}^{\omega_o} = S_\alpha^{\omega_o} = S_\beta^{\omega_o} = 0 \tag{2.47}$$

Thus the proposed circuits enjoy low active and passive ω_o-sensitivities

2.3.4 Simulation Results and Discussion

The three-phase and the six-phase sinusoidal oscillators shown in Fig2.11 (a) and (b) were obtained from Fig.2.8 and Fig.2.10. To investigate the workability of these MPSOs, both circuits were simulated using Pspice simulation circuit program. The simulation was performed using the modified version, shown in Fig.2.5(c), of the circuit proposed by Svoboda[55]. Fig 2.13 (a) and (b) shows the simulated

oscillations obtained from the circuits of Fig. 2.11 a and b for three-phase and six-phase oscillations obtained with $R_1=4.5k\Omega$ and $R_2=10k\Omega$.

From (2.34), (2.35), (2.44) and (2.45), we can see that while the frequency of oscillation will not be affected by the current and voltage tracking errors of the CCII, the condition of oscillation will be slightly affected. The proposed circuits prove that, they can absorb the effect of the nonidealites shown in the model of Fig 2.5 (c). To show the effect of other possible sources of nonidealties of the current conveyors of the proposed circuits of Fig2.11 (a) and (b) have been simulated using the modified version of the Bruun-model [59], shown in Fig.2.12. Fig.2.13(c) shows the theoretical results of the frequencies of oscillation at different values of Cz obtained by using (2.34) and (2.45) with ($R_1=4.5k\Omega$, $R2=10k\Omega$, $R_y=10M\Omega$, and $R_z=3M\Omega$) and the simulation results obtained by using the Bruun-model. The simulation results deviate from the theoretical results by an error less than 2%.

Since, the frequency of oscillation can be adjusted by tuning the total parasitic grounded capacitor without disturbing the condition of oscillation, then obtaining a voltage controlled multiphase oscillator is feasible by connecting a voltage controlled grounded-capacitor at terminal Z of the CCII. Such a capacitor can be realized in active-R technique using the voltage-feedback operational amplifier pole[60].

To show the merits and demerits of this MPSOs, Table 2.7 shows a comparison between the proposed MPSOs and the most recently published MPSOs. Comparison shows that the proposed MPSOs and the MPSOs published in [28] are able to produce even or odd numbers of phases while the MPSOs published in

1992[26] and 195[31] can produce odd number of phases only. However, the proposed MPSOs use less number of active and passive elements than what has been reported in 1995 [29]. For (n) odd-phase MPSOs, the proposed MPSOs use the same number of passive elements as what has been reported in [31] but all of them are grounded. Moreover, the MPSOs in [31] use (n) floating elements. The proposed MPSOs has the ability to control ω_0 through grounded capacitor without changing the condition of oscillation while the other can't do that.

	MPSOs using OTA[26] 1992	MPSOs using CFA [31] 1995	MPSOs using CCII [29] 1995	Proposed active-R MPSOs
No. of active devices for (2n) EVEN-MPSOs	---------	----------	(2n)	(n)
No. of passive elements for (n) EVEN-MPSOs	---------	----------	(5n)	(3n)
No. of Active Devices for (n) ODD-MPSOs	(2n)	(n)	(n)	(n)
No. of passive elements for (n) ODD-MPSOs	(n)	(2n) (n) of them floating	(3n)	(2n)
The ability of controlling ω_0 without changing the condition of oscillation through grounded resistor or through gm of the OTA	No	No	No	Yes

Table 2.7 Comparison between the latest MPSOs and the proposed one
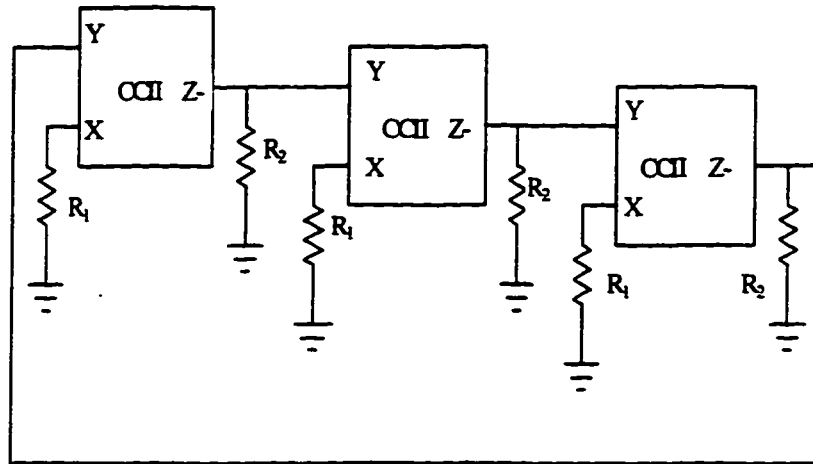
Fig. 2.11 (a) Three-phase sinusoidal oscillator
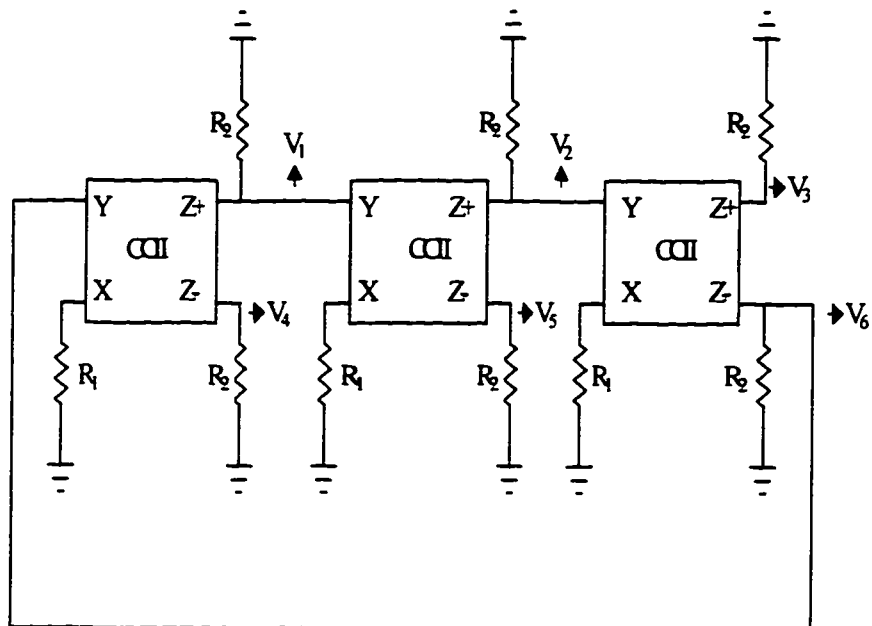
Fig. 2.11 (b) Six-phase sinusoidal oscillator
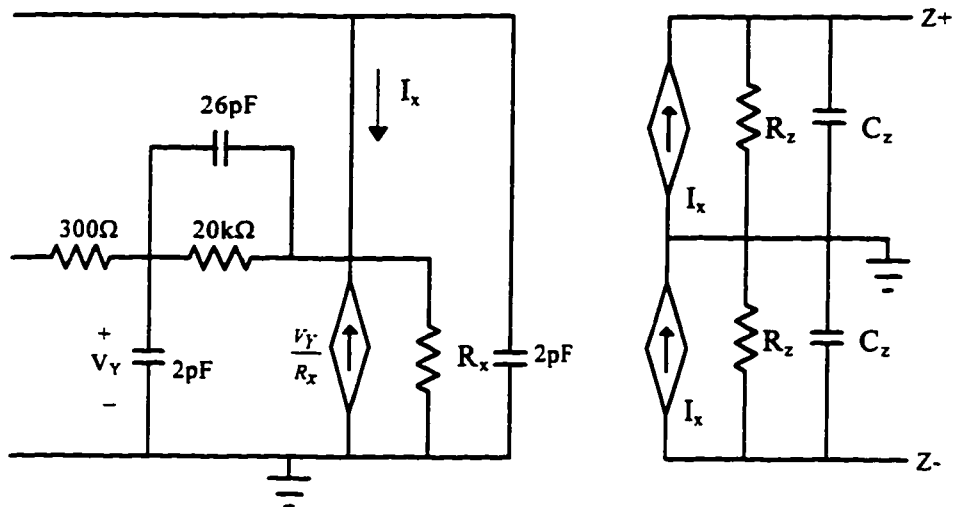
Fig.2.12 A modified version of Bruun-model for the modelling of the dual-output current conveyor $R_x=50\Omega$, $R_z=3M\Omega$ and $C_z=4.5pF$
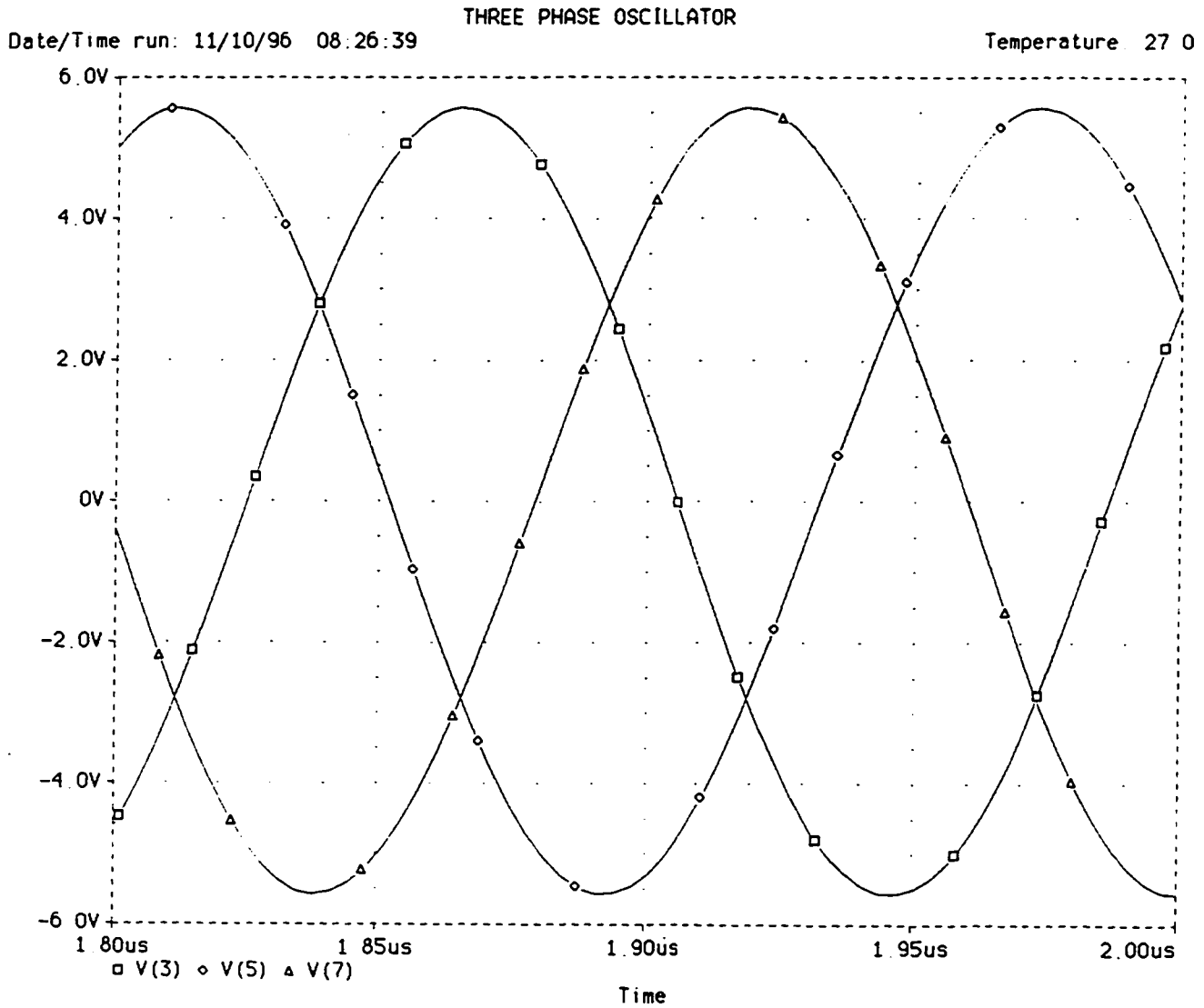
Fig 2.13 (a) Three-phase output obtained from
2.11(a) with
$R_1=4.5k\Omega, R_2=10k\Omega$

SIX PHASE OSCILLATOR

Date/Time run: 11/10/96   07:59:59

Temperature: 27 0

6 0V

4.0V

2.0V

0V

-2.0V

-4 0V

-6 0V

1.80us   1.85us   1.90us   1.95us   2.00us

□ V(3) ◇ V(5) ▵ V(7) ▽ V(8) ○ V(9) + V(10)

Time
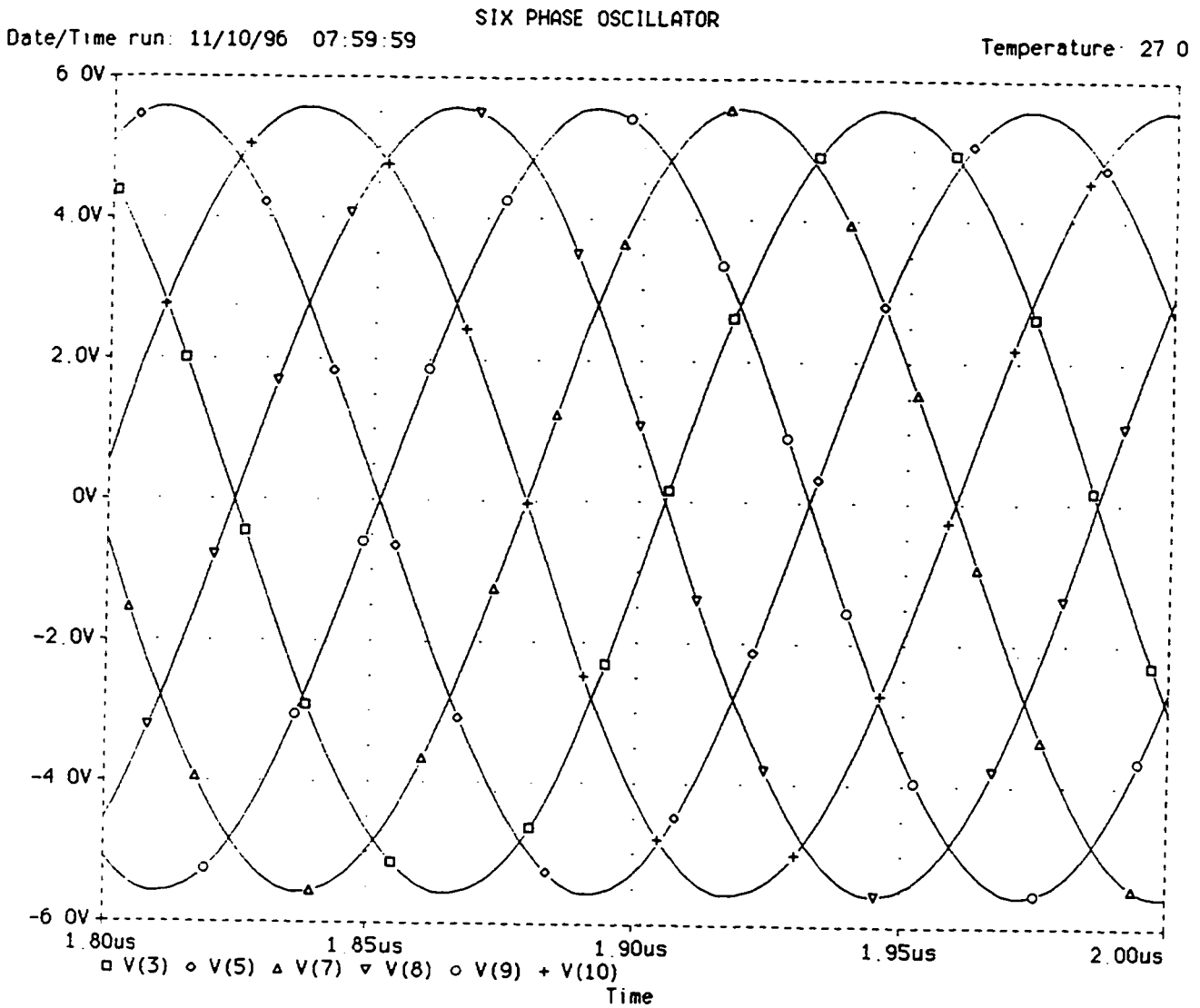
Fig 2.13 (b) Six-phase output obtained from
2.11(b) with
R₁=4.5kΩ,R₂=10kΩ
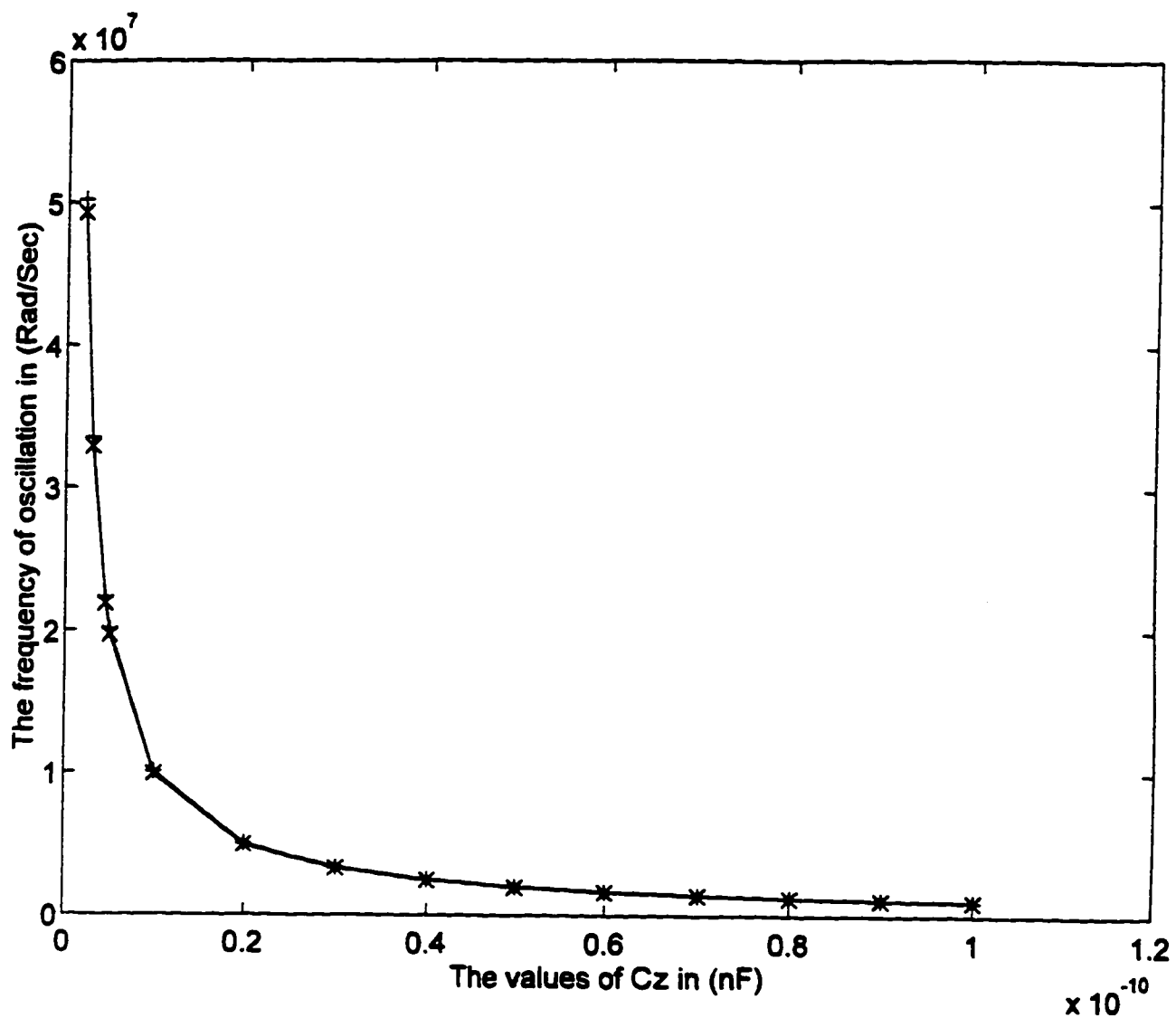
+ The theoretical results obtained using (2.34) and (2.45)
x The simulation results obtained using the Bruun-model

Fig 2.13 (c) The frequency of oscillation (ω_o) in (rad/second) vs.
the values of C_z in (nF)
with
$R_1=4.5k\Omega$, $R_2=10k\Omega$, $R_y=10M\Omega$, $R_z=3M\Omega$

2.4 Active-C Multiphase Oscillator

A new active-C multiphase oscillator structure using CCCIIs will be presented. The use of second-generation current controlled conveyor (CCCII) allows MPSO to be electronically programmable. The proposed structure can be configured to produce an even-number or odd-number of equal-amplitude equally-spaced-in-phase output currents. This structure enjoys the following attractive features: the use of grounded capacitors only without using any external resistors, independent current-control of the frequency of oscillation using the bias current of the CCCII and low active and passive sensitivities. The proposed active-C MPSO has two schemes, one can realize even or odd number of phases while the other can realize odd number of phases only.

2.4.1 Even/odd-phase sinusoidal oscillator

Fig. 2.13 shows the proposed even/odd-phase sinusoidal oscillator structure using the current controlled current conveyors CCCII deduced from the block diagram of Fig.2.7. Each phase requires a first-order lowpass section consisting of a CCCII and two grounded capacitors. The use of multiple output CCCII provides an inverted version of the output current. Thus for n-building block there are 2n-phase oscillator. Assuming identical CCCII and using the standard notation, the CCCII can be characterized by $i_Y=0$, $V_x=V_y+R_x i_x$ and $i_z=\pm i_x$ where $R_x=V_T/(2I_o)$, V_T is the thermal voltage and I_o is the bias current of the CCCII. Routine analysis yields the current transfer function of a single stage of Fig. 2.14 (a) which can be expressed as

$$T(s) = \frac{\alpha\beta(C_1 / C_2)}{s + (1/C_1 R_x)} \qquad (2.48)$$
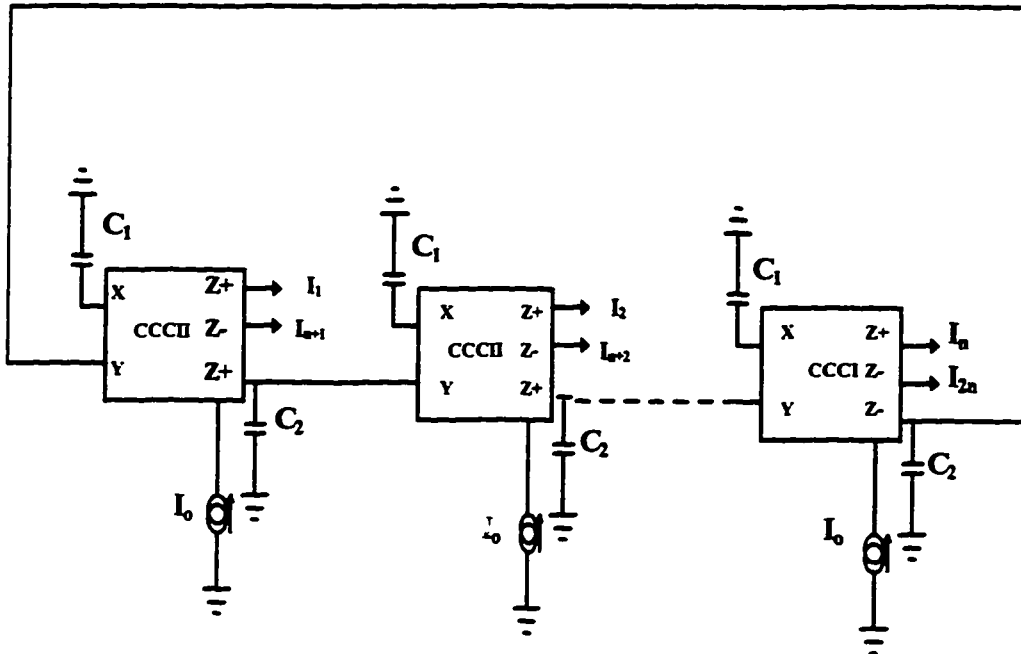
Fig. 2.14 (a) Generalized circuit for realizing a multiphase oscillator

The loop-gain between the points X and Y can be expressed for n (odd integer) sections by

$$L(s) = -(\frac{\alpha\beta(C_1 / C_2)}{s + (1/C_1 R_x)})^n \qquad (2.49)$$

If the loop gain is unity, this structure can be set to provide and sustain sinusoidal oscillation. Thus, the characteristic equation of the scheme of Fig. 2.13 can be expressed as

$$(\frac{\alpha\beta(C_1 / C_2)}{s + (1/C_1 R_x)})^n_{s=jw_o} = -1 \qquad (2.50)$$

$$(j\omega_o + (1/C_1 R_x))^n + (\alpha\beta(C_1 / C_2))^n = 0 \qquad (2.51)$$

From (2.51) the condition of the magnitude can be expressed as

$$\omega_o^2 + (1/C_1 R_x)^2 = (\alpha\beta(C_1 / C_2))^2 \qquad (2.52)$$

and the condition of the phase can be expressed as

$$\frac{180}{n} = \arctan(\omega_o R_x C_1) \qquad (2.53)$$

Using (2.52) and (2.53) the frequency of oscillation for different values of n can be expressed as

$$\omega_o = \frac{1}{R_x C_1}(\tan\frac{180}{n}) = \frac{2I_o}{C_1 V_T}(\tan\frac{180}{n}) \qquad (2.54)$$

and the condition of oscillation can be expressed as

$$C_1 = C_2 \sqrt{((\tan\frac{180}{n})^2 + 1)} \qquad (2.55)$$

Using (2.54) and (2.55) the frequency and the condition of oscillation for different values of n can be calculated. Sample results are shown in Table 2.8.

No. of building blocks (n)	No. of phases	Condition of oscillation	Frequency of oscillation (ω_o)
3	3,6	$\alpha\beta C_1 = 2C_2$	$1.732/(C_1R_x)$
4	4,8	$\alpha\beta C_1 = 1.414C_2$	$1/(C_1R_x)$
5	5,10	$\alpha\beta C_1 = 1.237C_2$	$0.728/(C_1R_x)$
6	6,12	$\alpha\beta C_1 = 1.154C_2$	$0.577/(C_1R_x)$
7	7,14	$\alpha\beta C_1 = 1.11C_2$	$0.482/(C_1R_x)$
8	8,16	$\alpha\beta C_1 = 1.082C_2$	$0.414/(C_1R_x)$

Table 2.8. Condition and frequency of oscillation of even/odd-phase sinusoidal oscillators.

From (2.54) and (2.55) it can be seen that the frequency of oscillation can be adjusted linearly by tuning I_o without disturbing the condition of oscillation which can be adjusted by tuning the grounded capacitor C_1 without disturbing the frequency of oscillation. Thus obtaining a current controlled multiphase oscillator is feasible. Also, we can see that while the frequency of oscillation will not be affected by the current and voltage tracking errors of the CCCII, the condition of oscillation will be slightly affected.

2.4.2 Odd-phase sinusoidal oscillator

Fig. 2.14 (b) shows the proposed odd-phase MPSOs oscillator structure deduced from the block diagram of Fig.2.9 using the CCCII. Each phase requires a first-order lowpass section consisting of a CCCII and two grounded capacitors.

Assuming identical current conveyors and using the standard notation of the CCCII, routine analysis yields the current transfer function of a single stage of Fig. 2.14 which can be expressed as

$$T(s) = \frac{\alpha\beta(C_1/C_2)}{s+(1/C_1 R_x)}$$

(2.56)
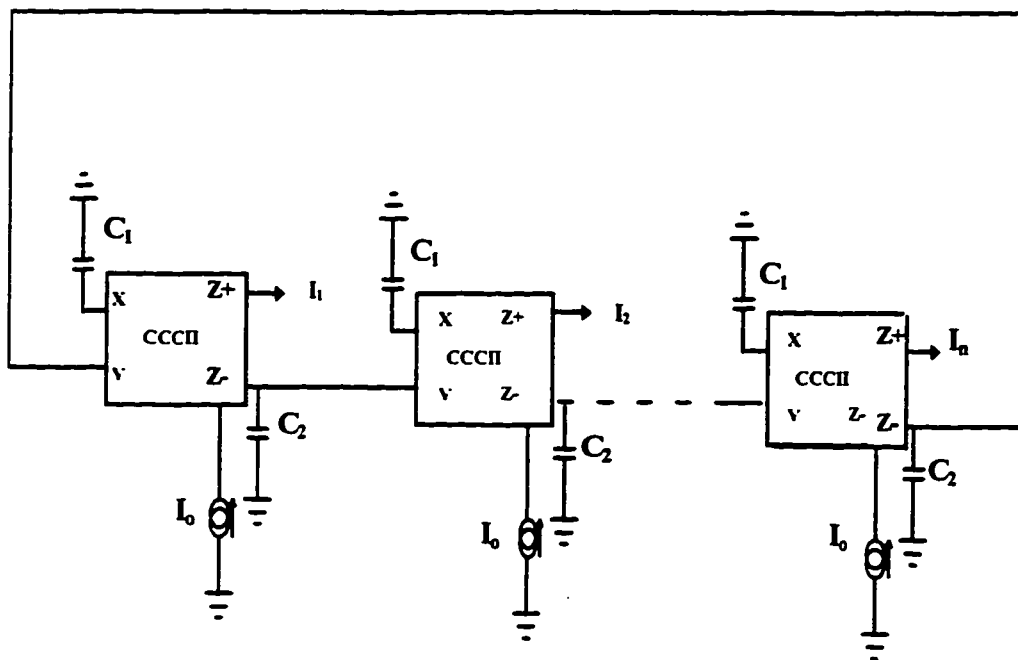
Fig. 2.14 (b) Generalized circuit for realizing an odd-phase sinusoidal oscillator

The loop-gain between the points X and Y can be expressed for n (odd integer) sections by

$$L(s) = -(\frac{\alpha\beta(C_1/C_2)}{s + (1/C_1R_x)})^n$$

(2.57)

If the loop gain is unity, this structure can be set to provide and sustain sinusoidal oscillation. Thus, the characteristic equation of the scheme of Fig. 2.14 can be expressed as

$$(\frac{\alpha\beta(C_1/C_2)}{s + (1/C_1R_x)})^n{}_{s=jw_o} = -1$$

(2.58)

$$(j\omega_o + (1/C_1R_x))^n + (\alpha\beta(C_1/C_2))^n = 0$$

(2.59)

From (2.59) the condition of the magnitude can be expressed as

$$\omega_o^2 + (1/C_1R_x)^2 = (\alpha\beta(C_1/C_2))^2$$

(2.60)

and the condition of the phase can be expressed as

$$\frac{180}{n} = \arctan(\omega_o R_x C_1)$$

(2.61)

Using (2.60) and (2.61) the frequency of oscillation for different values of n can be expressed as

$$\omega_o = \frac{1}{R_x C_1}(\tan\frac{180}{n}) = \frac{2I_o}{C_1V_T}(\tan\frac{180}{n})$$

(2.62)

and the condition of oscillation can be expressed as

$$C_1 = C_2 \sqrt{((\tan\frac{180}{n})^2 + 1)}$$

(2.63)

Using (2.62) and (2.63) the frequency and the condition of oscillation for different values of n can be calculated. Sample results are shown in Table 2.9.

No. of phase (n)	Condition of oscillation	Frequency of oscillation (ω_o)
3	$\alpha\beta C_1 = 2C_2$	$1.732/(C_1 R_X)$
5	$\alpha\beta C_1 = 1.237 C_2$	$0.728/(C_1 R_X)$
7	$\alpha\beta C_1 = 1.11 C_2$	$0.482/(C_1 R_X)$
9	$\alpha\beta C_1 = 1.063 C_2$	$0.364/(C_1 R_X)$

Table 2.9. Condition and frequency of oscillation of odd-phase sinusoidal oscillators.

From (2.62) and (2.63) it can be seen that the frequency of oscillation can be adjusted by tuning I_o without disturbing the condition of oscillation which can be adjusted li..early by tuning the grounded capacitor C_1 without disturbing the frequency of oscillation. Also, we can see that while the frequency of oscillation will not be affected by the current and voltage tracking errors of the current conveyors, the condition of oscillation will be slightly affected.

2.4.3 Sensitivity Analysis

From (2.21), (2.54), and (2.62) it is easy to show that the active and passive sensitivities of the frequency of oscillation of Fig. 2.13 and Fig. 2.14 are given by

$$S_C^{\omega_o} = -1 \tag{2.64}$$

$$S_{I_o}^{\omega_o} = 1 \tag{2.65}$$

$$S_\alpha^{\omega_o} = S_\beta^{\omega_o} = 0 \tag{2.66}$$

2.4.4 Simulation Results and Discussion

The three-phase MPSO shown in Fig 2.15 and the six-phase MPSO shown in Fig.2.16 were deduced from Fig.2.14 (a) and (b). To investigate the workability of these oscillators, both circuits were simulated using ICAPS circuit simulation program. The multiple output plus/minus CCCIIs were simulated using realization of Fig.1.10 proposed in [20] by adding current mirrors and cross-coupled current mirrors. The PNP and NPN transistors were simulated using the parameters of the PR200N and NR200N bipolar transistors[61]. The results obtained for C_1=41.5nF, C_2=20nF and I_o=50uA are shown in Fig. 2.17 and Fig. 2.18 for n=3 and and n=6 respectively. Fig 2.19 shows the frequency of oscillation vs. control current. As shown in Fig 2.19, the simulated values of frequency of oscillation are in good accordance with theoretical ones. Deviations less than 6% were obtained on the range 1–200uA for I_o. The most important deviations, which appear for the very high values of I_o principally come from the diminutions of the betas of the transistors of the translinear loop of the CCCII (betas used in simulation equals 137.5 for NPN transistors and 110 for PNP transistors). To reduce these deviations, transistors with higher values of beta should be used in realizing the CCCII. By

using smaller capacitors, we can work at higher frequencies. For oscillation at 22.053MHz with I_o=100uA and C_1=100pF the frequency obtained from simulation is 20.9MHz with error 5.2%.

To show the merits and demerits of this MPSOs, Table 2.10 show a comparison with the previously published MPSOs. It can be seen that, the proposed MPSOs are able to produce even or odd numbers of phases using less number of active devices and grounded elements than the previously published MPSOs. While MPSOs published in [31] and [29] lacks programmability, MPSOs published in [26] are not able to tune ω_o without changing the condition of oscillation. However, the big advantage of the proposed MPSOs is the ability of controlling ω_o through I_o of the CCCIIs without changing the condition of oscillation and without using any external resistors.

	MPSOs using OTA [26] 1992	MPSOs using CFA[31] 1995	MPSOs using CCII [29] 1995	Proposed MPSOs
No. of active devices for (2n)EVEN-MPSOs	----------	----------	(2n)	(n)
No. of passive elements (2n)for EVEN-MPSOs	----------	----------	(5n)	(2n)
No. of Active Devices (n)for ODD-MPSOs	(2n)	(n)	(n)	(n)
No. of passive elements (n)for ODD-MPSOs	(n)	(2n) (n)of them floating	(3n)	(2n)
The ability of programming ω_0 without cnanging the condition of oscillation through external current or voltage	we can't program ω_0 through gm without changing the condition of oscillation	lakes programm -ability	lakes programm-ability	we can program ω_0 through Ic without changing the condition of oscillation

Table 2.10 Comparison between the latest MPSOs and the proposed one
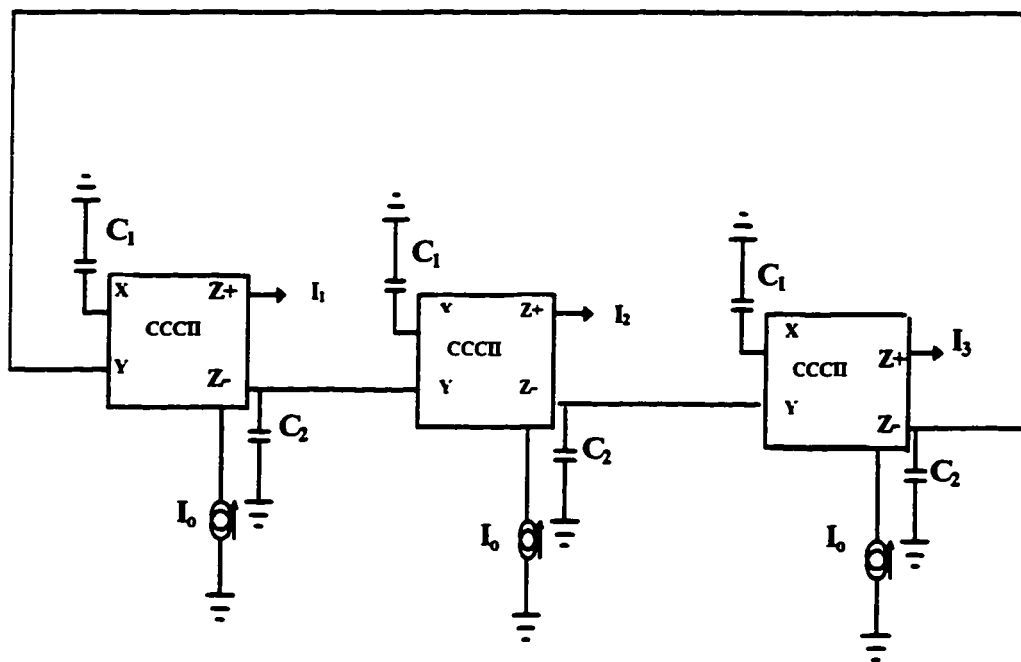
Fig 2.15 Three-phase sinusoidal oscillatore
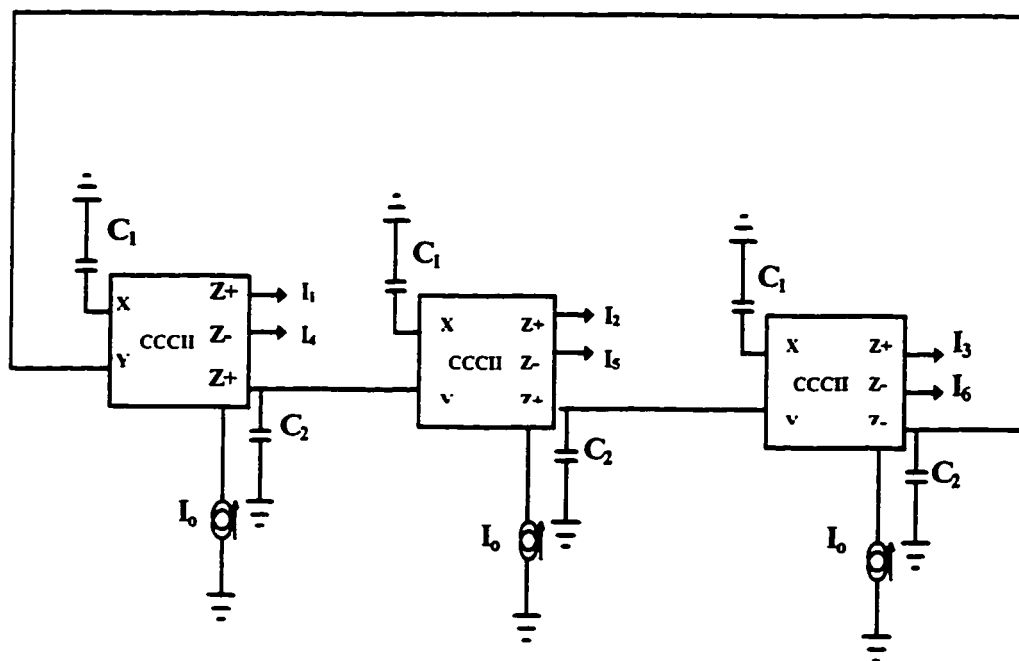
Fig 2.16 Six-phase sinusoidal oscillatore
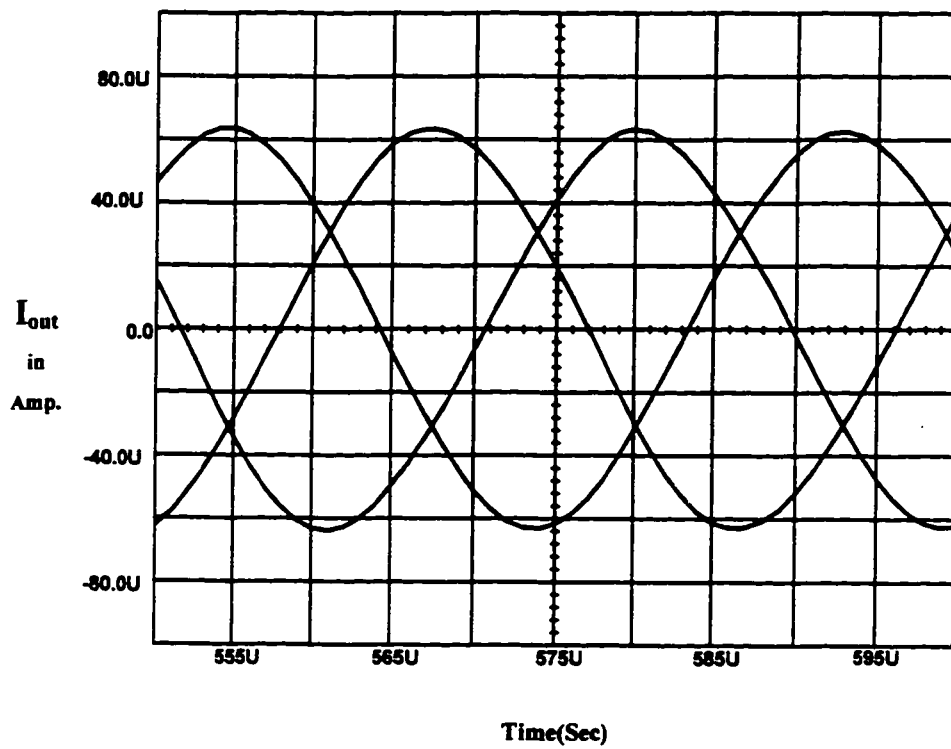
Fig 2.17 Simulated result of the three-
phase oscillator
$C_1=41.5nF$, $C_2=20nF$, $I_0=50uA$
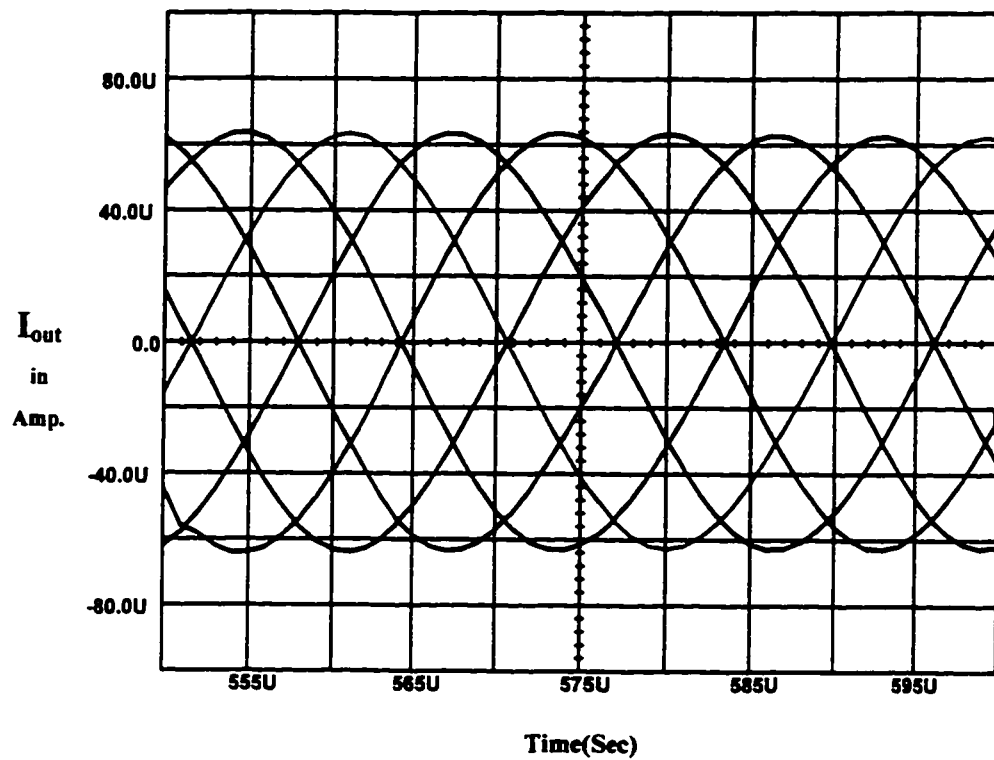
Fig 2.18 Simulated result of the six-
phase oscillator
$C_1=41.5nF$, $C_2=20nF$, $I_o=50uA$
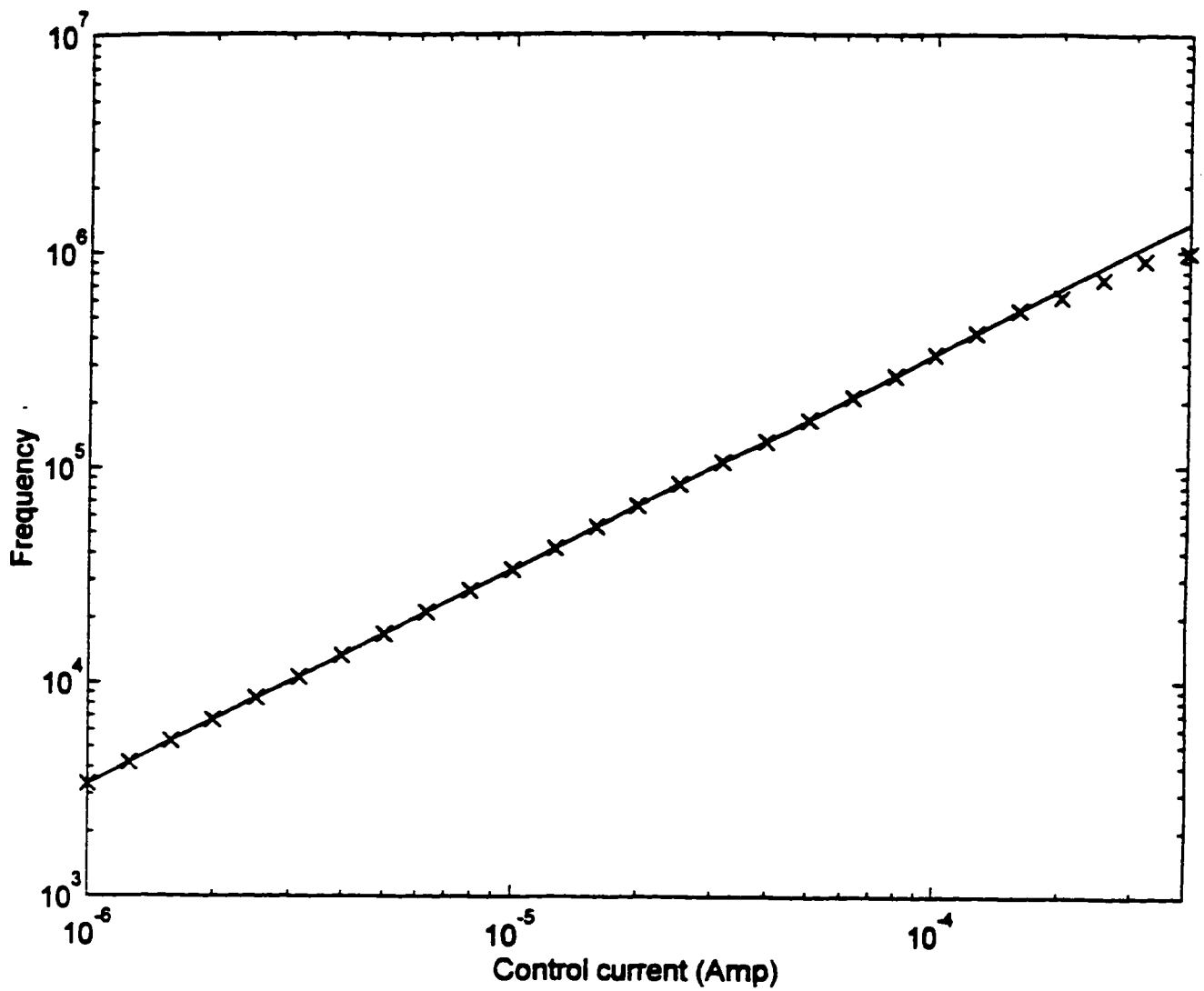
Fig. 2.19 Frequency of oscillation
in(rad/sec)
vs.
control current in (Amp) where
$C_1 = 41.5nF, C_2 = 20 nF$

Chapter 3

Active-RC Universal Filter using unity gain cells

3.1 Introduction

The active-RC filter is the filter implemented by embedding active devices within a passive RC network. It is desirable to minimize the complexity of the active circuitry required. Consequently, the use of simple active devices like the unity gain current and voltage followers to realize active-RC filters has been receiving considerable attention [33-35] and results in the merits of greater linearity, larger dynamic range and wider bandwidth which is not inversely related to the closed-loop gain. A universal filter which can realize different responses i.e. lowpass,

highpass, bandpass, notch and allpass has been reported by [36]. However, it can't realize the different responses without changing the circuit topology. In this chapter, we will investigate the use of unity gain cells in designing both current and voltage mode universal filters which can realize different responses without changing the circuit topology.

3.2 Universal Current-mode Multiple Inputs-Single Output Filter

A new universal current-mode filter with three inputs and one output using unity gain cells will be presented. It can realize lowpass, bandpass and highpass responses without changing the circuit topology. The circuit can also realize notch and allpass responses without using additional active or passive elements. The proposed filter circuit enjoys high output impedance, independent tuning of the parameters ω_0 and ω_0/Q_0, independent tuning of the gain without changing ω_0 and ω_0/Q_0, employment of grounded capacitors which paves the way for high frequency operation and low active and passive sensitivities [62].

3.2.1 Proposed Circuit

The proposed circuit is shown in Fig. 3.1. Using standard notations, the current-follower CF± can be characterized by $i_z = \pm \alpha_n i_x$, $n=1-4$ and the unity gain voltage follower can be characterized by $V_{out} = \beta_n V_{input}$, $n=1-3$ where $\alpha_n = 1-\varepsilon_n$, $|\varepsilon_n| \ll 1$ represents the current tracking error of the n-th current follower and $\beta_n = 1-\delta_n$,

$|\delta_n|<<1$ represents the voltage tracking error of the n-th voltage follower. Routine analysis of Fig.3.1 yields the current transfer function given by
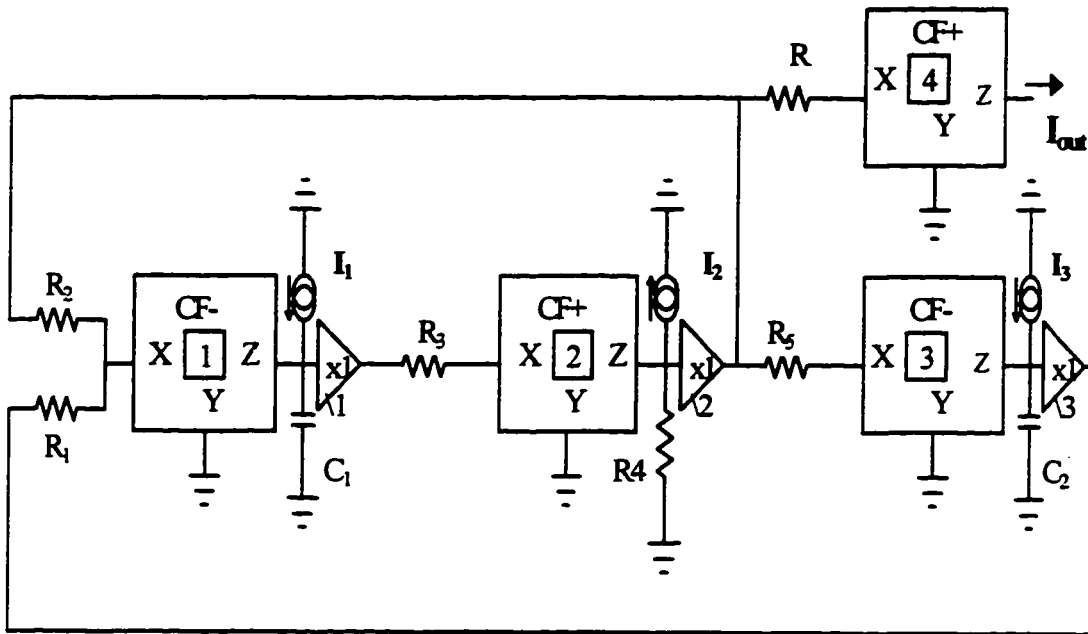
**Fig 3.1 Proposed universal current-mode filter
with three inputs and one output**

$$I_{out} = \alpha_2\alpha_4\beta_2 \frac{R_4}{R} \frac{I_2(s^2) + I_1(s\dfrac{\beta_1}{C_1R_3}) + I_3(\dfrac{\alpha_1\beta_1\beta_3}{C_1C_2R_1R_3})}{s^2 + s\dfrac{\alpha_1\alpha_2\beta_1\beta_2R_4}{C_1R_2R_3} + \dfrac{\alpha_1\alpha_2\alpha_3\beta_1\beta_2\beta_3R_4}{C_1C_2R_1R_3R_5}} \qquad (3.1)$$

From (3.1) the parameters ω_0 and ω_0/Q_0 can be expressed as

$$\omega_o^2 = \frac{\alpha_1 \alpha_2 \alpha_3 \beta_1 \beta_2 \beta_3 R_4}{C_1 C_2 R_1 R_3 R_5} \qquad (3.2)$$

$$\frac{\omega_o}{Q_o} = \frac{\alpha_1 \alpha_2 \beta_1 \beta_2 R_4}{C_1 R_2 R_3} \qquad (3.3)$$

From (3.1) it can be seen that

(i) the lowpass response can be realized with

$$I_1 = I_2 = 0,$$

(ii) the highpass response can be realized with

$$I_1 = I_3 = 0,$$

(iii) the bandpass response can be realized with

$$I_2 = I_3 = 0,$$

(ii) the notch response can be realized with

$$I_1 = 0 \text{ and } I_2 = I_3 \text{ and } R_5 = R_4$$

(ii) the allpass response can be realized with

$$I_2 = I_3 = -I_1, \text{ and } R_2 = R_4 = R_5$$

From (3.1) it can also be seen that the lowpass dc gain is equal to,

$$G_{LP} = \frac{\alpha_4 R_5}{\alpha_3 R} \qquad (3.4)$$

the high frequency gain of the highpass response is equal to,

$$G_{HP} = \frac{\alpha_2 \alpha_4 \beta_2 R_4}{R} \qquad (3.5)$$

and the bandpass gain at ω_0 is equal to

$$G_{BP} = \frac{\alpha_4 R_2}{\alpha_1 R} \qquad (3.6)$$

From (3.2)–(3.6) it can be seen that the parameter ω_0 can be adjusted by controlling the resistors R_1, R_5 and/or the capacitor C_2 without disturbing the parameter ω_0/Q_o. Moreover, the parameter ω_0/Q_o can be adjusted by controlling the resistor R_2 without disturbing the parameter ω_0. However, controlling the resistance R_2 and/or R_5 will disturb the lowpass and the bandpass gains. A possible strategy for adjusting the parameters ω_0, ω_0/Q_o, the lowpass gain, the highpass gain and the bandpass gain, is therefore as follows: first the resistor R_2 is adjusted to control the parameter ω_0/Q_o, then the resistor R is adjusted to control the highpass gain or the bandpass gain; the resistor R_5 is adjusted to control the lowpass gain, and finally the resistor R_1 is adjusted to control the parameters ω_0.

3.2.2 Sensitivity Analysis

Using (2.21), (3.2) and (3.3), Table 3.1 show the active and passive sensitivities of the proposed filter of Fig. 3.1.

S	ω_o	Q_o
α_1	0.5	-0.5
α_2	0.5	-0.5
α_3	0.5	0.5
β_1	0.5	-0.5
β_2	0.5	-0.5
β_3	0.5	0.5
C_1	-0.5	-0.5
C_2	-0.5	-0.5
R_1	-0.5	0.5
R_2	0.0	1
R_3	-0.5	0.5
R_4	0.5	-0.5
R_5	-0.5	-0.5
R	0.0	0.0

Table 3.1 The active and passive sensitivities of
the proposed filter in Fig.3.1

From Table 3.1, it is clear that the active and passive sensitivities are small.

3.2.3 Simulation and Experimental Results and Discussion

The proposed circuit was tested experimentally using the AD844; the AD844 contains a unity-gain follower and a second-generation current-conveyor which can be converted into a current-follower by grounding its high-impedance terminal. The circuit was also simulated using Pspice. The simulation was performed using the model of AD844, shown in Fig. 3.2, proposed by Svoboda 1994[55]. Fig. 3.3 (a,b,c,d and e) show the simulation and the experimental results obtained from the lowpass, bandpass, highpass, notch and allpass responses. It appears that the simulation and the experimental results are in fairly good agreement with the presented theory. However, it can be seen that there are some deviation between the theoretical, the simulation and the experimental results. That is due to the nonidealties of the active devices. The major source of the nonidealites is the parasitic resistance that appears at port X of the CF. We can take care of R_{x2}, R_{x3} and R_{x4} by adding them in series to R_3, R_5 and R respectively.

For the natural frequency (ω_o) the deviation between the theoretical, simulation and experimental results is less than 5%.

For the gain the deviations between the theoretical, simulation and experimental results can be summarized as follows:

1. the lowpass gain deviates by a percentage error less than 1%,

2. the bandpass gain deviates by a percentage error less than 6%,

3. the highpass gain deviates a percentage error less than 4% for frequencies < 1MHz,

4. the notch response deviates by a percentage error less than 10%,

5. the allpass response deviates by a percentage error less than 10%. while the phase of the allpass responce deviates by a percentage error less than 12%.

In order to explore the possible reasons for the deviation between the theoretical and experimental results, the analysis was repeated, in Appendix A, using a more sophisticated model, shown in Fig. 3.2, for the CCII which includes the effect of the parasitic resistance that appears at port X, voltage and current tracking error and the poles of the CCIIs. As shown in Appendix A, the deviation between practical results and theoretical results are due mainly to the R_{x1} and the pole of the current conveyor (R_z and C_z). It must also be mentioned that the stray capacitance may affect the operation of the circuit for the discrete implementation. Thus, designing this filter in integrated form will improve the accuracy of the results.

Table 3.2 shows a comparison between the proposed filter and Celma's universal filter [36] which is the only proposed one in the literature using unity gain cells. Comparison shows that the proposed filter uses same number of active devices and less number passive elements to achieve all of the feature of the previously published universal filter. The big advantage of the proposed universal filer over the previous filter is the ability of realizing all of the five responses i.e. lowpass, bandpass, highpass, notch and allpass response without changing the circuit typology.

	Celma Universal filter [36]1995	Proposed Universal Filter in Fig 3.1
No. of active elements	Three current and voltage follower & additional current follower to sense the output	Three current and voltage follower & additional current follower to sense the output
No. of passive elements	7-Resistor 3-Capacitor	6-Resistor 2-Capacitor
No. of input and output	Single input Single output	Three inputs One output
It can realize lowpass, bandpass and highpass without changing the circuit typology	No	Yes
Does not require additional active or passive element to realize notch and allpass response	No	Yes

Table 3.2 Comparison between Celma's universal filter and the proposed current-mode universal filter
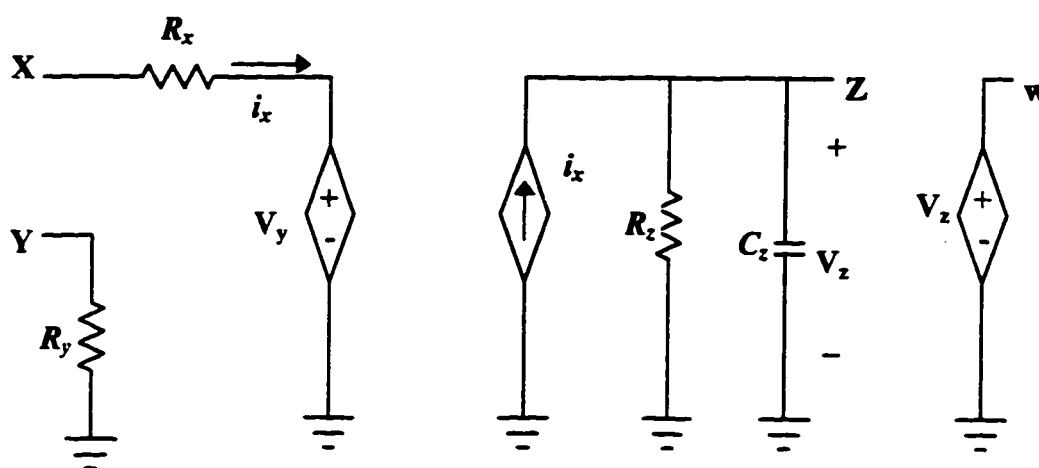
Fig. 3.2 Model of the negative-type current-conveyor CCII- which can be converted into CF- by grounding terminal Y. The VCVS V_z simulates the unity-gain voltage follower. $R_x=50\Omega$, $R_y=10Meg\Omega$, $R_z=3Meg\Omega$, $C_z=4.5PF$.
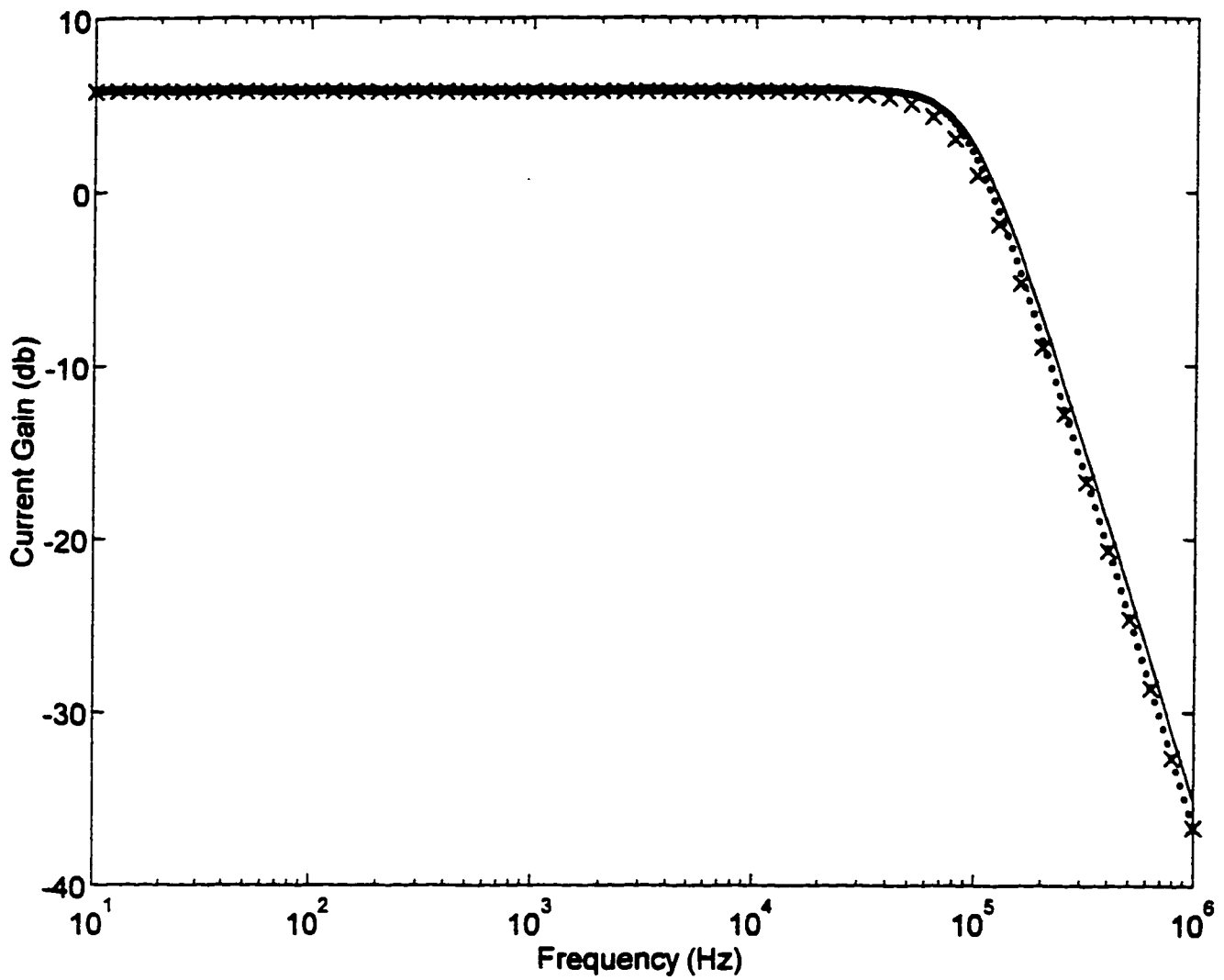
- Theoretical
o simulation
x Experimental

Fig. 3.3 (a) The lowpass response with
$R_1=R_2=R=1 \ k\Omega, \ R_3=R_4=R_5=2k\Omega$
$C_1=C_2 =1.2nF$
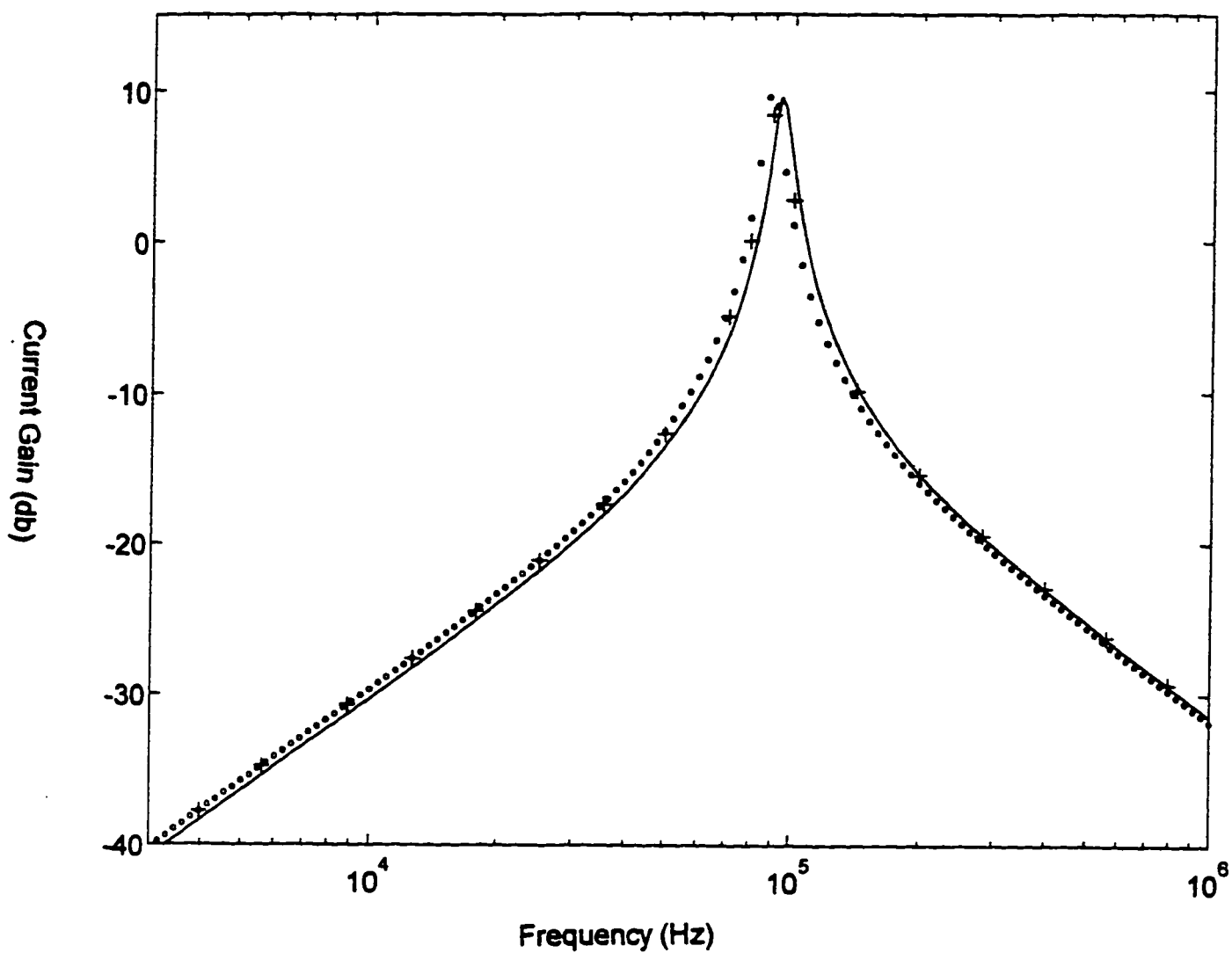
- Theoretical
o simulation
+ Experimental

Fig. 3.3 (b) The bandpass response with
$R_1 = 1\ k\Omega,\ R_3 = R_4 = R_5 = 2k\Omega,\ R_2 = 15\ k\Omega,$
$R = 5k\Omega,\ C_1 = C_2 = 1.2nF$
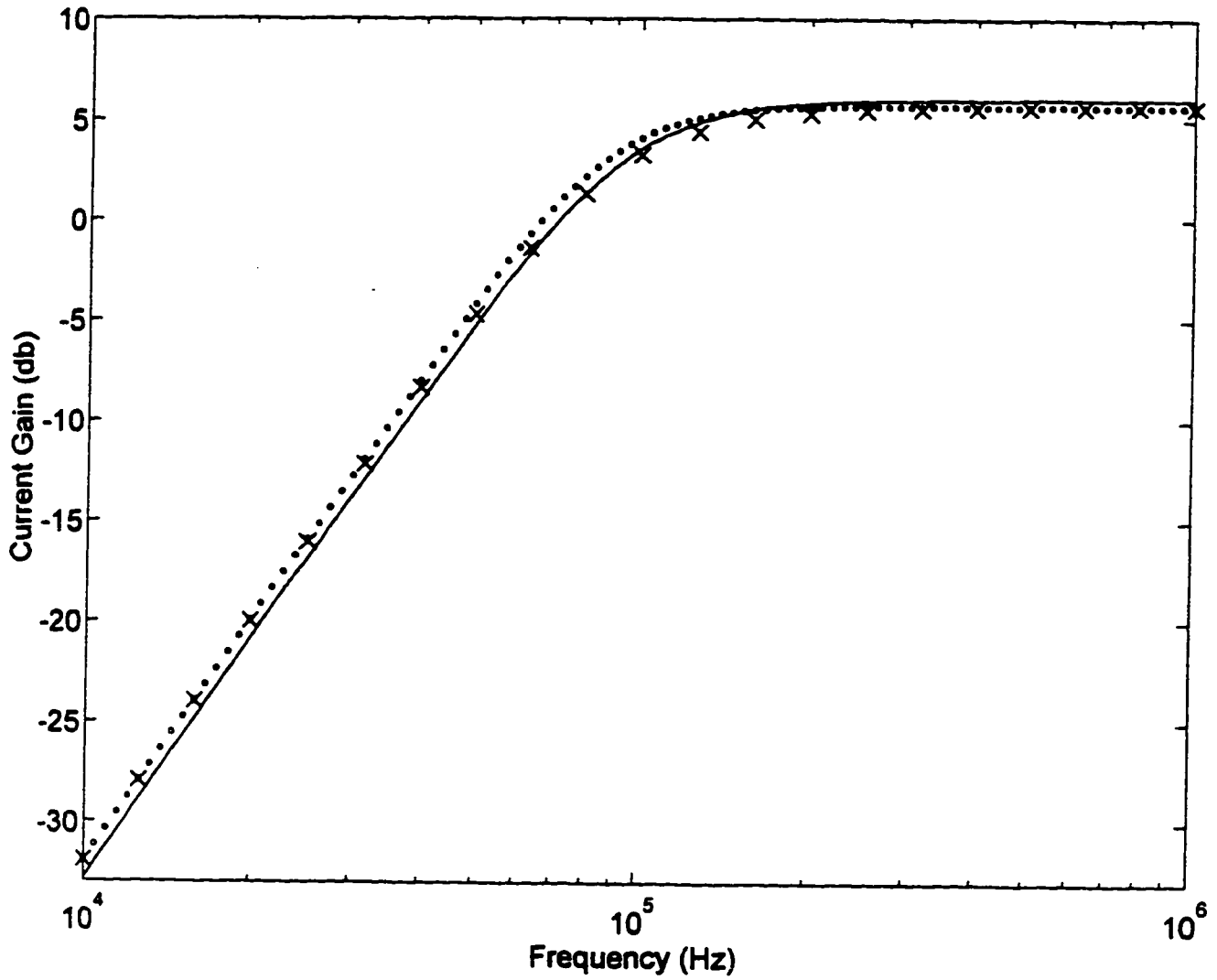
- Theoretical
o simulation
x Experimental

Fig. 3.3 (c) The highpass response with
$R_1 = R_2 = R = 1 \ k\Omega, \ R_3 = R_4 = R_5 = 2k\Omega$
$C_1 = C_2 = 1.2nF$
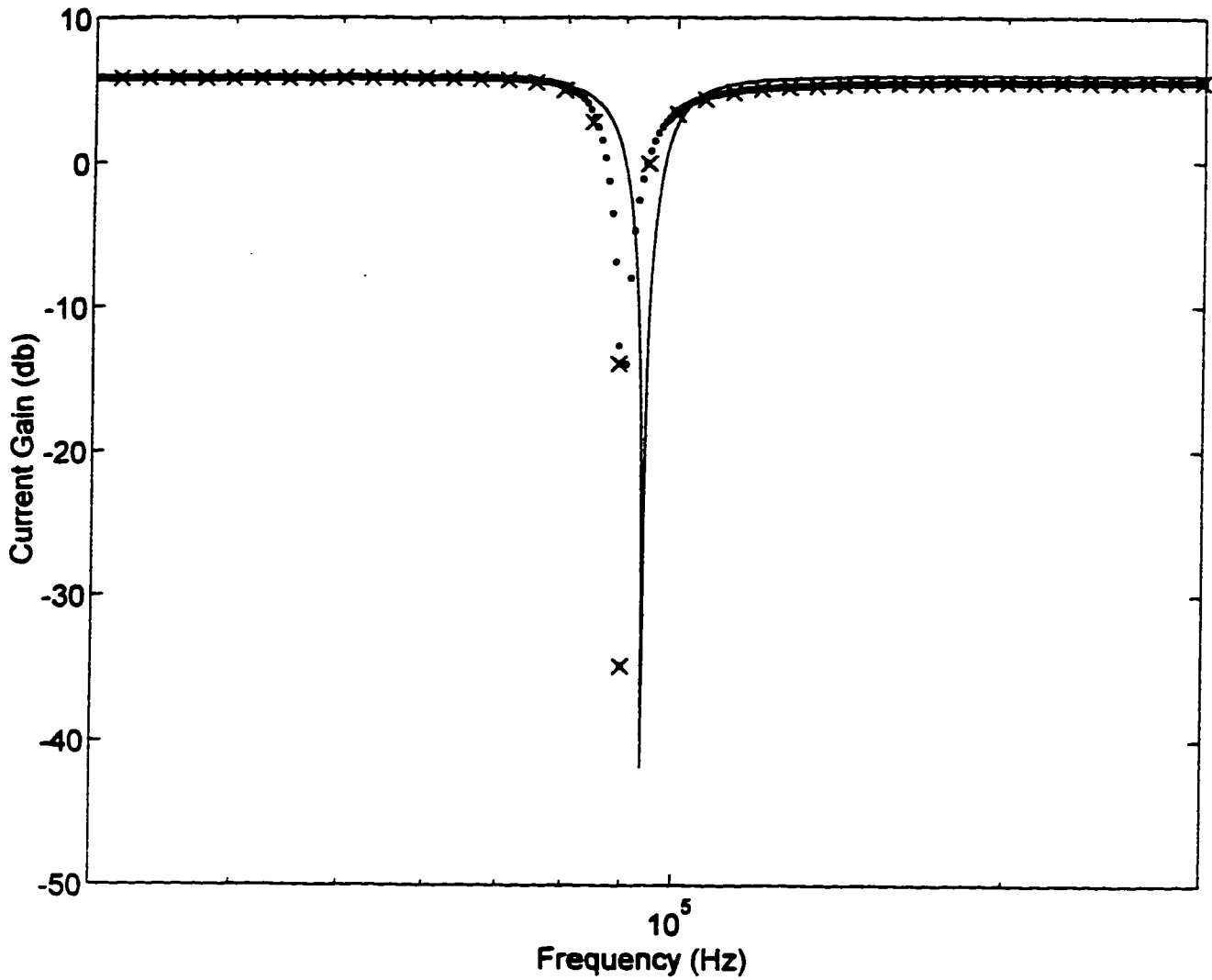
- Theoretical
o simulation
x Experimental

Fig. 3.3 (d) The notch (bandreject)
response with
$R_1= R=1\ k\Omega,\ R_3=R_4=R_5=2k\Omega,\ R_2=10\ k\ \Omega$
$C_1=C_2=1.2nF$
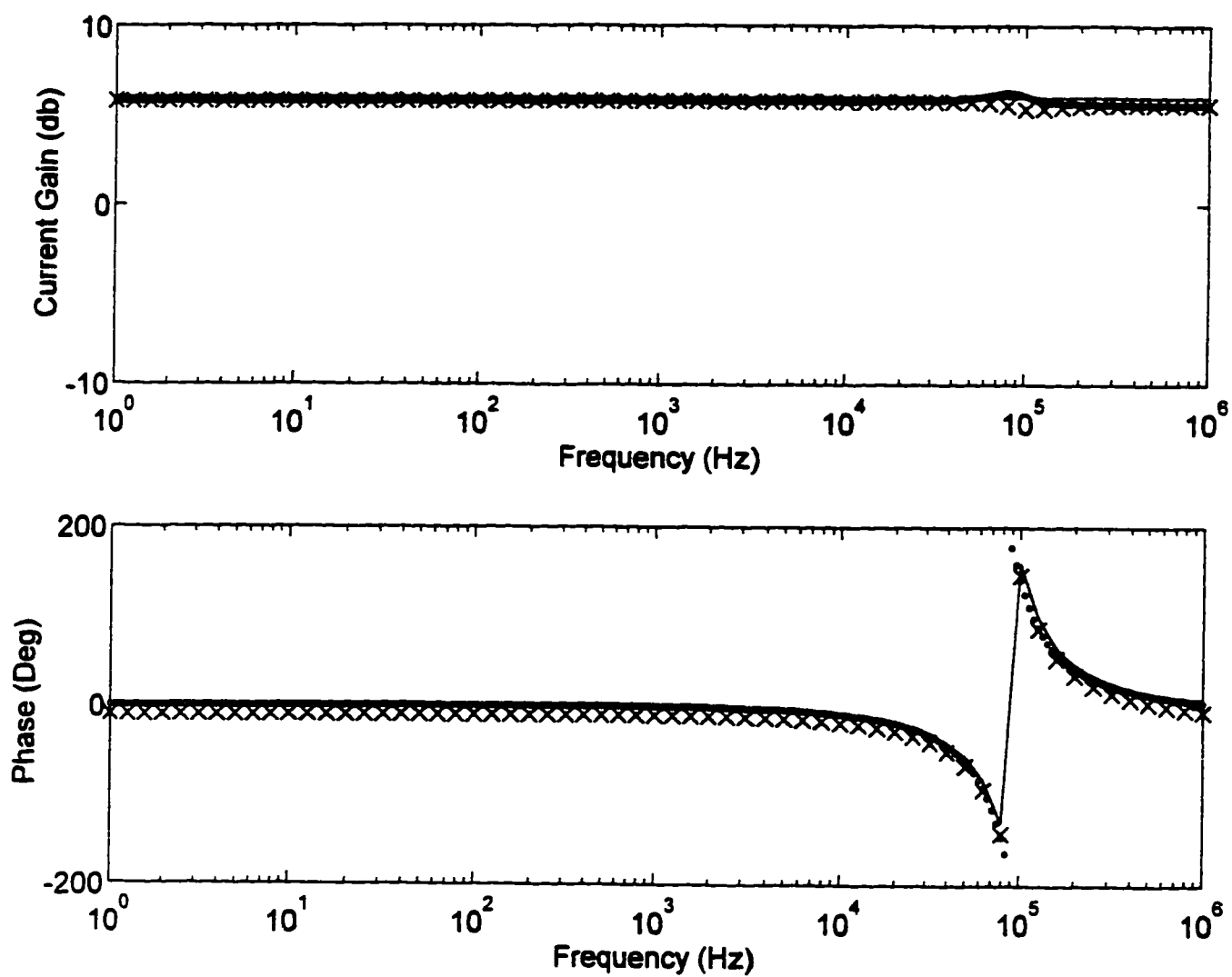
- Theoretical
o simulation
x Experimental

Fig. 3.3 (e) The magnitude and the phase
of the allpass response with
$R_1 = R = 1 \ k\Omega, \ R_2 = R_3 = R_4 = R_5 = 2k\Omega,$
$C_1 = C_2 = 1.2nF$

3.3 Universal Current-mode Single Input – Multiple Outputs Filter

The previous proposed universal filter can realize one function at a time by controlling the input current. In this section, a new universal current-mode filter with one input and three outputs which can simultaneously realize lowpass, bandpass and highpass responses will be presented. The circuit can also realize notch and allpass responses without using additional active or passive elements. The proposed filter enjoys high output impedance, low input impedance, independent tuning of the parameters ω_0 and ω_0/Q_0, employment of grounded capacitors which pave the way for high frequency operation and low active and passive sensitivities [62].

3.3.1 Proposed Circuit

The proposed circuit is shown in Fig. 3.4. Using standard notations of the two output current-follower CF and the unity gain voltage follower, routine analysis yields the current transfer functions
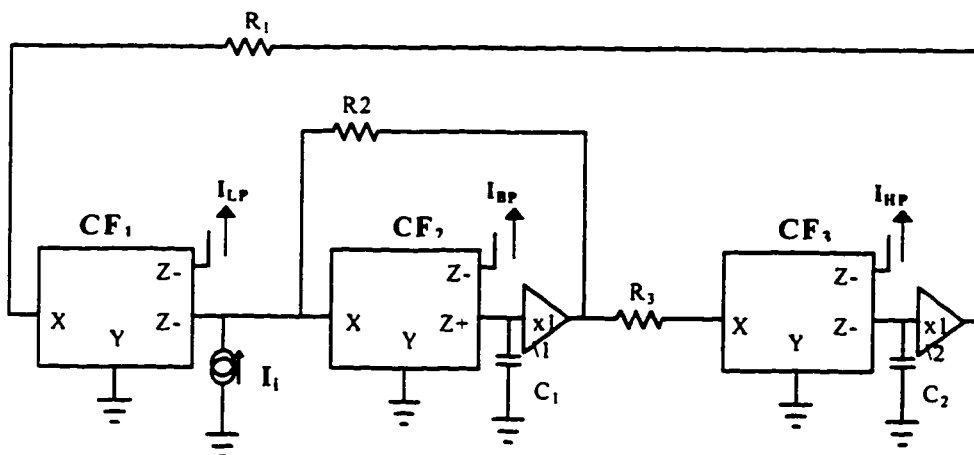
Fig 3.4 Proposed universal current-mode filter with single input and three outputs

$$\frac{I_{HP}}{I_i} = \frac{-\beta_1 s^2}{s^2 + s\frac{\alpha_2 \beta_1 \beta_2}{C_1 R_2} + \frac{\alpha_1 \alpha_2 \alpha_3 \beta_1 \beta_2}{C_1 C_2 R_1 R_3}} \qquad (3.7)$$

$$\frac{I_{LP}}{I_i} = \frac{-\frac{\alpha_2 \alpha_3 \beta_1 \beta_2}{C_1 C_2 R_1 R_3}}{s^2 + s\frac{\alpha_2 \beta_1 \beta_2}{C_1 R_2} + \frac{\alpha_1 \alpha_2 \alpha_3 \beta_1 \beta_2}{C_1 C_2 R_1 R_3}} \qquad (3.8)$$

$$\frac{I_{BP}}{I_i} = \frac{s\frac{\alpha_2 \beta_1}{C_1 R_3}}{s^2 + s\frac{\alpha_2 \beta_1 \beta_2}{C_1 R_2} + \frac{\alpha_1 \alpha_2 \alpha_3 \beta_1 \beta_2}{C_1 C_2 \ R_1 R_3}} \qquad (3.9)$$

From equations (3.7-3.9) the parameters ω_0 and ω_o/Q_o can be expressed as

$$\omega_o^2 = \frac{\alpha_1 \alpha_2 \alpha_3 \beta_1 \beta_2}{C_1 C_2 R_1 R_3} \qquad (3.10)$$

$$\frac{\omega_o}{Q_o} = \frac{\alpha_2 \beta_1 \beta_2}{C_1 R_2} \qquad (3.11)$$

From (3.7)–(3.9) it can be seen that the lowpass dc gain and the high frequency gain

of the highpass are approximately equal to unity and the bandpass gain at ω_o equals

$$G_{BP} = \frac{R_2}{\beta_2 R_3}$$

(3.12)

From (3.7)–(3.9), it can also be seen that an inverting notch response can be realized by connecting the I_{HP} and I_{LP} output terminals. An inverting allpass response can be obtained by connecting I_{HP}, I_{BP} and I_{LP} output terminals provided that $R_3 = R_2$. Thus no additional current followers are required for realizing notch and allpass responses.

From (3.10)–(3.12) it can be seen that the parameter ω_0 can be adjusted by controlling the resistors R_1, R_3 and/or the capacitor C_2 without disturbing the parameter ω_0/Q_0. Moreover, the parameter ω_0/Q_0 can be adjusted by controlling the resistor R_2 without disturbing the parameter ω_0. However, controlling the resistance R_2 and/or R_3 will disturb the bandpass gain. A possible strategy for adjusting the parameters ω_0, ω_0/Q_0 and the bandpass gain, is therefore as follows: first the resistor R_2 is adjusted to control the parameter ω_0/Q_0 then the resistor R_3 is adjusted to control the bandpass gain; and finally the resistor R_1 is adjusted to control the parameters ω_0.

3.3.2 Sensitivity Analysis

Using (2.21), (3.10) and (3.11), the sensitivities of the proposed filter shown in Fig.3.4 were calculated and the results are shown in Table 3.3.

S	ω_o	Q_o
α_1	0.5	0.5
α_2	0.5	-0.5
α_3	0.5	0.5
β_1	0.5	-0.5
β_2	0.5	-0.5
C_1	-0.5	0.5
C_2	-0.5	-0.5
R_1	-0.5	-0.5
R_2	0.0	1
R_3	-0.5	-0.5

Table 3.3 The active and passive sensitivities of
the proposed filter in Fig.3.4

From Table 3.3, it is clear that the active and passive sensitivities are small.

3.3.3 Simulation Results and Discussion

The proposed circuit was simulated using Pspice. The simulation was performed using the modified version of Svoboda model [55] shown in Fig.3.5. Fig. 3.6 (a,b,c,d and e) show the theoretical and the simulation results obtained from the lowpass, bandpass, highpass, notch and allpass responses. It appears that the simulation

results are in fairly good agreement with the presented theory. However, it can be seen that there are some deviation between the theoretical, the simulation and the results that is due to the nonidealties of the active devices. The major source of the nonidealites is the parasitic resistance that appears at port X of the CF. We can take care of R_{x1} and R_{x3} by adding them in series to R_1, and R_3 respectively.

For values of the natural frequency (f_o)<60MHz, the deviation between the theoretical results and the simulation results is less than 3%.

For the gain, the deviation between the simulation and theoretical results can be summarized as follows:

1. the bandpass gain deviates by a percentage error less than 5%,

2. the highpass gain deviates by a percentage error less than 2% for f_o<100MHz,

3. the lowpass, notch and allpass gains deviate by a percentage error less than 1%, while the phase of the allpass responce deviates by a percentage error less than 4%.

Similar to circuit of Fig. 3.1, these errors are attributed to the effect of the parasitic resistance R_{x2} and the finite pole of the current conveyor (R_z and C_z).

Table 3.4 shows a comparison between the proposed filter and Celma's Universal filter [36]. Comparison shows that the proposed filter uses less number of active devices and passive elements to achieve all of the features of the previously published universal filter. However, the big advantage of the proposed filter is the ability of realizing lowpass, bandpass and highpass responses simultaneously. Also

notch and allpass responses can be achieved without using additional active or

passive elements.

	Celma Universal filter [36]1995	Proposed Universal Filter in Fig 3.4
No. of active elements	Three current and voltage follower & additional current follower to sense the output	Three dual output current follower and Three voltage follower
No. of passive elements	7-Resistor 3-Capacitor	3-Resistor 2-Capacitor
No. of input and output	Single input Single output	One input Three outputs
It can realize lowpass, bandpass and highpass without changing the circuit typology	No	Yes Simultaneously
Does not require additional active or passive element to realize notch and allpass response	No	Yes

Table 3.4 Comparison between Celma's universal filter and the proposed current-mode universal filter
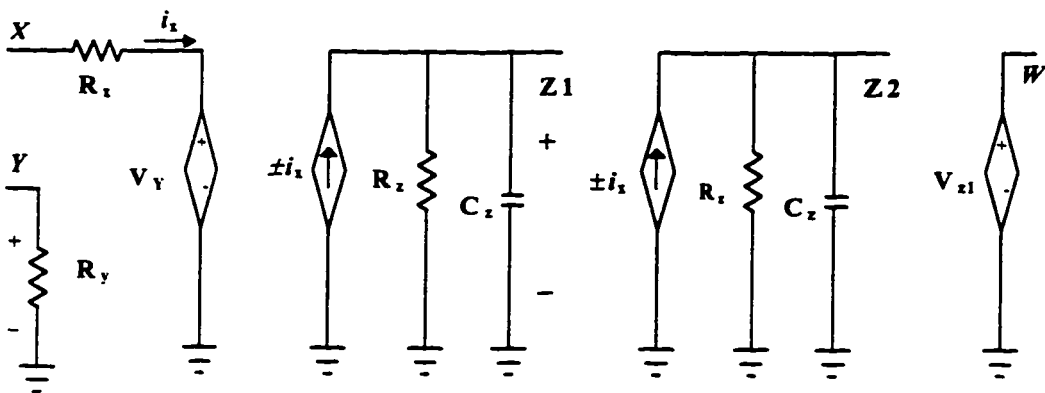
Fig. 3.5 Model of the dual outputs current-conveyor CCII which can be converted into dual output CF by grounding terminal Y. The VCVS V_{z1} simulates the unity-gain voltage follower. $R_x=50\Omega$, $R_y=10M\Omega$, $R_z=3M\Omega$, $C_z=4..5PF$
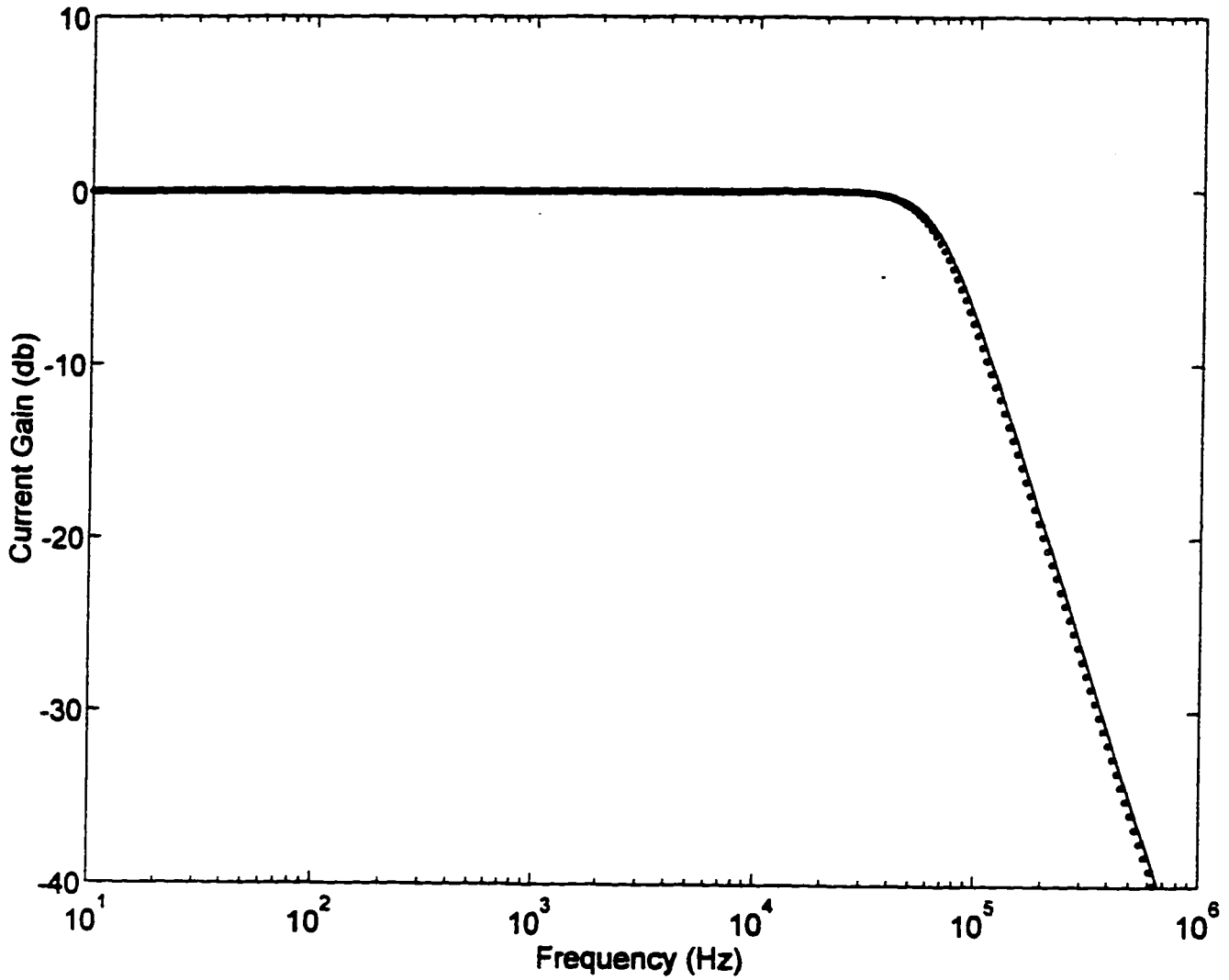
- Theoretical
o simulation

Fig. 3.6 (a) The lowpass response with
$R_1=R_3=2\ k\Omega,\ R_2=1.5k\Omega$
$C_1=C_2=1.2nF$
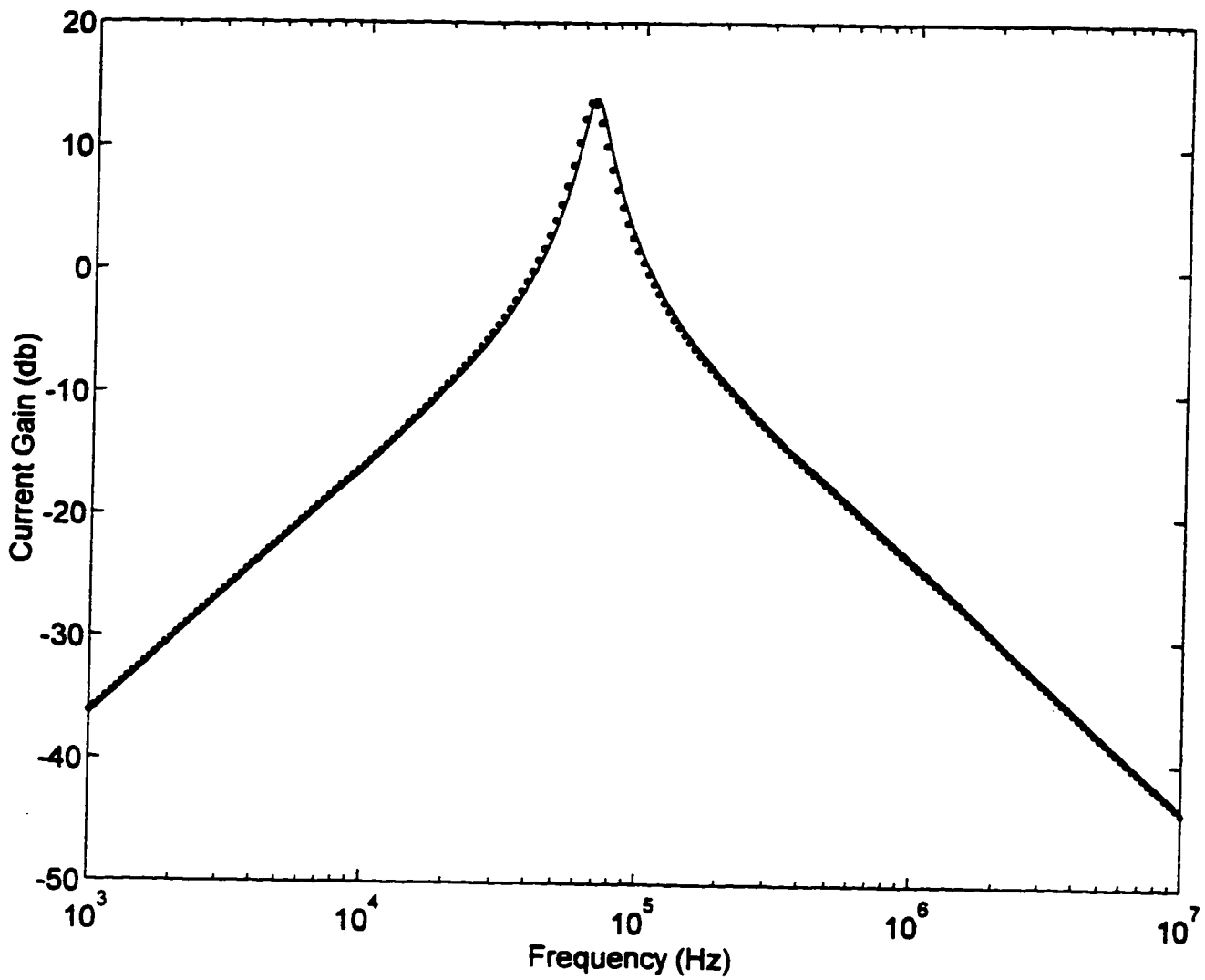
- Theoretical
o simulation

Fig. 3.6 (b) The bandpass response with
$R_1 = R_3 = 2$ $k\Omega$, $R_2 = 10$ $k\Omega$,
$C_1 = C_2 = 1.2nF$
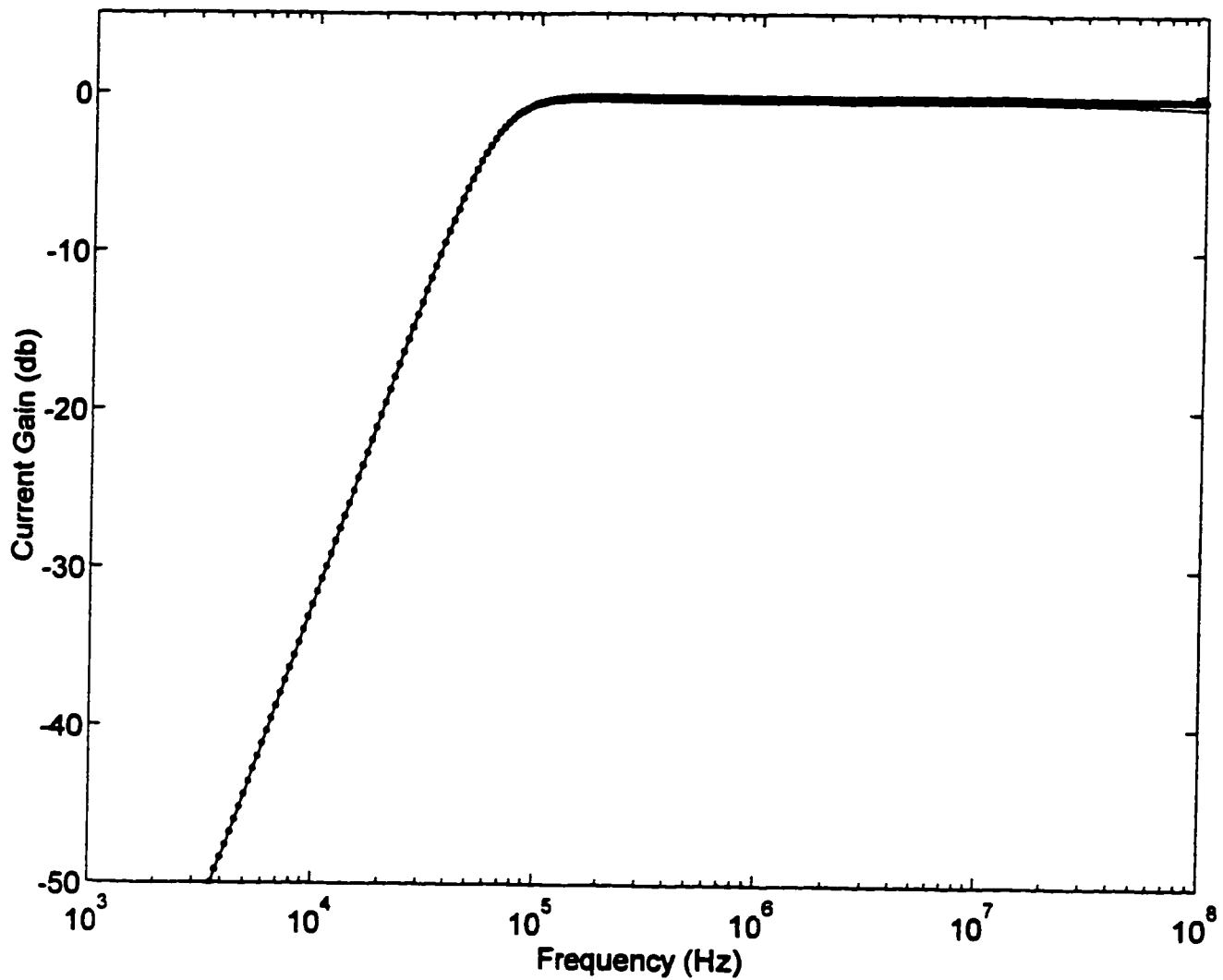
- Theoretical
o simulation
Fig. 3.6 (c) The highpass response with
$R_1 = R_3 = 2 \ k\Omega, \ R_2 = 1.5 \ k\Omega$
$C_1 = C_2 = 1.2nF$
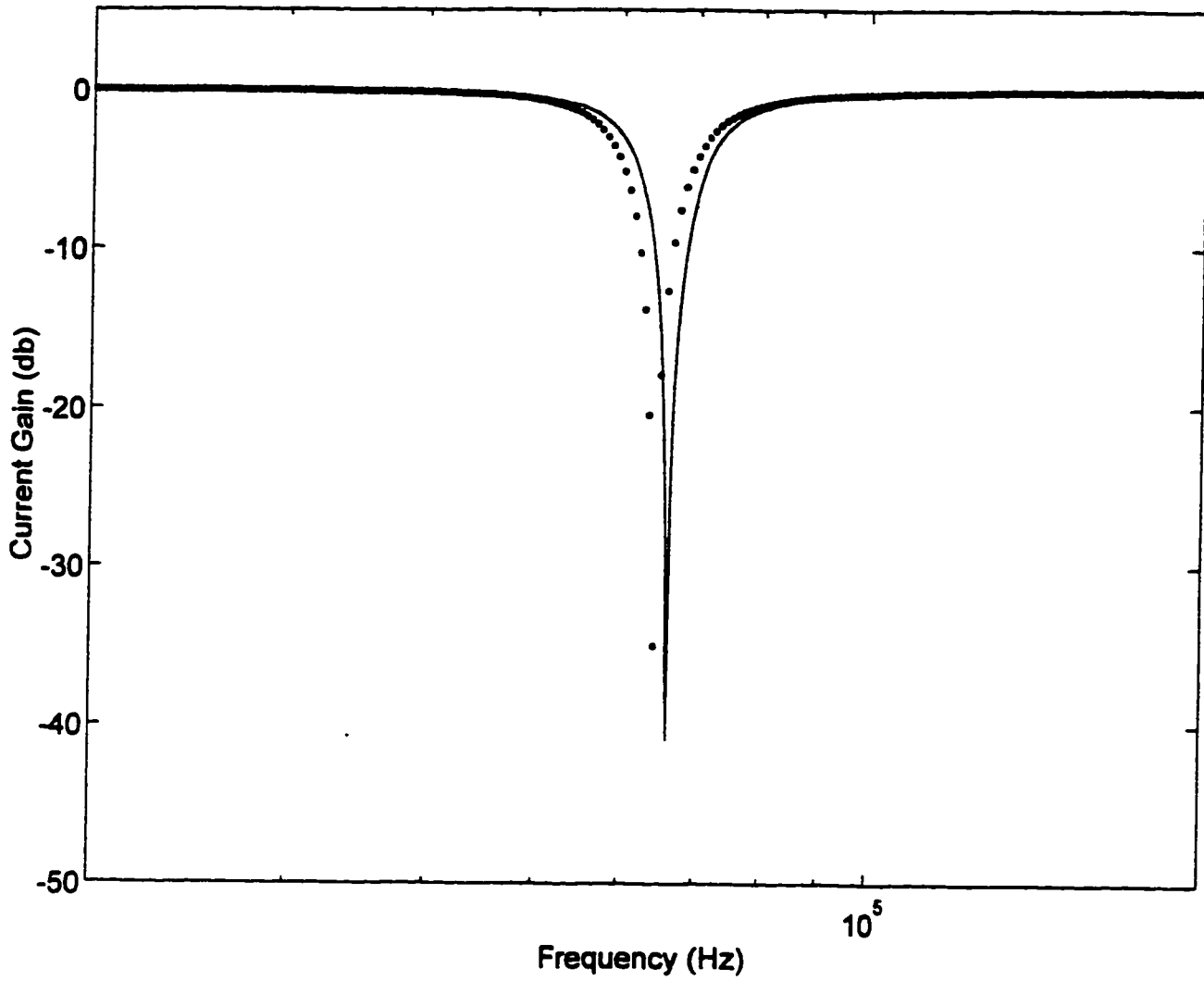
- Theoretical
o simulation

Fig. 3.6 (d) The notch (bandreject)
response with
$R_1 = R_3 = 2\ k\Omega,\ R_2 = 10\ k\ \Omega$
$C_1 = C_2 = 1.2nF$
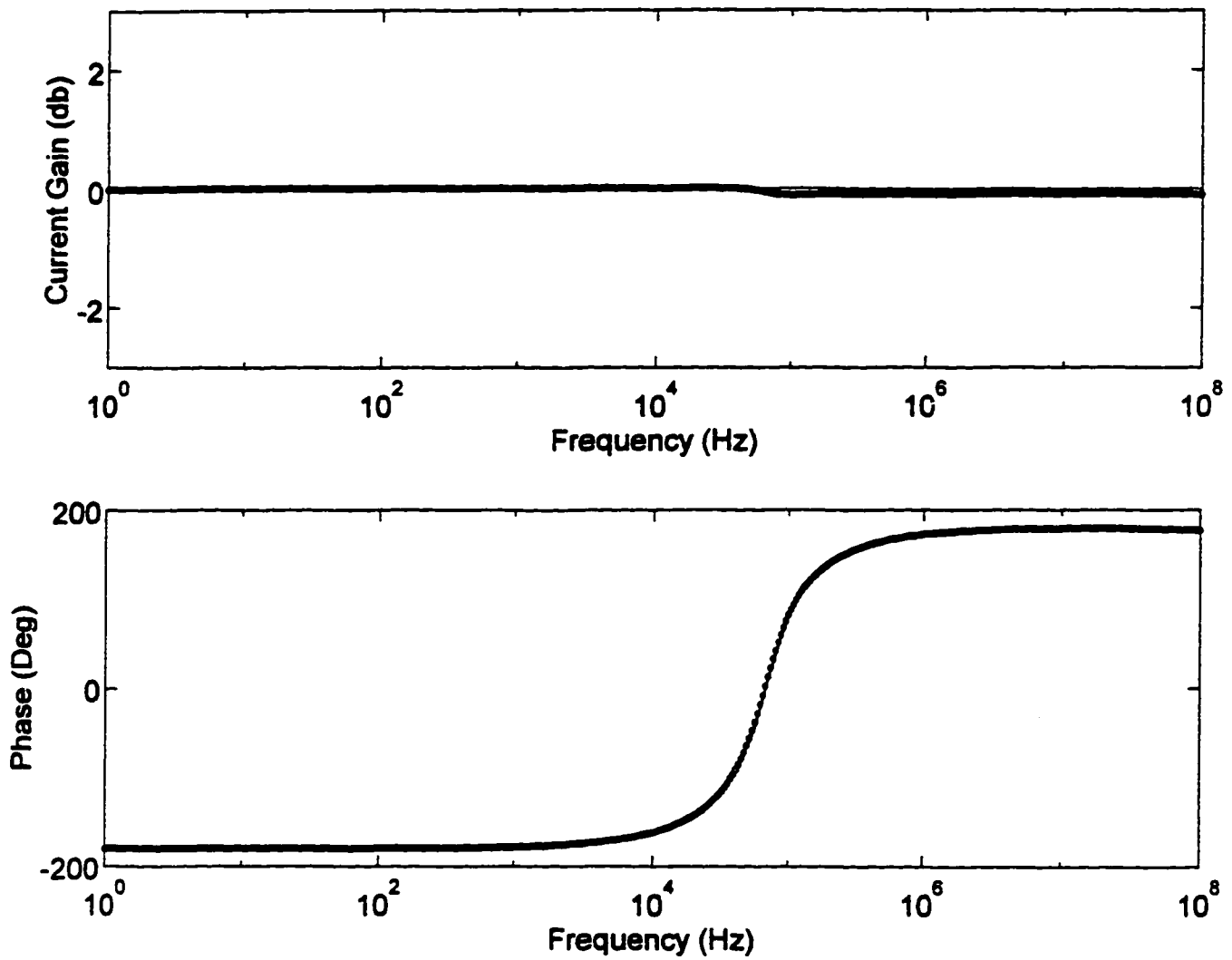
- Theoretical
o simulation

Fig. 3.6 (e) The magnitude and the phase
of the allpass response with
$R_1=R_2=R_3=2\ k\Omega,$
$C_1=C_2=1.2nF$

3.4 Voltage-mode Filter with Single Input and two Outputs

The previous proposed universal filters are current-mode filters. However, analog voltage-mode signal processing needs voltage-mode filters. In this regard, a new voltage-mode bandpass/lowpass filter using unity gain cells will be presented. It can simultaneously realize lowpass and bandpass responses. The proposed filter enjoys low output impedance, independent tuning of the parameters ω_0 and ω_0/Q_o, independent tuning of the lowpass and bandpass responses gains without changing ω_0 and ω_0/Q_o, employment of grounded capacitors and low active and passive sensitivities.

3.4.1 Proposed Circuit

The proposed circuit is shown in Fig. 3.7. Using the standard notations of the current-follower CF± and the unity gain voltage follower, routine analysis yields the voltage transfer functions:
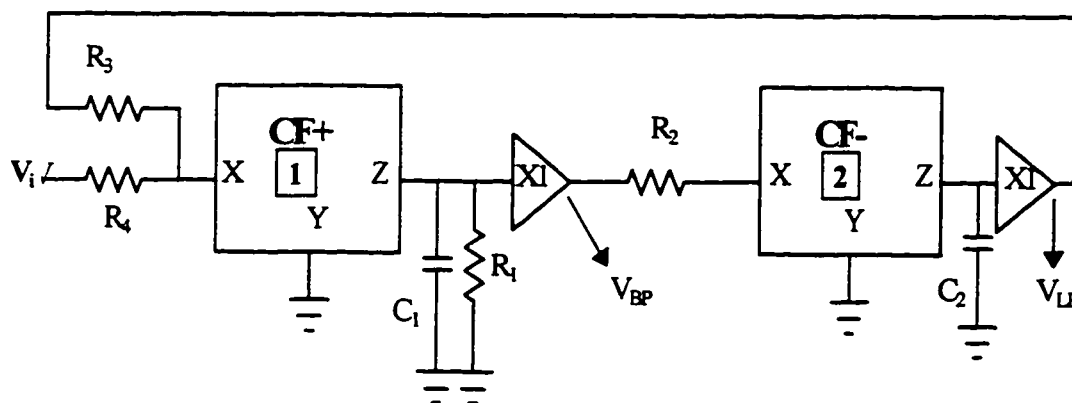
Fig 3.7 Proposed bandpass/lowpass filter voltage-mode filter with single input and two outputs

$$\frac{V_{BP}}{Vi} = \frac{-s\dfrac{\alpha_1}{C_1 R_4}}{s^2 + \dfrac{s}{C_1 R_1} + \dfrac{\alpha_1 \alpha_2 \beta_1 \beta_2}{C_1 C_2 R_2 R_3}} \qquad (3.14)$$

From (3.13) and (3.14) the parameters ω_0 and ω_0/Q_0 can be expressed as

$$\omega_o^2 = \frac{\alpha_1 \alpha_2 \beta_1 \beta_2}{C_1 C_2 R_2 R_3} \qquad (3.15)$$

$$\frac{\omega_o}{Q_o} = \frac{1}{C_1 R_1} \qquad (3.16)$$

From (3.15) and (3.16) it can be seen that the lowpass dc gain and the bandpass gain at ω_0 are equal to

$$G_{LP} = \frac{R_3}{R_4} \qquad (3.17)$$

$$G_{BP} = \frac{\alpha_1 R_1}{R_4} \qquad (3.18)$$

From (3.15)–(3.18) it can be seen that the parameter ω_0 can be adjusted by controlling the resistors R_2, R_3 and/or the capacitor C_2 without disturbing the parameter ω_0/Q_0. Moreover, the parameter ω_0/Q_0 can be adjusted by controlling the resistor R_1 without disturbing the parameter ω_0. However, controlling the resistance R_1 and/or R_3 will disturb the bandpass and/or the lowpass gain. A possible strategy

for adjusting the parameters ω_o, ω_o/Q_o, the lowpass and the bandpass gains, is therefore as follows: first the resistor R_1 is adjusted to control the parameter ω_o/Q_o then the resistor R_4 is adjusted to control the bandpass gain, the resistor R_3 is adjusted to control the lowpass gain and finally the resistor R_2 is adjusted to control the parameters ω_o.

3.4.2 Sensitivity Analysis

Using (2.21), (3.15) and (3.16), the sensitivities of the proposed filter shown in Fig.3.7 were calculated and the results are shown in Table 3.5.

S	ω_o	Q_o
α_1	0.5	0.5
α_2	0.5	0.5
β_1	0.5	0.5
β_2	0.5	0.5
C_1	-0.5	0.5
C_2	-0.5	-0.5
R_1	0.0	1.0
R_2	-0.5	-0.5
R_3	-0.5	-0.5

Table 3.5 The active and passive sensitivities of
the proposed filter in Fig.3.7

From Table 3.5, it is clear that the active and passive sensitivities are small

3.4.3 Simulation and Experimental Results and Discussion

The proposed circuit was tested experimentally using the AD844. The circuit was also simulated using Pspice. The simulation was performed using the model of AD844 proposed by Svoboda [55] shown in Fig.3.2. Fig. 3.8 (a,b,c,d and e) show the simulation and the experimental results obtained from the lowpass, bandpass, highpass, notch and allpass responses. It appears that the simulation and the experimental results are in fairly good agreement with the presented theory. However, it can be seen that there are some deviation between the theoretical, the simulation and the experimental results that is due to the nonidealties of the active devices. The major source of the nonidealites is the parasitic resistance that appears at port X of the CF. We can take care of R_{x2} by adding it in series to R_2.

For the natural frequency (ω_o) the deviation between the theoretical, simulation and experimental results is less than 5%.

For the gain, the deviations between the theoretical, simulation and experimental results can be summarized as follows:

1. the bandpass gain deviates by a percentage error less than 6%,

2. the lowpass gain deviates by a percentage error less than 2%,

Similar to circuit of Fig. 3.1, these errors are attributed to the effect of the parasitic resistance R_{x1} and the finite pole of the current conveyor (R_z and C_z).

Table 3.6 shows a comparison between the proposed filter and Celma's universal

voltage-mode filter [36]. Comparison shows that the proposed filter has the ability

to simultaneously realize lowpass and bandpass responses while Celma's filter can't

do that. The proposed filter uses less number of active devices and passive elements.

However, It can't realize the highpass response.

	Celma Universal filter [36]1995	Proposed Universal Filter in Fig 3.7
No. of active elements	Three current and voltage follower	Two current and voltage follower
No. of passive elements	7-Resistor 3-Capacitor	4-Resistor 2-Capacitor
No. of input and output	Single input Single output	One input Two outputs
It can realize lowpass, bandpass and highpass without changing the circuit typology	No	Yes, it can simultaneously realize lowpass and bandpass.

Table 3.6 Comparison between Celma's universal filter and the proposed voltage-mode lowpass/bandpass filter
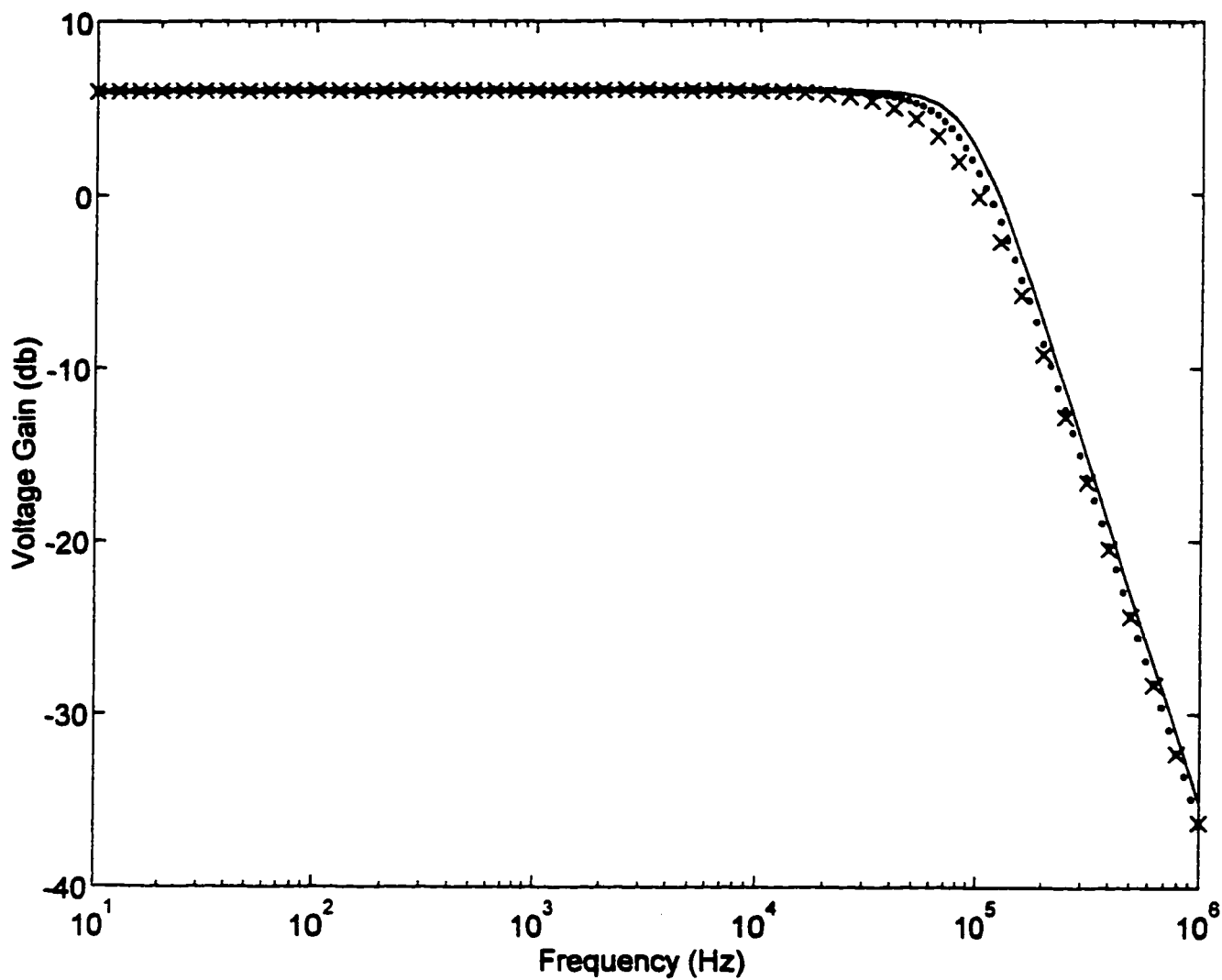
- Theoretical
o Simulation
x Experimental

Fig. 3.8 (a) The lowpass response with
$R_1 = R_2 = R_4 = 1\ k\Omega,\ R_3 = 2k\Omega$
$C_1 = C_2 = 1.2nF$
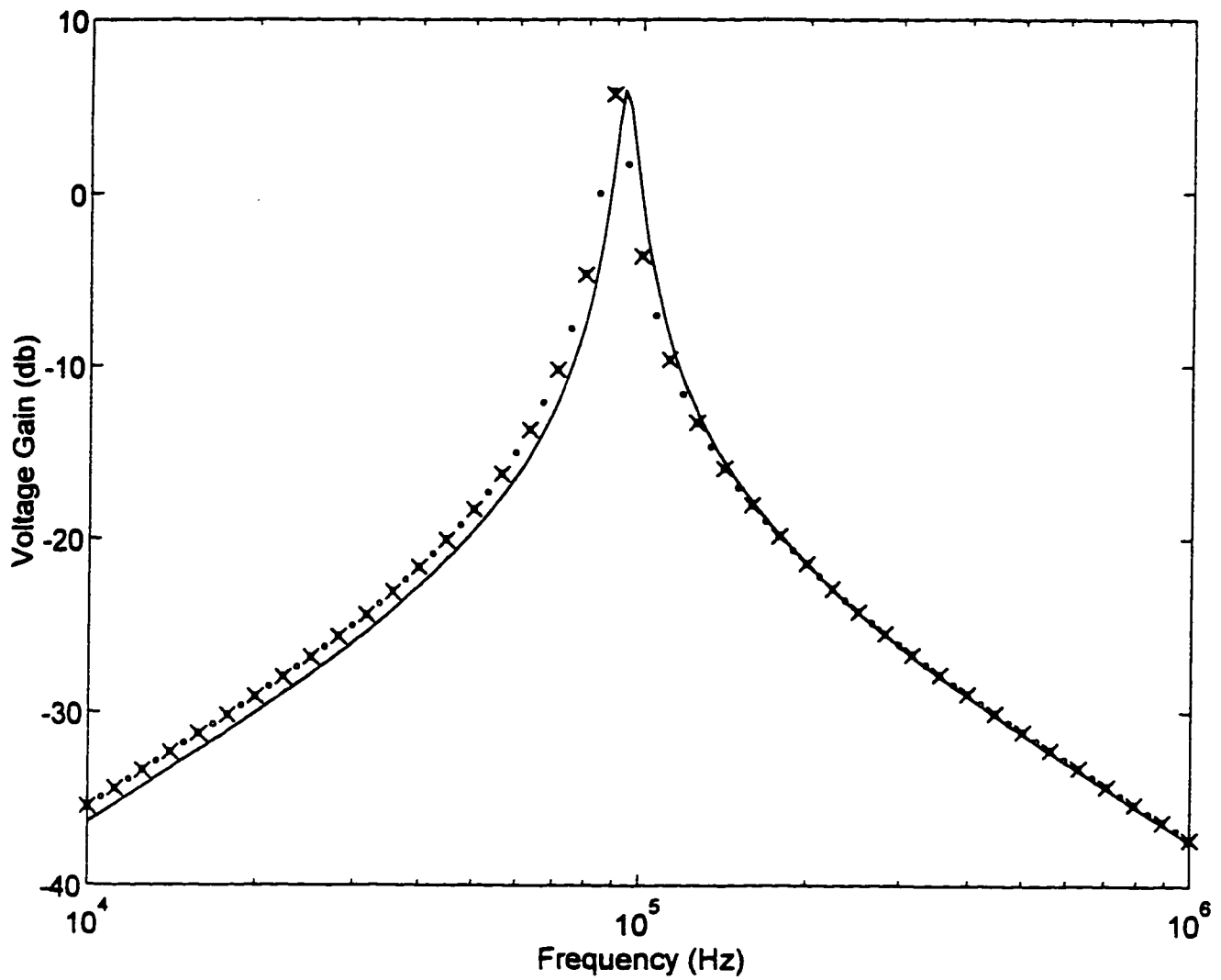
- Theoretical
o Simulation
x Experimental

Fig. 3.8 (b) The bandpass response with
$R_1=20\ k\Omega$, $R_2=1\ k\Omega$, $R_3=2\ k\Omega$, $R_4=10k$
$C_1=C_2=1.2nF$

3.5 Voltage-mode Filter with Single Input and Three Outputs

The previous voltage-mode filter can realize lowpass and bandpass responses only. A new voltage-mode universal filter with single input and three outputs which can simultaneously realize lowpass, bandpass and highness responses will be presented. The proposed filter enjoys low output impedance, independent tuning of the parameters ω_o and ω_o/Q_o, independent tuning of the lowpass, bandpass and highpass responses gains without disturbing ω_o and ω_o/Q_o, employment of grounded capacitors and low active and passive sensitivities.

3.5.1 Proposed Circuit

The proposed circuit is shown in Fig. 3.9. Using the standard notations of the current-follower CF± and the unity gain voltage follower, routine analysis yields the voltage transfer functions:
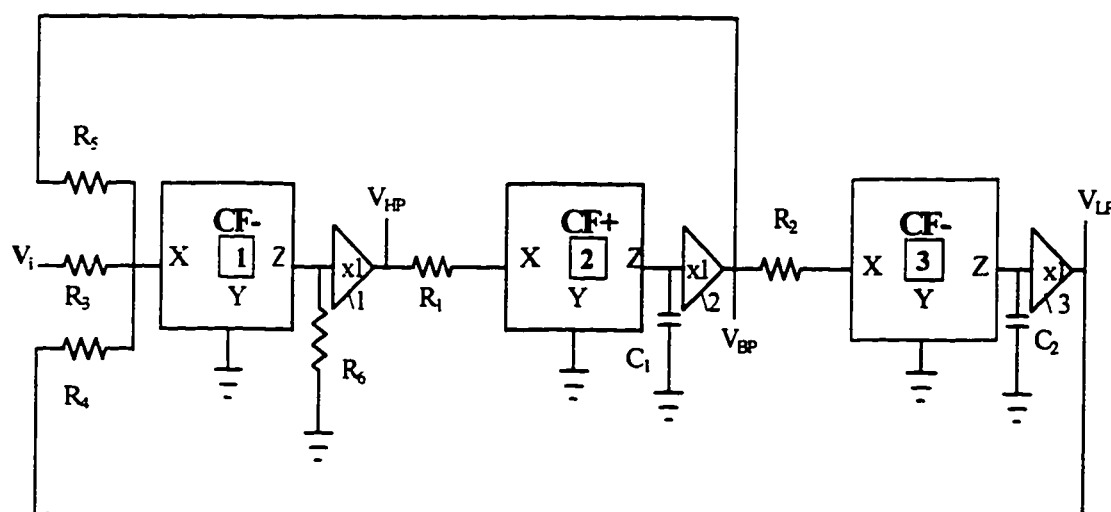

Fig 3.9 Proposed universal voltage-mode filter with single input and three outputs

$$\frac{V_{LP}}{Vi} = \frac{-\dfrac{\alpha_1 \alpha_2 \alpha_3 \beta_1 \beta_2 \beta_3 R_6}{C_1 C_2 R_1 R_2 R_3}}{s^2 + s\dfrac{\alpha_1 \alpha_2 \beta_1 \beta_2 R_6}{C_1 R_1 R_4} + \dfrac{\alpha_1 \alpha_2 \alpha_3 \beta_1 \beta_2 \beta_3 R_6}{C_1 C_2 R_1 R_2 R_5}} \qquad (3.19)$$

$$\frac{V_{BP}}{Vi} = \frac{-s\dfrac{\alpha_1 \alpha_2 \beta_1 \beta_2 R_6}{C_1 R_1 R_3}}{s^2 + s\dfrac{\alpha_1 \alpha_2 \beta_1 \beta_2 R_6}{C_1 R_1 R_4} + \dfrac{\alpha_1 \alpha_2 \alpha_3 \beta_1 \beta_2 \beta_3 R_6}{C_1 C_2 R_1 R_2 R_5}} \qquad (3.20)$$

$$\frac{V_{HP}}{Vi} = \frac{s^2\dfrac{\alpha_1 \beta_1 R_6}{R_3}}{s^2 + s\dfrac{\alpha_1 \alpha_2 \beta_1 \beta_2 R_6}{C_1 R_1 R_4} + \dfrac{\alpha_1 \alpha_2 \alpha_3 \beta_1 \beta_2 \beta_3 R_6}{C_1 C_2 R_1 R_2 R_5}} \qquad (3.21)$$

From (3.19)–(3.21) the parameters ω_0 and ω_0/Q_0 can be expressed as

$$\omega_o^2 = \frac{\alpha_1 \alpha_2 \alpha_3 \beta_1 \beta_2 \beta_3 R_6}{C_1 C_2 R_1 R_2 R_5} \qquad (3.22)$$

$$\frac{\omega_o}{Q_o} = \frac{\alpha_1 \alpha_2 \beta_1 \beta_2 R_6}{C_1 R_1 R_4} \qquad (3.23)$$

From (3.19)–(3.21) it can be seen that the lowpass dc gain, the high frequency gain of the highpass and the bandpass gain at ω_0 are equal to

$$G_{\mathrm{LP}} = \frac{R_5}{R_3} \qquad\qquad (3.24)$$

$$G_{\mathrm{HP}} = \frac{\alpha_1 \beta_1 R_6}{R_3} \qquad\qquad (3.25)$$

$$G_{\mathrm{BP}} = \frac{R_4}{R_3} \qquad\qquad (3.26)$$

From (3.15)–(3.26) it can be seen that the parameter ω_0 can be adjusted by controlling the resistors R_2, R_3 and/or the capacitor C_2 without disturbing the parameter ω_o/Q_o. Moreover, the parameter ω_o/Q_o can be adjusted by controlling the resistor R_1 without disturbing the parameter ω_o. However, controlling the resistance R_1 and/or R_3 will disturb the bandpass and/or the lowpass gain. A possible strategy for adjusting the parameters ω_0, ω_o/Q_o, the lowpass and the bandpass gains, is therefore as follows: first the resistor R_1 is adjusted to control the parameter ω_o/Q_o then the resistor R_4 is adjusted to control the bandpass gain, the resistor R_3 is adjusted to control the lowpass gain and finally the resistor R_2 is adjusted to control the parameters ω_0.

3.5.2 Sensitivity Analysis

Using (2.21), (3.22) and (3.23), the sensitivities of the proposed filter shown in Fig.3.9 were calculated and the results are shown in Table 3.7.

S	ω_o	Q_o
α_1	0.5	-0.5
α_2	0.5	-0.5
α_3	0.5	0.5
β_1	0.5	-0.5
β_2	0.5	-0.5
β_3	0.5	0.5
C_1	-0.5	0.5
C_2	-0.5	-0.5
R_1	-0.5	0.5
R_2	-0.5	-0.5
R_3	0.0	0.0
R_4	0.0	1
R_5	-0.5	-0.5
R_6	0.5	-0.5

Table 3.7 The active and passive sensitivities of the proposed filter in Fig.3.9

From Table 3.7, it is clear that the active and passive sensitivities are small

3.5.3 Simulation and Experimental Results

The proposed circuit was tested experimentally using the AD844. The circuit was also simulated using Pspice. The simulation was performed using the model of AD844 proposed by Svoboda [55] shown in Fig.3.2. Fig. 3.10 (a,b,c,d and e) show the simulation and the experimental results obtained from the lowpass, bandpass, highpass, notch and allpass filters. It appears that the simulation and experimental results are in good agreement with the theory presented. However, it can be seen that there are some deviation between the theoretical, the simulation and the experimental results that is due to the nonidealties of the active devices. The major source of the nonidealites is the parasitic resistance appears at port X of the CF. We can take care of R_{x2} and R_{x3} by adding them in series to R_1 and R_2 respectively.

For the natural frequency (ω_o) the deviation between the theoretical, simulation and experimental results is less than 5%.

For the gain the deviation between the theoretical, simulation and experimental results can be summarized as follows:

1. the lowpass gain deviates by a percentage error less than 3% due to the effect of the parasitic resistance R_{x1}.

2. the bandpass gain deviates by a percentage error less than 4% due to the effect of the parasitic resistance R_{x1}.

3. the highpass gain deviates by a percentage error of less than 7% for frequencies<2MHz.

Similar to circuit of Fig. 3.1, these errors are attributed to the effect of the parasitic resistance R_{x1} and the finite pole of the current conveyor (R_z and C_z).

Table 3.8 shows a comparison between the proposed filter and Celma's universal voltage-mode filter [36]. Comparison shows that using the same number of active devices and less number of passive elements the proposed universal filter has all of the features of the previously published universal filter. The big advantage of the proposed universal filer over the previously published filter is the ability of realizing lowpass, bandpass and highpass simultaneously.

	S. Celma Universal filter [36]1995	Proposed Universal Filter in Fig 3.9
No. of active elements	Three current and voltage follower	Three current and voltage follower
No. of passive elements	7-Resistor 3-Capacitor	6-Resistor 2-Capacitor
No. of input and output	Single input Single output	One input Three outputs
It can realize lowpass, bandpass and highpass without changing the circuit typology	No	Yes, it can simultaneously realize lowpass, bandpass and highpass.

Table 3.8 Comparison between S. Celma's universal filter and the proposed voltage-mode universal active filters

Voltage Gain (db)

10

0

-10

-20

-30

-40

10^1 10^2 10^3 10^4 10^5 10^6

Frequency (Hz)
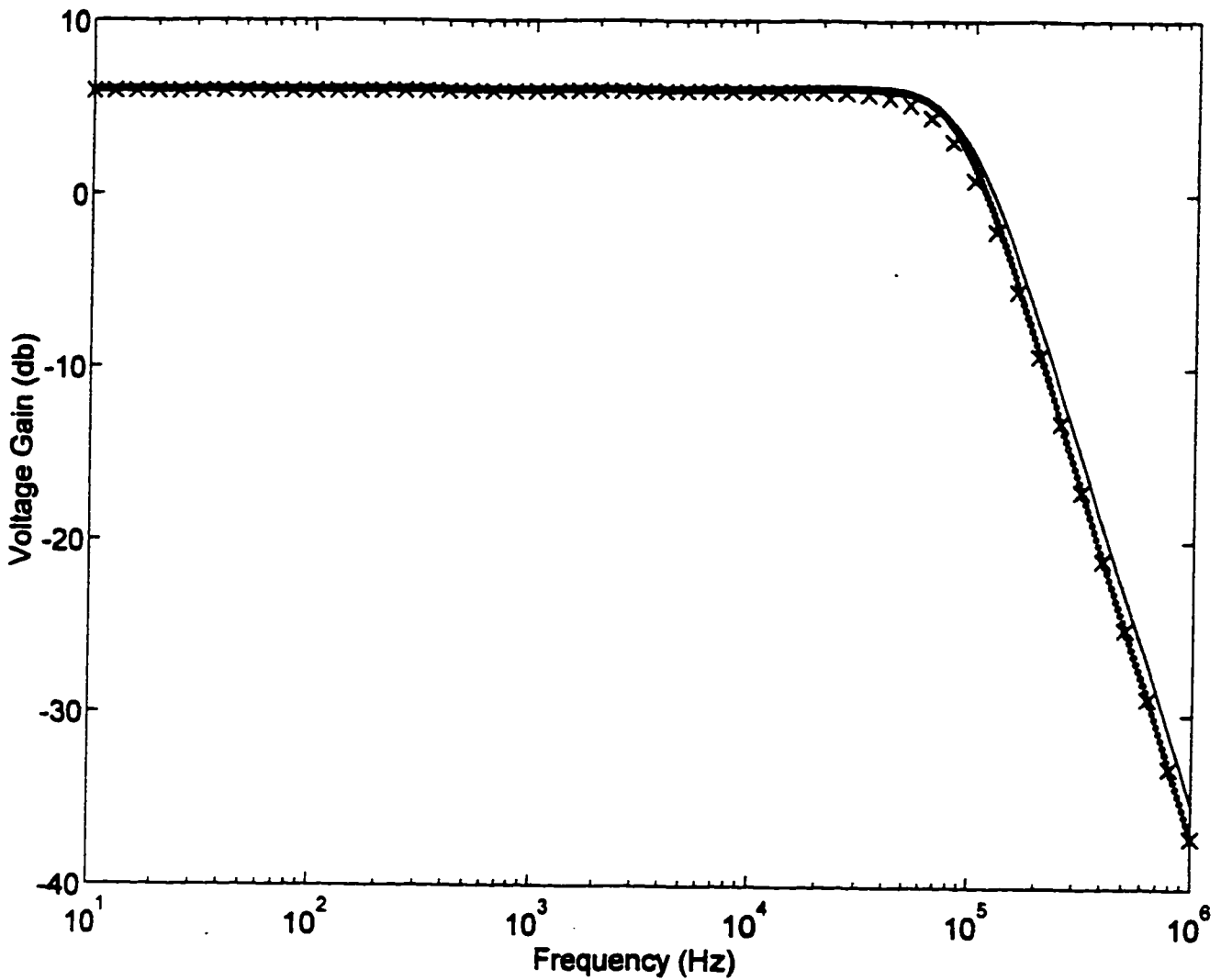
- Theoretical
o Simulation
x Experimental

Fig. 3.10 (a) The lowpass response with
$R_1=R_2= R_3= R_4=R_6=1 \ k\Omega, \ R_5=2k\Omega,$
$C_1=C_2=1.2nF$
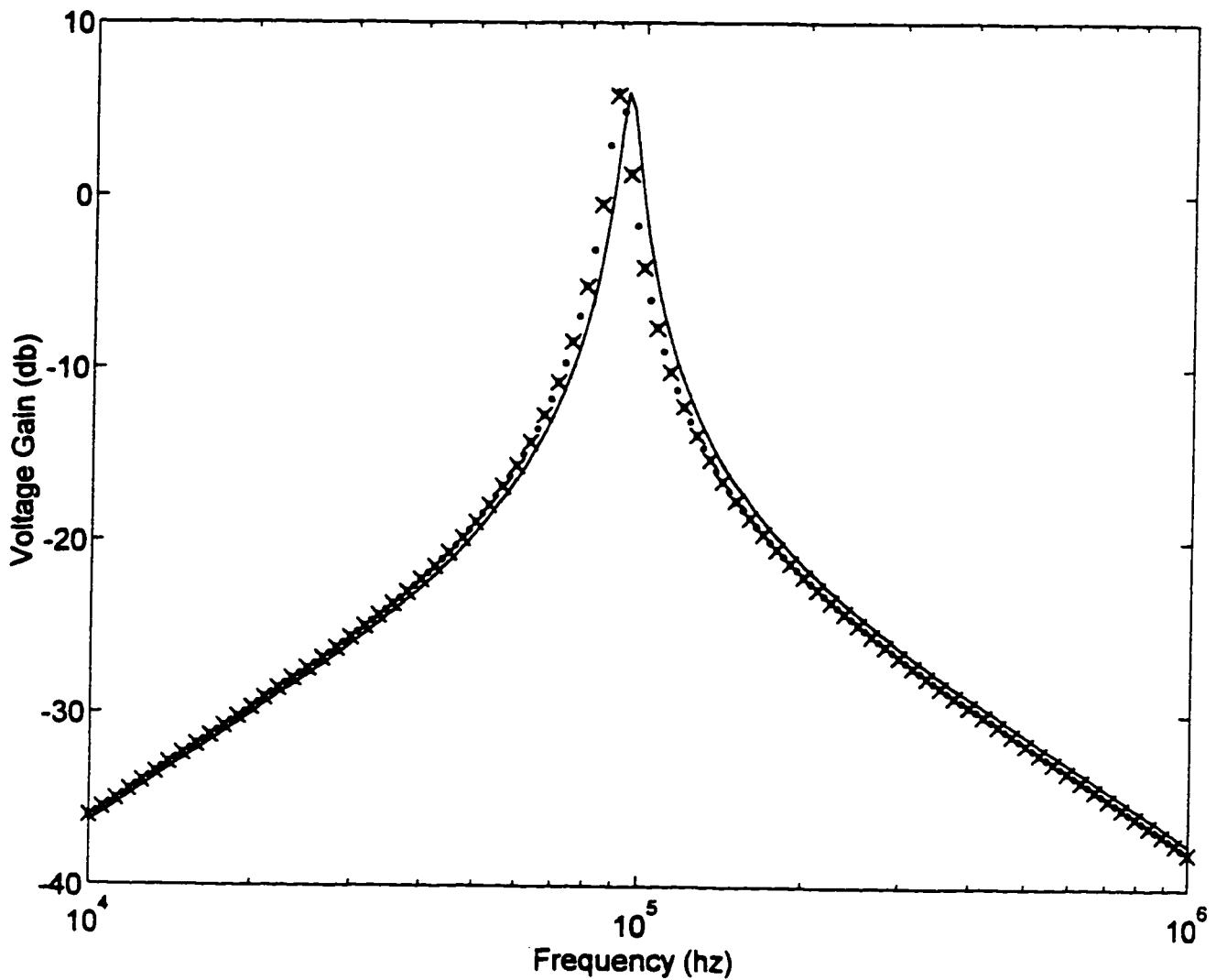
- Theoretical
o Simulation
x Experimental

Fig. 3.10 (b) The bandpass response with
$R_1=R_2=R_6=1\ k\Omega$, $R_3=10\ k\Omega$, $R_4=20\ k\Omega$,
$R_5=2k\Omega$,
$C_1=C_2=1.2nF$
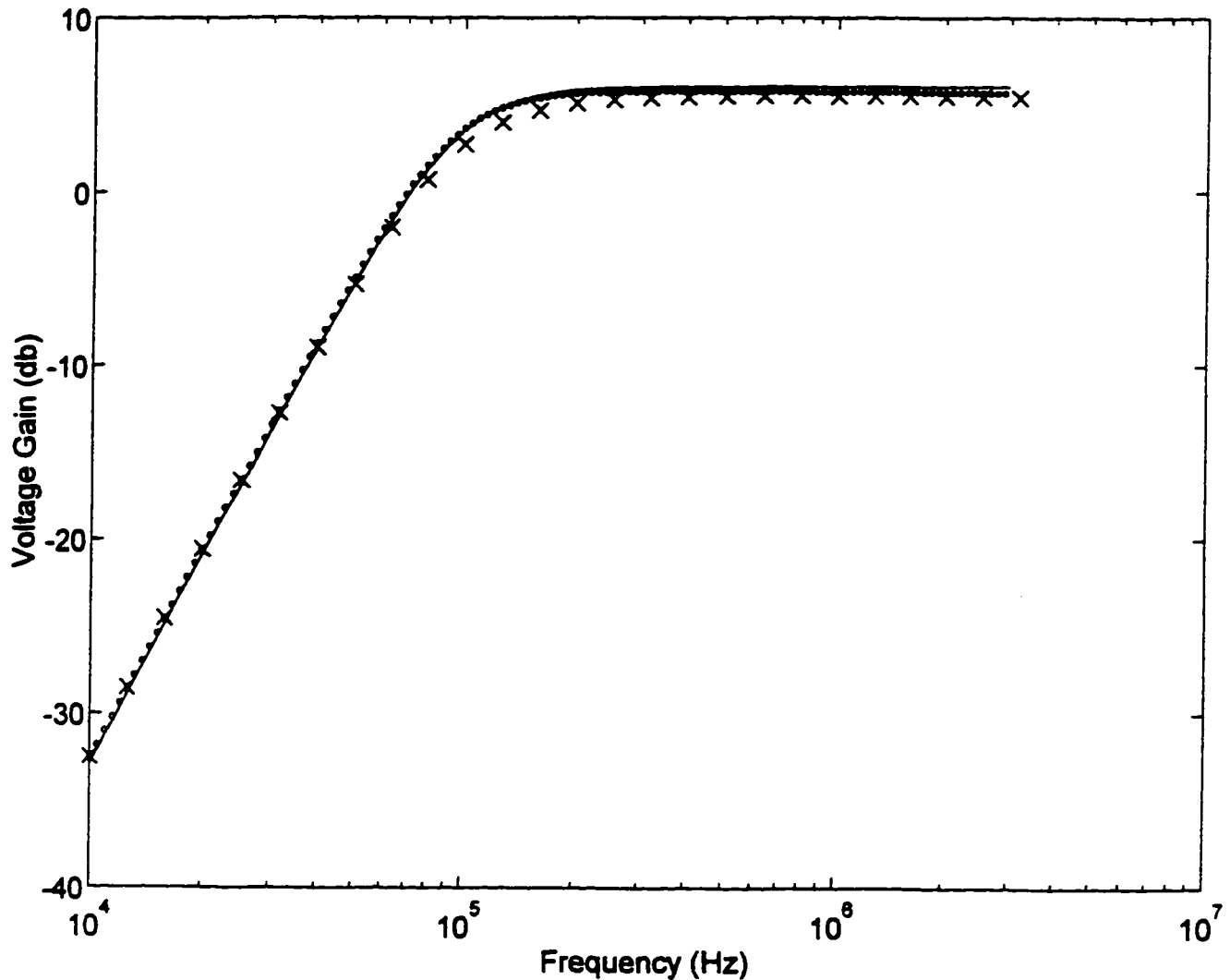
- Theoretical
o Simulation
x Experimental

Fig. 3.10 (c) The highpass response with
$R_2=R_3=R_4=1\ k\Omega,\ R_5=R_1=R_6=2k\Omega$
$C_1=C_2=1.2nF$

Chapter 4

Active-C Programmable Universal Filter using CCCIIs

4.1 Introduction

The popularity of programmable active filters have increased over the past decade[37-54]. Using OTAs to implement this type of filters is one of the most successful methods due to its simplicity [37-41]. However, performance limitations of OTAs such as poor bandwidths and poor output drive capabilities will restrict the overall operating performance of the filter. On the other hand, current-mode

current-conveyor based filters can offer wider signal bandwidths, greater linearity and wider dynamic ranges of operation [42-54]. However, they lack programmability. With the advent of current control conveyors CCCIIs, filter parameters such as the natural frequency and bandwidth can be continuously tuned by varying the bias current I_o of the CCCII. Using two CCCII+ and two grounded capacitors a current-mode band pass filter was reported by Fabre et al, 1995 [19] and a voltage-mode bandpass filter was reported by Fabre et al, 1996 [20]. No attempt has been reported, so far, to present universal second-order filter using CCCIIs. In this regard, a new universal programmable current-mode second-order filter with three-inputs and one-output will be presented. The proposed filter enjoys the following advantages:

(i) current control of the parameters ω_o and ω_o/Q_o of the filter and the gains of the bandpass and the lowpass responses,

(ii) high output impedance,

(iii) independent control of the parameter ω_o without disturbing the parameter ω_o/Q_o and the bandpass and the lowpass gains,

(iv) no externally connected resistors,

(v) employment of grounded capacitors which pave the way for high frequency operation and

(vi) low active and passive sensitivities.

4.2 Proposed Circuit

The proposed circuit is shown in Fig. 4.1. Using standard notations, the CCCII± of Fig.1.10 can be characterized by $i_Y=0$, $V_x=V_y+R_x i_x$ and $i_z=\pm i_x$, where $R_x=V_T/(2I_o)$, V_T is the thermal voltage and I_o is the bias current of the CCCII. Routine analysis yields the current transfer function which can be expressed by

$$I_{out} = -\frac{s^2 I_3 + s\dfrac{1}{C_2 R_{x2}} I_2 + \dfrac{1}{C_1 C_2 R_{x1} R_{x2}} I_1}{s^2 + s\dfrac{R_{x3}}{C_2 R_{x2} R_{x4}} + \dfrac{R_{x3}}{C_1 C_2 R_{x1} R_{x2} R_{x5}}} \tag{4.1}$$

Now, a current-mode bandpass filter is obtained if we choose $I_1=I_3=0$, thus,

$$\frac{I_{BP}}{I_2} = -\frac{s\dfrac{1}{C_2 R_{x2}}}{s^2 + s\dfrac{R_{x3}}{C_2 R_{x2} R_{x4}} + \dfrac{R_{x3}}{C_1 C_2 R_{x1} R_{x2} R_{x5}}} \tag{4.2}$$

A current-mode lowpass filter is obtained if we choose $I_2=I_3=0$, thus,

$$\frac{I_{LP}}{I_1} = -\frac{\dfrac{1}{C_1 C_2 R_{x1} R_{x2}}}{s^2 + s\dfrac{R_{x3}}{C_2 R_{x2} R_{x4}} + \dfrac{R_{x3}}{C_1 C_2 R_{x1} R_{x2} R_{x5}}} \qquad (4.3)$$
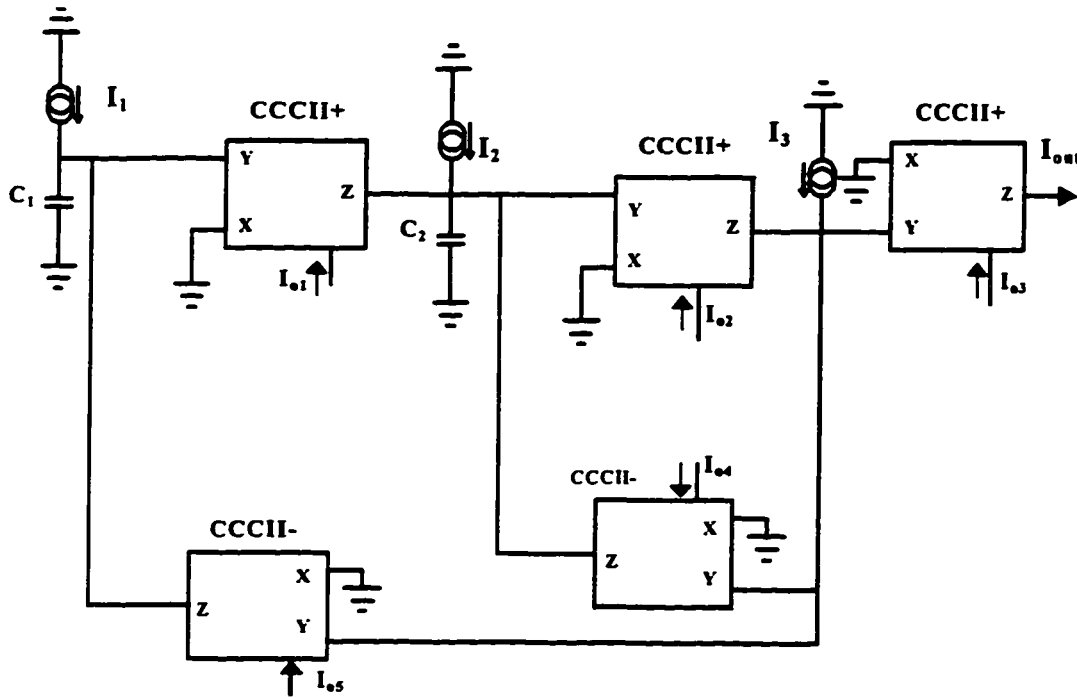
Fig 4.1 Proposed universal current-mode filter with three inputs and single output

A current-mode highpass filter is obtained if we choose $I_1=I_2=0$, thus

$$\frac{I_{HP}}{I_3} = -\frac{s^2}{s^2 + s\dfrac{R_{x3}}{C_2 R_{x2} R_{x4}} + \dfrac{R_{x3}}{C_1 C_2 R_{x1} R_{x2} R_{x5}}} \qquad (4.4)$$

A current-mode notch (bandreject) filter is obtained if we choose $I_2=0$, $I_1=I_3=I_i$ and $R_{x3}=R_{x5}$ thus

$$\frac{I_{NOTCH}}{I_i} = -\frac{s^2 + \dfrac{1}{C_1 C_2 R_{x1} R_{x2}}}{s^2 + s\dfrac{R_{x3}}{C_2 R_{x2} R_{x4}} + \dfrac{1}{C_1 C_2 R_{x1} R_{x2}}} \tag{4.5}$$

A current-mode allpass filter is obtained if we choose $I_1=I_2=I_3=I_i$ and $R_{x3}=R_{x4}$

$=R_{x5}$ thus

$$\frac{I_{AP}}{I_i} = -\frac{s^2 - s\dfrac{1}{C_2 R_{x2}} + \dfrac{1}{C_1 C_2 R_{x1} R_{x2}}}{s^2 + s\dfrac{1}{C_2 R_{x2}} + \dfrac{1}{C_1 C_2 R_{x1} R_{x2}}} \tag{4.6}$$

From eqn. 4.1-4.6 the parameters ω_0 and ω_o/Q_o can be expressed as

$$\omega_o^2 = \frac{R_{x3}}{C_1 C_2 R_{x1} R_{x2} R_{x5}} \tag{4.7}$$

$$\frac{\omega_o}{Q_o} = \frac{R_{x3}}{C_2 R_{x2} R_{x4}} \tag{4.8}$$

From equations (4.1-4.6), it can also be seen that the high frequency gain of the highpass filter is equal to unity, the dc gain of the lowpass filter is equal to

$$G_{LP} = \frac{R_{x5}}{R_{x3}} \tag{4.9}$$

and the bandpass gain at ω_0 is equal to

$$G_{BP} = \frac{R_{x4}}{R_{x3}}$$
(4.10)

From equations. (4.7-4.10), it can be seen that the parameter ω_0 can be adjusted by controlling the resistance R_{x1}, that is the bias current I_{o1}, without disturbing the parameters ω_0/Q_0, the lowpass gain G_{LP} and the bandpass gain G_{BP}. Moreover, the parameter ω_0/Q_0 can be adjusted by controlling the resistance R_{x2}, that is the bias current I_{o2}, without disturbing the parameters ω_0, the lowpass gain G_{LP} and the bandpass gain G_{BP}. Furthermore, the bandpass gain can be adjusted by controlling the resistance R_{x4}, that is the bias current I_{o4}, without disturbing the parameter ω_0. However, this will disturb the parameter ω_0/Q_0. Finally, the lowpass gain can be adjusted by controlling the resistance R_{x5}, that is the bias current I_{o5}, without disturbing the parameter ω_0/Q_0. However, this will disturb the parameter ω_0. A possible strategy for adjusting the parameters ω_0, ω_0/Q_0, the bandpass and the lowpass gain is therefore as follows: first the resistor R_{x4}, that is the bias current I_{o4} is adjusted to control the bandpass gain G_{BP} and R_{x5}, that is the bias current I_{o5}, is adjusted to control the lowpass gain G_{LP}, then the bias current I_{o2} is adjusted to control the parameter ω_0/Q_0 and finally the bias current I_{o1} is adjusted to control the parameter ω_0.

4.3 Sensitivity Analysis

Using (2.21) and (4.1) the sensitivities of the parameters ω_0 and Q_0 of the proposed filter were calculated and the results are given in Table 4.1.

S	ω_o	Q_o
C_1	-0.5	-0.5
C_2	-0.5	0.5
R_{x1}	-0.5	-0.5
R_{x2}	-0.5	0.5
R_{x3}	0.5	0.0
R_{x4}	0.0	1.0
R_{x5}	-0.5	-0.5

Table 4.1 The active and passive sensitivities

of the proposed filter in Fig. 4.1

Thus, the active and passive sensitivities of the proposed filter are small.

4.4 Simulation Results and Discussion

The proposed universal filter in Fig. 4.1 has been simulated using ICAPS circuit simulation program. The CCCII± have been simulated using the schematic implementation of Fig. 1.10, proposed by Faber et al, [20] with dc supply voltage=±2.5V. The PNP and NPN transistors were simulated using the parameters of the PR200N and NR200N bipolar transistors [61].

Fig. 4.2 (a) shows the theoretical and the simulation results of the gain-frequency characteristics of the lowpass filter with $C_1=C_2=1nF$ $I_{o3}=$ $I_{o4}=100uA$ and $I_{o5}=50uA$ tuned at three different values of (ω_o) with ($I_{o1}=I_{o2}$ =1uA, $I_{o1}=I_{o2}$ =10uA, $I_{o1}=I_{o2}$ =100uA) respectively. The simulated results of the frequencies deviate from the

theoretical results by a percentage error less than 3% and the simulated results of the gains deviate from the theoretical results by a percentage error less than 5%.

Fig. 4.2 (b) shows the theoretical and the simulation results of the gain-frequency characteristics of the bandpass filter with $C_1=C_2=1nF$ $I_{o3}=$ 100uA, $I_{o4}=$ 25uA and $I_{o5}=50uA$ tuned at three different center frequencies (ω_o) with ($I_{o1}=I_{o2}=1uA$, $I_{o1}=I_{o2}$ =10uA, $I_{o1}=I_{o2}$ =100uA) respectively. The simulation results of the frequencies deviate from the theoretical results by a percentage error less than 3.5% and the simulated results of the gains deviate from the theoretical results by a percentage error less than 5%.

Fig. 4.2 (c) shows the theoretical and the simulation results of the gain-frequency characteristics of the highpass filter with $C_1=C_2=1nF$ $I_{o3}=I_{o4}=100uA$ and $I_{o5}=50uA$ tuned at three different values of (ω_o) with ($I_{o1}=I_{o2}$ =1uA, $I_{o1}=I_{o2}$ =10uA, $I_{o1}=I_{o2}$ =100uA) respectively. The simulated results of frequencies deviates from the theoretical results by a percentage error less than 3.5% and the simulated results of the gains deviate from the theoretical results by a percentage error less than 7% for frequencies less than 100MHz. The most important deviations appear at very high frequencies due to the cut off frequency of the transistors. To reduce these deviations, transistors with higher cutoff frequencies should be used in realizing the CCCII.

Fig. 4.2 (d) shows the theoretical and the simulation results of the gain-frequency characteristics of the notch (band reject) filter with $C_1=C_2=1nF$ $I_{o3}=$ $I_{o5}=$ 100uA and $I_{o4}=25uA$ tuned at three different values of (ω_o) with ($I_{o1}=I_{o2}$ =1uA, $I_{o1}=I_{o2}$ =10uA,

$I_{o1}=I_{o2}$ =100uA) respectively. The simulation results deviates from the theoretical results by a percentage error less than 5% and the simulated results of the gains deviate from the theoretical results by a percentage error less than 7%.

Fig. 4.2 (e) shows the theoretical and the simulation results of the gain-frequency characteristics of the allpass filter with $C_1=C_2=1nF$ $I_{o1}=I_{o2}=10uA$, $I_{o3}=I_{o4}=I_{o5}=100uA$. The simulation results deviates from the theoretical results by percentage of error less than 7%.

Fig. 4.2 (f) shows the theoretical and the simulation results of the phase-frequency characteristics of the allpass filter with $C_1=C_2=1nF$ $I_{o3}=I_{o4}=I_{o5}=$ 100uA and tuned at three different values of (ω_o) with ($I_{o1}=I_{o2}=1uA$, $I_{o1}=I_{o2}$ =10uA, $I_{o1}=I_{o2}$ =100uA) respectively. The simulated results of phase deviates from the theoretical results by a percentage error less than 6%.

Fig 4.3 show ω_o vs. the control current . It appears that the simulation results are in fairly good agreement with the presented theory. Deviations less than 6% were obtained on the range 1–150uA for I_o. The most important deviations, which appear for the very high values of I_o principally come from the diminutions of the beta of the transistors in the translinear loop of the CCCII (beta used in the simulation equal to 137.5 for NPN transistors and 110 for PNP transistors). To reduce these deviations, transistors with higher value of beta should be used in realizing the CCCII.

To show the merits and demerits of the proposed filter, Table 4.2 shows a comparison with the most recently published active-C programmable current mode

universal filters. Comparison shows that, the proposed filter and the previously published filter enjoy the independent tuning of ω_0 and ω_0/Q_o. The proposed filter use same number of active devices and same or less number of grounded capacitors. For conventional bipolar OTA, the value of $gm=I_o/(2V_T)$ while for the CCCII, R_x can be expressed as $V_T/2I_o$. It can be seen that for a second order filter with same ω_0, an OTA implementation needs 4 times the value of the control current needed by an CCCII implementation. Thus at high ω_0, the OTA implementation will suffer from the diminutions of the beta of the transistors more than CCCII implementation. The proposed filter has better performance at high frequencies and less power consumption than the filters using OTAs.

	OTA-C Universal filter 1996[41]	OTA-C and CCII Universal filter 1995[54]	Proposed CCCII-C Universal filter
No. of active devices	Five OTA-C with two output	Four OTA-C and One CCII	Five CCCII
No. of capacitors	Two	Three	Two
Independent tuning of ω_0 and ω_0/Q_0	Yes	Yes	Yes
Perfomance at high frequinces	————	————	Better than both of them
Power Consumption	> Three units	> Three units	One unit

Tabel 4.2 show a comparison betwwen the proposed filter and the previously published Active-C programmable current mode universal filter.
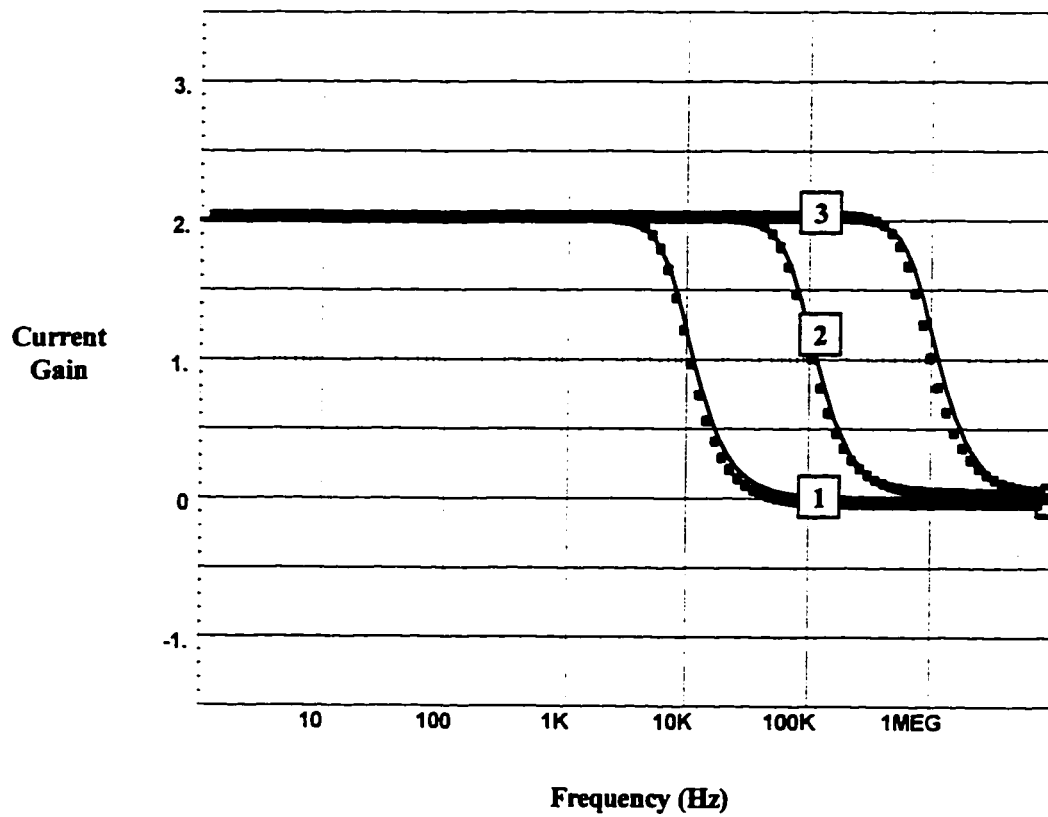
Fig. 4.2 (a) Gain-frequency characteristics of the lowpass
filter with
$$C_1 = C_2 = 1nF$$
$$I_{o3} = I_{o4} = 100uA, \; I_{o5} = 50uA$$
(1) $I_{o1} = I_{o2} = 1uA$
(2) $I_{o1} = I_{o2} = 10uA$
(3) $I_{o1} = I_{o2} = 100uA$
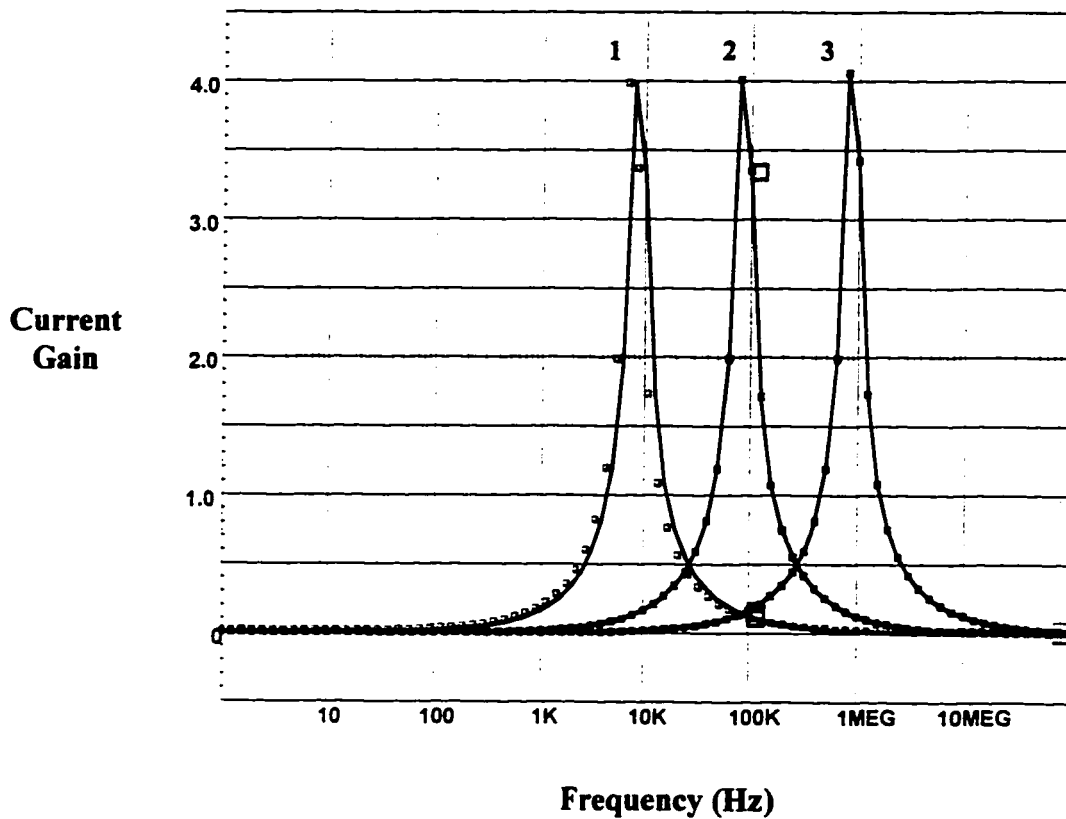
Fig. 4.2 (b) Gain-frequency characteristics of the bandpass
filter with
$C_1=C_2=1nF$
$I_{o3}= 100uA, I_{o4}= 25uA\ I_{o5}=50uA$
(1) $I_{o1}=I_{o2}=1uA$
(2) $I_{o1}=I_{o2}=10uA$
(3) $I_{o1}=I_{o2}=100uA$
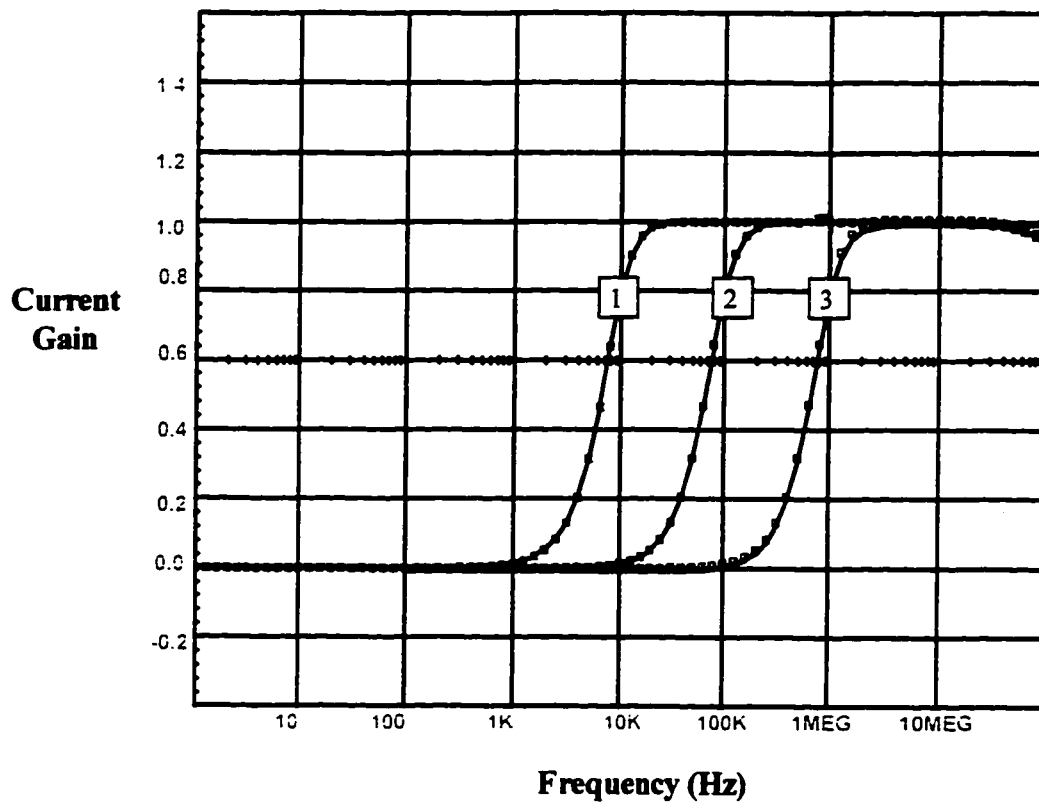
- Theoretical
≃ Simulation

Fig. 4.2 (c) Gain-frequency characteristics of the highpass
filter with
$C_l=C_2=lnF$
$I_{o3}=I_{o4}=100uA$, $I_{o5}=50uA$
(1) $I_{o1}=I_{o2}=1uA$
(2) $I_{o1}=I_{o2}=10uA$
(3) $I_{o1}=I_{o2}=100uA$

Current
Gain
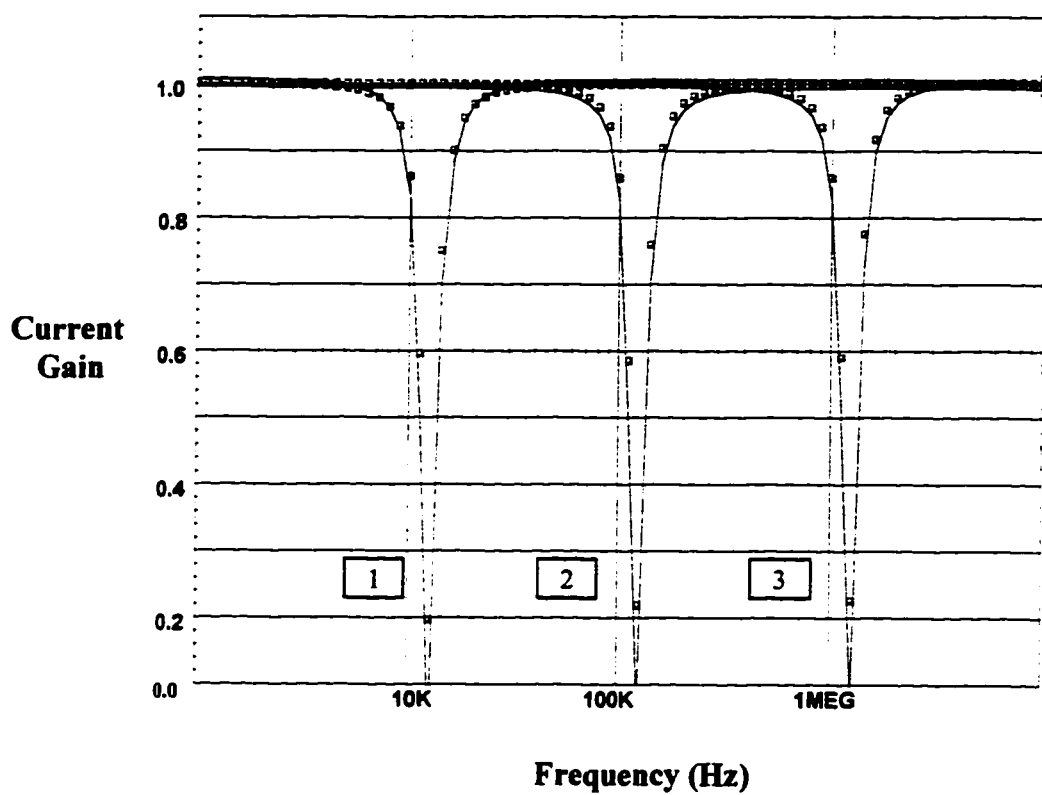
Frequency (Hz)

- Theoretical
≈ Simulation

Fig. 4.2 (d) Gain-frequency characteristics of the notch filter
with
$C_1 = C_2 = 1nF$
$I_{o3} = I_{o5} = 100uA, I_{o4} = 25uA$
(1) $I_{o1} = I_{o2} = 1uA$
(2) $I_{o1} = I_{o2} = 10uA$
(3) $I_{o1} = I_{o2} = 100uA$

Current 1.0
Gain

0.0

10   100   1K   10K   100K   1MEG   10MEG
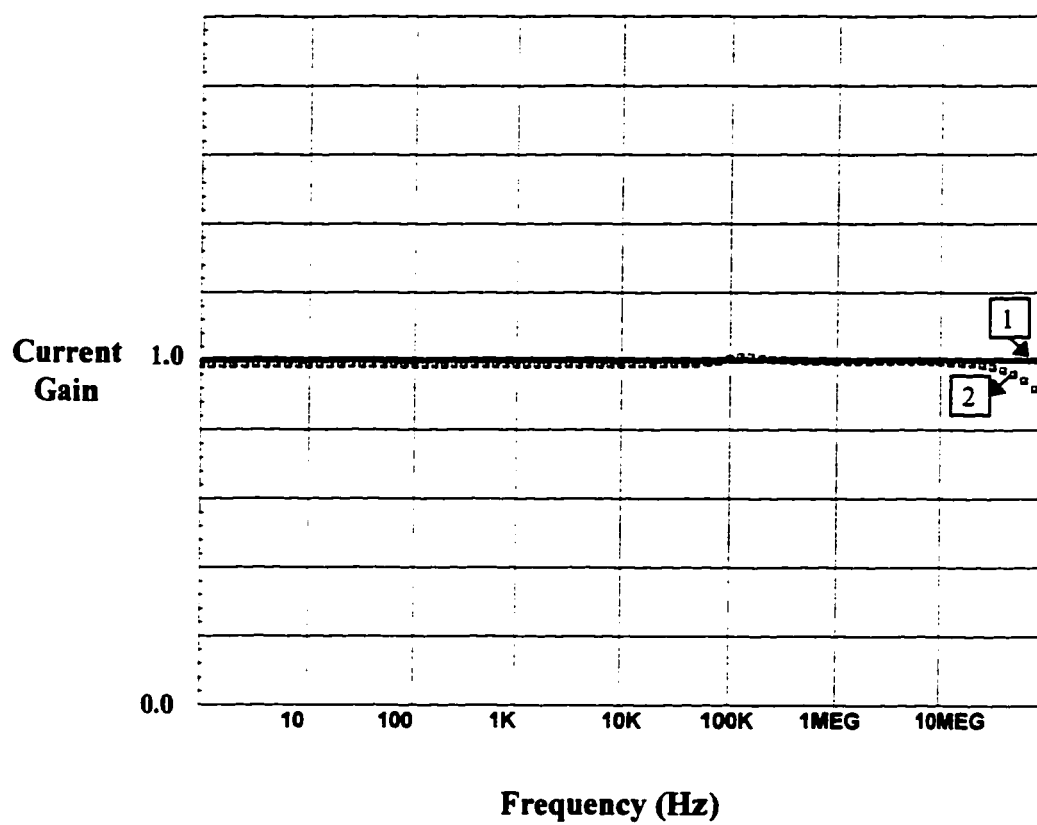
Frequency (Hz)

- Theoretical
∷ Simulation

Fig. 4.2 (e) Gain-frequency characteristics of the allpass filter with
$$C_1 = C_2 = 1nF$$
$$I_{o1} = I_{o2} = 10uA,, \quad I_{o3} = I_{o4} = I_{o5} = 100uA$$
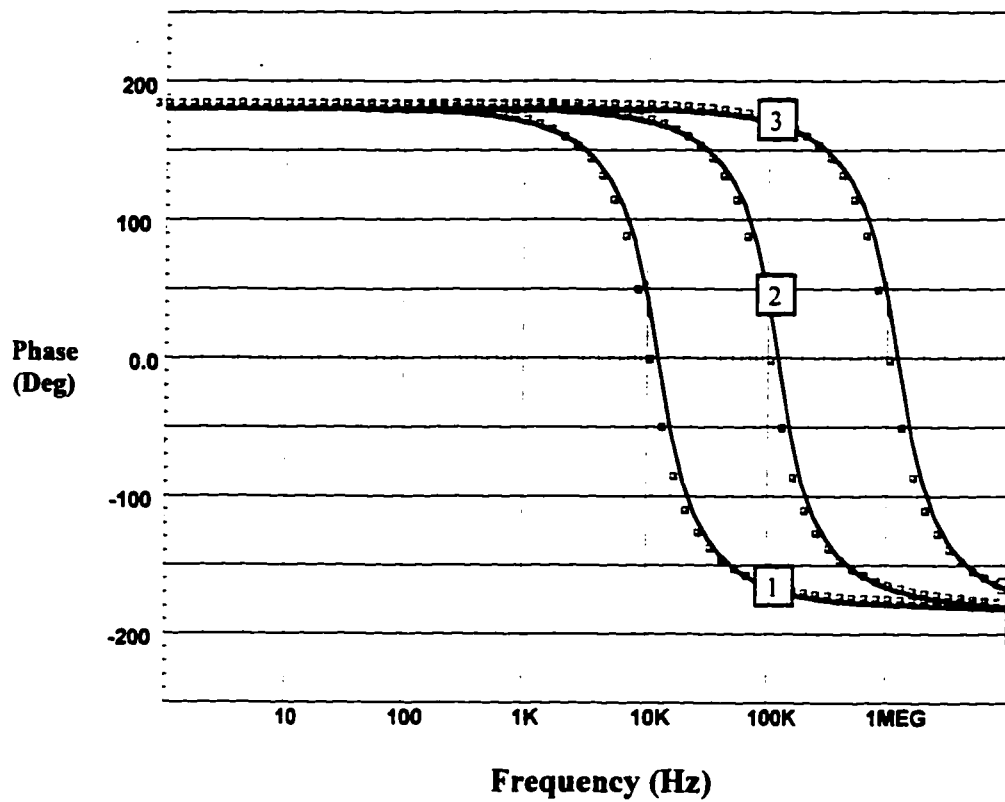
- Theoretical
= Simulation

Fig. 4.2 (f) Phase-frequency characteristics of the notch filter with
$$C_1 = C_2 = 1nF$$
$$I_{o3} = I_{o5} = 100uA, \ I_{o4} = 25uA$$
(1) $I_{o1} = I_{o2} = 1uA$
(2) $I_{o1} = I_{o2} = 10uA$
(3) $I_{o1} = I_{o2} = 100uA$
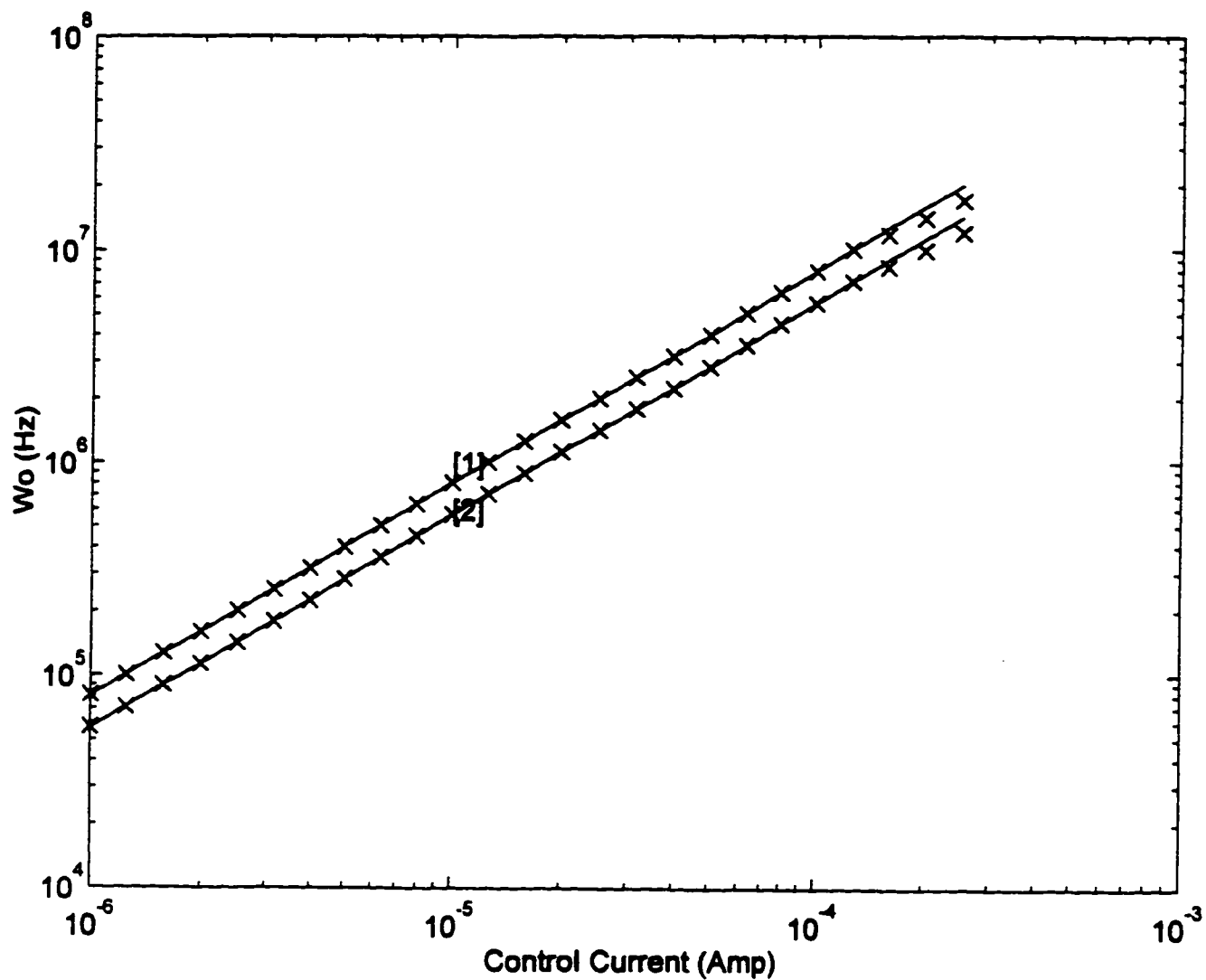
-Theoretical
x Simulation

Fig. 4.3 ω_0 in (rad/sec) vs. the control current=I_{o1}=I_{o2}
[1] I_{o3}= I_{o5}=100μA C_1=C_2=1nF
[2] I_{o5}=50μA I_{o3}=100μA C_1=C_2=1nF

Chapter 5

A CCCII-based Current-Mode Analog

Multiplier/Divider

5.1 Introduction

Analog Multipliers and dividers are widely used in telecommunications, control, instrumentation and signal processing. The application of the second-generation current-conveyor (CCII) in realizing voltage-mode multiplier circuits has been demonstrated, but these circuits invariably use MOS transistors [55-57]. In order to

avoid the effect of the nonlinearities of the MOS transistors, it is essential to ensure the operation of the MOS transistors in the linear region. This requires some operation constraints [55-57].

The major intention of this chapter is to present a current-mode analog multiplier/divider circuit using only two CCCII and without using MOS transistors or resistors. Thus, avoiding the operation constraints required for linear operation of the MOS transistors used in the available voltage-mode multiplier/divider circuits. The proposed multiplier/divider enjoys temperature independent performance.

5.2 Proposed Circuit

The proposed current-mode analog multiplier/divider circuit using only two second-generation current-controlled current-conveyors is shown in Fig. 5.1.

Fig. 5.1 Proposed Multiplier/Divider Circuit

The results obtained are shown in Fig. 5.2 for $i_l=1\sin(2\pi.1000t)mA$, $i_2=1\ \sin(2\pi.30000t)\ mA$, I=2mA. The deviations of the simulation results from the theory presented is less than 2%. For higher values of current this deviations will increase due to the diminutions of the beta of the transistors of CCCII, (beta used in simulation equals to 500).

Another test for multiplying a triangular signal by factors of 2 and -2 was performed. The results are shown in Fig. 5.3 for $i_l=\pm200\mu A$, $I=100\mu A$ and i_2 as triangular wave with amplitude $10\mu A$ and period $=2$msec. The simulation results are in fairly good agreement with the presented theory. The deviations of the simulation results from the theory presented is less than 1%.

The divider function was also tested. The results obtained are shown in Fig. 5.4 for $i_l=20\mu A$, $i_2=100\mu A$ and I as a triangular wave with amplitude $20\mu A$, dc component $=10\mu A$ and period = 2msec. The deviations of the simulation results from the theory presented is less than 2%.

To show the merits and demerits of the proposed multiplier/divider, Table 5.1 shows a comparison with the most recently published multipliers/dividers. Comparison shows that the proposed multiplier/divider are current-mode while the other multipliers/dividers are voltage mode. The proposed multiplier/divider has been realized using only two CCCII and without using MOS transistors. Thus avoiding the operation constraints required for linear operation of the MOS transistors used in the available voltage-mode multiplier/divider circuits. Moreover, the proposed

multiplier/divider enjoys larger dynamic range and temperature independent

performance.

	Multiplier and divider [55] (1993)	Multiplier / divider [56] (1996)	Proposed multiplier/ divider
No. of active devices	Two CCII and two MOS transistors for the multiplier Three CCII and six MOS transistors for the divider	One CCII and six MOS transistors	Two CCCII+
Mode	voltage-mode	voltage-mode	current-mode
Dynamic range	small	small	Large
Require some operation constraints for linear operation	Yes	Yes	No
Can realize multiplier and divider without changing the circuit typology	No	Yes	Yes
Temperature independent	No	No	Yes

Table 5.1 comparison between two of the most recently published
multipliers/dividers using current conveyor and the proposed
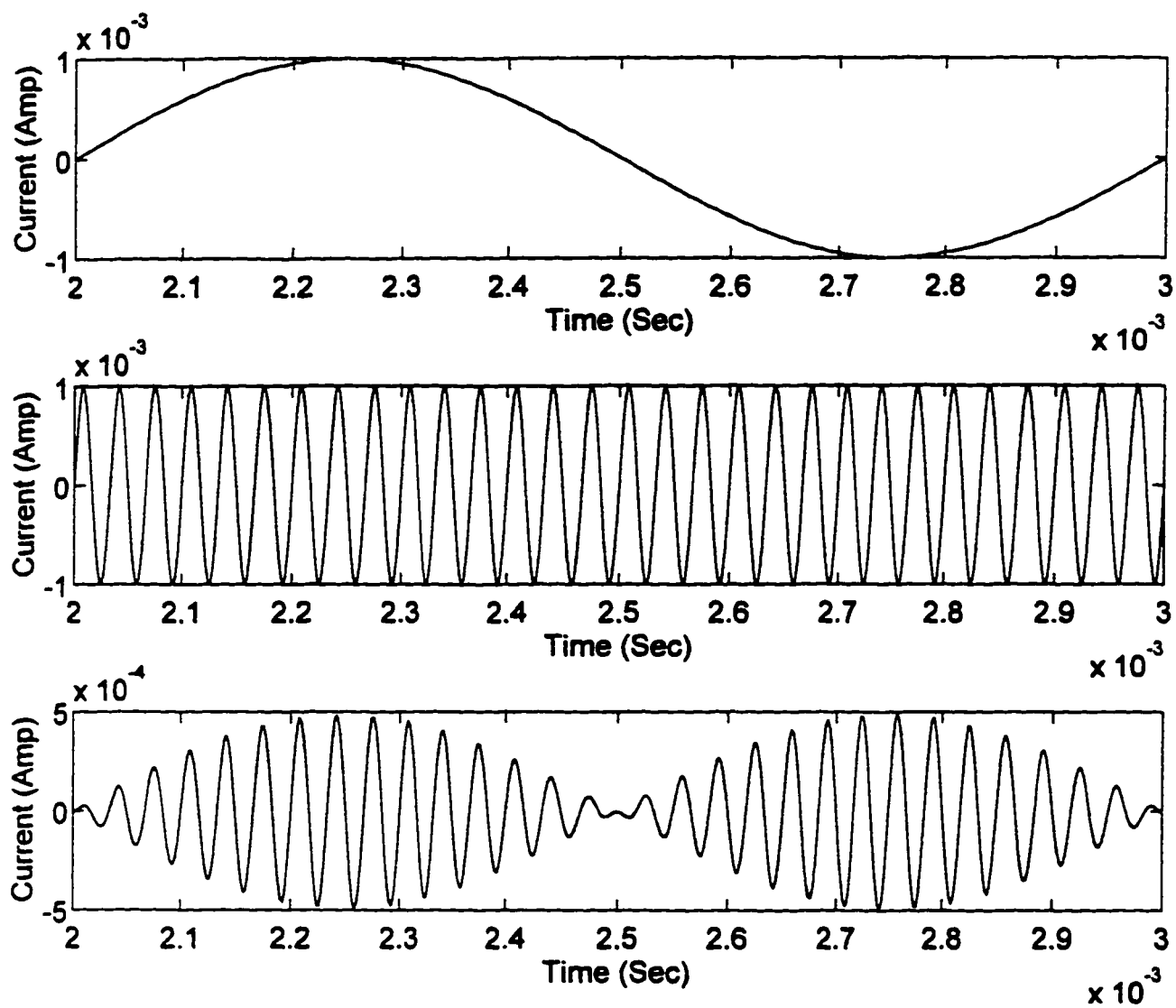
Fig 5.2 Output current obtained from the multiplier of Fig. 5.1 with $i_1=1\sin(2\pi1000t)$, $i_2=1\sin(2\pi30000t)$, I=2 all in mA.
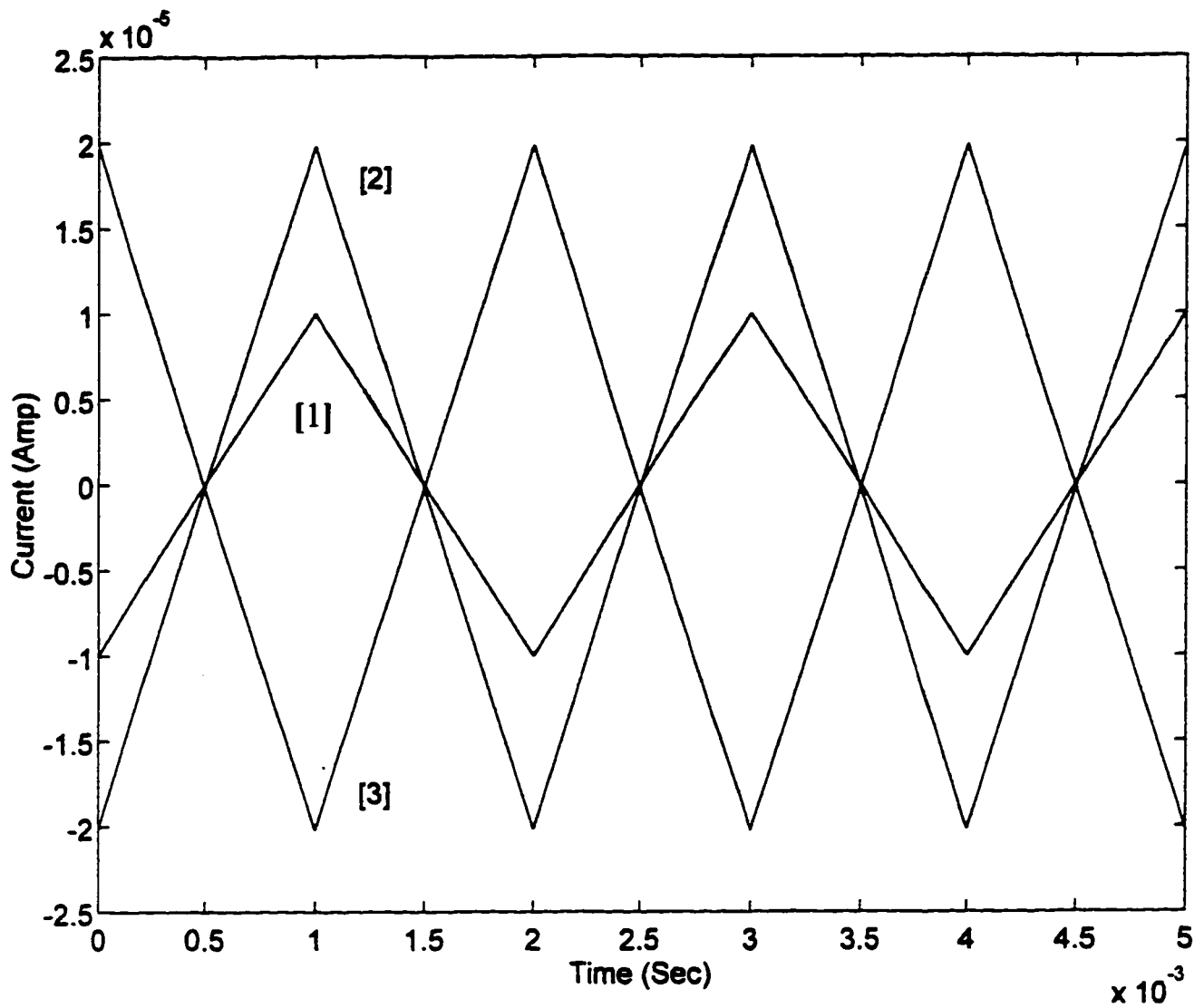
Fig. 5.3 Output currents obtained from the
multiplier of Fig. 5.1 with
$i_1 = \pm 200$ uA, I=100uA
i_2= triangular wave with amplitude 10uA and
period =2msec
[1] input signal
[2] output signal when i_2=-200uA
[3] output signal when i_2=-200uA
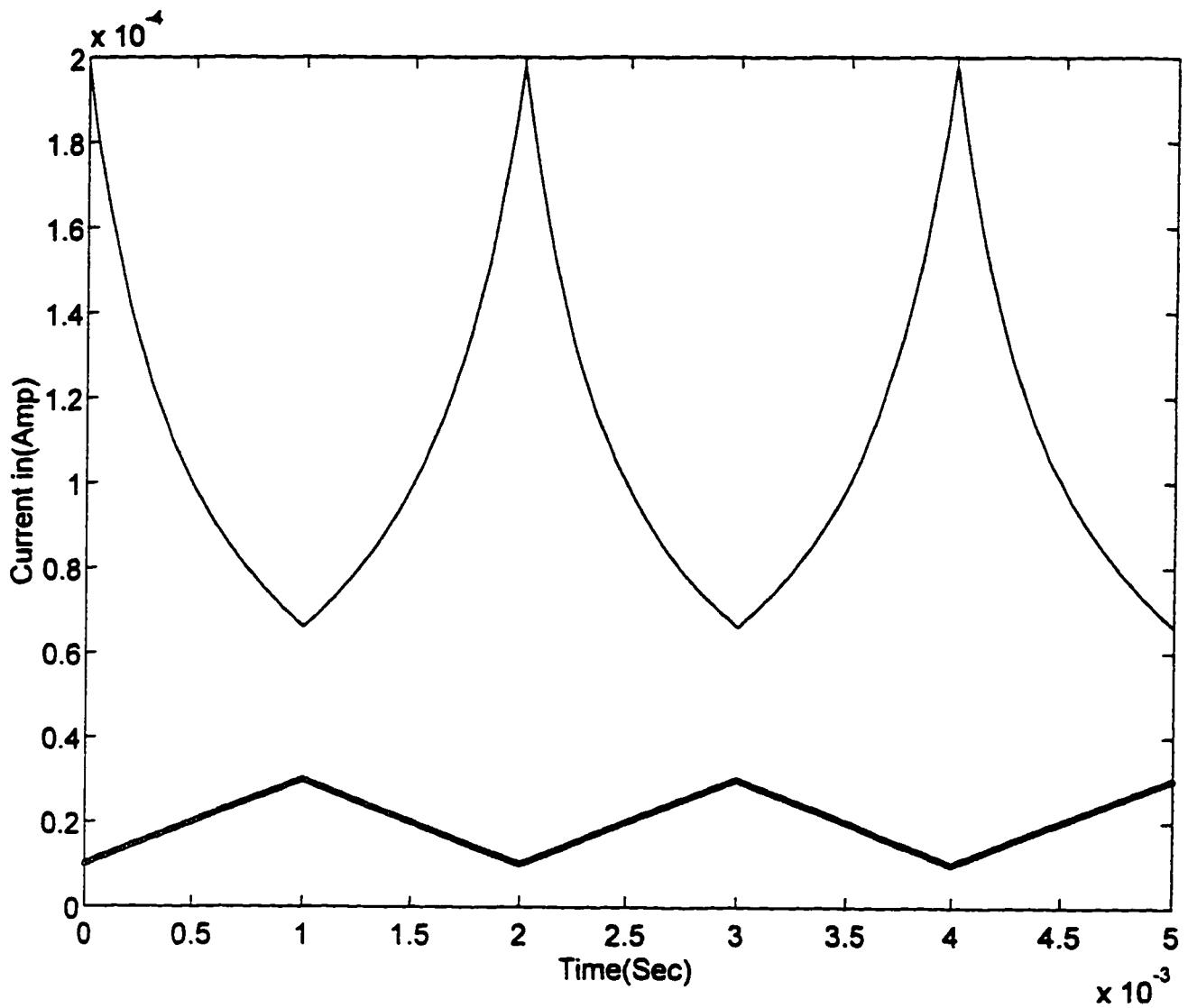
o input signal
- output signal

Fig. 5.4 Output current of the divider
with
i_1=20uA, i_2=100uA and I the triangular
waveform.

Chapter 6

Conclusion and Directions of Future Work

6.1 Conclusion

Current conveyors have proved to be functionally flexible and versatile. This is attributed to their higher signal bandwidths, greater linearity and larger dynamic range. In this thesis, we have developed MPSOs using second-generation current conveyors CCIIs, new universal filters based on current and voltage followers, a new programmable active-C current-mode universal filters using CCCII and we have extended the use of current conveyor to nonlinear applications.

The first part of this thesis investigated the feasibility of developing new MPSOs using second-generation current conveyors CCIIs which can generate (n) signals equal in amplitude and equally spaced in phase, with (n) either an even or an odd number. In this regard, active-RC, active-R and active-C MPSOs were presented. Their frequencies of oscillation can be controlled either by a grounded resistor as in the proposed active-RC MPSOs, or by a grounded capacitor as in the proposed active-R MPSOs or by the bias current of the CCCII as in the proposed active-C MPSOs. The three structures were simulated using Pspice and the results were in good agreement with the presented theory, with an error of the order of or less than 6%.

The second part of this thesis investigated the feasibility of developing new universal filters based on voltage and current followers which can be deduced from CCII by grounding the Y terminal. In this regard two current-mode universal filters were presented. The first filter has three inputs and one output and can realize lowpass, highpass, bandpass, notch and allpass responses without any changes in the circuit topology. The second filter has three inputs and one output and can simultaneously realize lowpass, highpass and bandpass responses. Realization of notch and allpass can be easily achieved without adding any additional active elements. On the other hand, two voltage-mode universal filter were also presented. The first filter can simultaneously realize lowpass and bandpass responses. The other filter can simultaneously realize lowpass, highpass and bandpass responses. Three of these filters were tested experimentally and all of them were simulated using Pspice. The

theoretical, the simulation and the experimental results were in good agreement.

with an error of the order of or less than 7%.

The third part of this thesis investigated the feasibility of taking advantage of the

parasitic resistance R_x (which appears when the input cell of CCII is implemented

from mixed translinear loop known as CCCII where the value of this resistance

depends on the bias current I_o of the CCII) in developing a new programmable

active-C current-mode universal filters. The proposed filter has three inputs and

one output and can realize lowpass, bandpass, highpass, notch and allpass

responses.

Comparisons between all of the proposed circuits and the previously published

circuits were included. All of the proposed MPSOs and universal filters enjoy:

1. the independent control of the basic parameters, like the frequecy of oscillation

and the condition of oscillation of the MPSO, or like the natural frequency and the

banwidth of the universal filter.

2. the use of grounded capacitors,

3. the use of minimum number of active and passive components,

and

4. the low active and passive sensitivities.

The last part of this thesis investigated the feasibility of extending the use of current

conveyor   to   nonlinear   applications.   A   simple   current-mode   analog

multiplier/divider circuit using only two CCCII was presented. No resistors, no capacitors and no MOS transistors are required. The circuit can perform multiplication and division without changing its topology. The proposed circuit enjoys the temperature independence and the large dynamic range of the input signals. Simulation results are included. Comparison with the most recently published multiplier/divider circuit shows that the proposed multiplier/divider circuit has superior advantages over them.

To conclude, it can be said that the proposed circuits in this thesis have attractive features for possible integration in comparsion with related existing circuits.

6.2 Directions of Future Work

There is always still a room for improvement. This work can be extended in many directions:

- The CCCIIs has been used in realizing programmable universal filter with multiple inputs and single output. In future, the CCCII can be used in realizing programmable universal filter with single input and multiple outputs.

- The CCCII has been used in realizing a programmable grounded resistor [20]. In future, the CCCII can be used in realizing programmable floating resistor and floating or grounded capacitor and may be inductor which enjoys the large dynamic range, temperature independence, using grounded capacitor and employing of minimum number of active and passive elements.

References

[1] K. C. Smith and A. Sedra, The current conveyor – a new circuit building block, IEEE Proc., Vol. 56, 1968, pp. 1368-1369

[2] A. Sedra and K. C. Smith, A second generation current conveyor and its applications, IEEE Trans. Circuit Theory, Vol. CT-17, 1970, pp. 132-134

[3] A. Fabre, Third-generation current conveyor: a new helpful active element, Electronic Letters, Vol. 31, No. 5, 1995, pp.338-339

[4] M. Sharif-Bakhtiar and P. Aronhime, A current conveyor realisation using operational amplifiers, Int. J. Electron., Vol.45, 1978, pp.225-226

[5] R. Senani, Novel circuit implementation of current conveyors using an OA and an OTA, Electronics Letters, Vol. 16, No. 1, 1980, pp.2-3

[6] B. Wilson, Recent Developments in Current Conveyors and Current-Mode Circuits, IEE Proceedings , Vol. 137, Pt. G, No. 2, April 1990, pp. 63-77

[7] B. Wilson, High-performance Current Conveyor Implementation, Electronics Letters, Vol. 20, NO. 24, 22nd November 1984, pp. 990-991

[8] B. Gilbert, Translinear Circuits: A Proposed Classification, Electronics Letters, Vol. 11, No. 1, 9th January 1975, pp. 14-16

[9] Fabre, Wideband Translinear Current Conveyor, Electronics Letters, Vol. 20, NO. 6, 15th March 1984, pp. 241-242

[10] P. L. Francois, F. Alard and J. F. Bayon, Ultra-Low-Distortion Current-Conversion Technique, Electronic Letters, Vol. 20, NO. 17, 16th August 1984, pp. 674-675

[11] A. Fabre, Translinear Current Conveyors implementation, Int. J. Electronics, Vol. 59, No. 5, 1985, pp. 619-623

[12] A. Fabre, Dual Translinear Voltage/Current Conveyor, Electronic Letters, Vol. 19, NO. 24, 24th November 1983, pp. 1030-1031.

[13] A. S. Sedra, G. W. Roberts and F. Gohh, The Current Conveyor: History, Progress and New Results, IEE Proceedings, Vol. 137, Pt. G, No. 2, April 1990, pp. 78-87

[14] A. Fabre, New Formulation to Describe Translinear mixed Cell Accurately, IEE Proc.-Circuits Devices Syst., Vol. 141, No. 3, June 1994, pp. 167-173

[15] Erik Bruun, A Combined first- and second-generation current conveyor structure, Int. J. Electronics, Vol. 78, No. 5, 1995, pp. 911-923

[16] C. Toumazou, F. J. Lidgey and C. A. Makris, Extending Voltage-Mode Op-Amps to Current-Mode Performance, IEE Proceedings, Vol. 137, Pt. G, No. 2, April 1990, pp.116-130

[17] F. J. Lidgey, Current Followers, Wireless World, February, Vol. 90, 1984, pp. 40-43

[18] F. J. Lidgey and C. Toumazou, Accurate Current Followers, Electronic and Wireless World, April, Vol. 91, 1985, pp. 17-19

[19] A. Fabre, O. Saaid, F. Wiest and C. Boucheron, Current Controlled Bandpass Filter Based on Translinear Conveyors, Electronics Letters, Vol. 31, No. 20, 28th September 1995, pp. 1727-1728

[20]A. Fabre, O. Saaid, F. Wiest and C. Boucheron, High Frequency Applications Based on a New Current Controlled Conveyor, IEEE Transactions on Circuits and Systems-I: Fundamental Theory and Applications. Vol. 43, No. 2, February 1996, pp. 82-91

[21] B. Z. Kaplan, and S. T. Bachar, A versatile voltage controlled three phase oscillator, IEEE Transactions on IECI, Vol.26, 1979, pp.192-195

[22] A. Rahman and S. E. Haque, A simple three-phase variable-frequency oscillator, International Journal of Electronics, Vol.53, 1982, pp.83-89

[23] V. P. Ramamurti and B. Ramaswami, A novel three-phase reference sinewave generator for PWM invertor, IEEE Transaction on Industrial Electronics, Vol.29, 1982, pp.235-240

[24] W. B. Mikhael and S. Tu, Continuous and switched-capacitor multiphase oscillators, IEEE Transaction on Circuit and Systems, Vol.31, 1984, pp.280-293

[25] R. Rabinovici, B. Z. Kaplan and D. Yardeni, Fundamental topologies of three-phase LC resonators and their applications for oscillators, Proceedings IEE, Pt. D , Vol. 140, 1987, pp.148-154

[26] I. A. Khan, M. T. Ahmed and N. Minhaj, Tunable OTA-based multiphase sinusoidal oscillators, International Journal of Electronics, Vol. 72, 1992, pp.443-450

[27] M. T. Abuelma'atti and W. A. Almansoury, Active-R multiphase oscillators, Proceedings IEE, Pt. G , Vol. 134, 1987,pp.292-293

[28] D. Stiurca, On the multiphase symmetrical active-R oscillators, IEEE Transaction on Circuit and Systems-II: Analog and Digital Signal Processing, Vol. 41, 1994, pp.156-158

[29] C.-L Hou and B. Shen, Second-generation current conveyor-based multiphase sinusoidal oscillators, International Journal of Electronics, Vol. 78, 1995, pp.317-325

[30] D.-S. Wu, S.-I. Liu, Y.-S. Hwang and Y.-P. Wu, Multiphase sinusoidal oscillator using second-generation current conveyors, International Journal of Electronics, Vol. 78, 1995, pp.645-651

[31] D.-S. Wu, S.-I. Liu, Y.-S. Hwang and Y.-P. Wu, Multiphase sinusoidal oscillators using the CFOA pole, IEE Proceedings-Circuits, Devices and Systems, Vol. 142, 1995, pp. 37-40

[32] M. T. Abuelma'atti, Current-mode multiphase oscillator using current followers, Microelectronics Journal, Vol. 25, 1994, pp. 457-461

[33] R. H. Zele, D. J. Allstot and T. S. Fiez,Fully balanced CMOS current-mode circuits, IEEE Journal of Solid-State Circuits, Vol .28, 1993, pp.569-575

[34] R. Ramirez Angulo and E. Sanchez-Sinecio, Two approaches for current-mode filters using voltage follower and transconductance multipliers building blocks, IEEE International Symposium on Circuits and Systems, 1994, Vol.5, pp.669-672

[35] Y.Tsividis and Y. Papananos, Continuous time filters using buffers with gain lower than unity, Electronics Letters , Vol. 30 , 1994, pp. 629-630

[36] S. Celma, J. Sabadell and P. Martinez, Universal filter using unity-gain cells, Electronics Letters, Vol. 31, No.21, 1995, pp. 1817-1818

[37] C.-M Chang and P.-C. Chen, Universal active current filter with current gain using OTAs, International Journal of Electronics, Vol. 71, 1991, pp.805-808

[38] J. Wu and C.-Y. Xie, New multifunction active filter using OTAs. International Journal of Electronics,Vol.74, 1993, pp. 235-239

[39] R. Nawrocki and U. Klein, New OTA-capacitor realization of a universal biquad, Electronics Letters, Vol. 22, 1986,pp. 50-51

[40] Y. Sun, J.K. Fidler, Novel OTA-C realization of biquadratic transfer functions, International Journal of Electronics, Vol.75,1993, pp.333-340

[41] Yichuang Sun and J. K. Fidler, Structure generation of current-mode two integrator loop dual output-OTA grounded capacitor filters, IEEE Transactions on Circuits and Systems-II, Analog and Digital Signal Processing, Vol.43, No. 9, 1996, pp.659-663.

[42] C.-M Chang and P.-C. Chen, Universal active current filter with three inputs and one output using current conveyors, International Journal of Electronics, Vol. 71, 1991, pp.817-819

[43]] C.-M Chang , C.-C. Chen and H.-Y. Wang, Universal active current filter with three inputs and one output using current conveyors-part2, International Journal of Electronics, Vol. 76, 1994, pp.87-89

[44] C.-M Chang, Universal active current filter with single input and three outputs using CCIIs, Electronics Letters, Vol. 29, 1993,pp. 1932-1933

[45] C.-M Chang, Novel universal current-mode filter with single input and three outputs using five current conveyors, Electronics Letters, Vol. 29, 1993,pp. 2005-2006

[46] C.-M Chang, Current-mode lowpass, bandpassand highpass biquads using two CCIIs, Electronics Letters, Vol. 29, 1993,pp.2020-2021

[47] C.-M Chang, Universal active current filters using single second-generation current conveyor, Electronics Letters, Vol. 29, 1993,pp. 1932-1933

[48] C.-M Chang, Current-mode allpass/notch and bandpass filter using single second-generation current conveyor, Electronics Letters, Vol. 27, 1993, pp. 1812-1813

[49] C.-M Chang , C.-C. Chen and H.-Y. Wang, Universal active current filters using single second-generation current conveyors, Electronics Letters, Vol. 29, 1993, pp. 1159-1160

[50] G. W. Roberts, A. S. Sedra, A general class of current amplifier-based biquadratic filter circuits, IEEE Transaction on Circuit and Systems,Vol. 39, 1992, pp.257-263

[51] R. Senani, New current-mode biquad filter, International Journal of Electronics, Vol.73,1992, pp.735-742

[52] Y. Sun and J. K. Fidler, Versatile active biquad based on second-generation current conveyors, International Journal of Electronics, Vol.76, 1994, pp.91-98

[53] D.-S. Wu.,Y.-S. Hwang, S.-I. Liu and Y.-P. Wu., New multifunction filter using an inverting CCII and a voltage follower, Electronic Letters, Vol.30, 1994, pp.551-552

[54] J.-W. Horng, M.-H Lee and C.-L. Hou, Universal active filter using four OTAs and one CCII, International Journal of Electronics, Vol.78,1995, pp.903-906

[55] S.-I. Liu , D.-S. Wu, H.-W. Tsao, J. Wu.and J.-H Tsay, Nonlinear circuit applications with current conveyors, IEE Proceeding-G, Vol.140, 1993, pp.1-6

[56] M.C. Piccirilli, A current-conveyor-based multiplier/divder cell, International Journal of Circuit Theory and Applications, Vol.24, 1996, pp.233-237

[57] S.-I. Liu and J.-J. Chen, Realisation of analogue divider using current feedback amplifiers, IEE Proc.-Circuits Devices Syst., Vol.142, No.1, February 1995, pp.45-47

[58] J. A. Svoboda, Comparison of RC op.-amp and RC current conveyor filters, International Journal of Electronics, Vol. 76,1994, pp. 615-626

[59] E. Bruun., A dual current feedback OpAmp in CMOS technology, Analog Integrated Circuits and Signal Processing, Vol.5, 1994, pp.213-217

[60] M. A. Siddiqi and M. T. Ahmed, Realization of grounded capacitor with operational amplifiers and resistance, Electronics Letters, Vol.14, 1978, pp.633-634

[61] D. R. Frey, Log-domain filtering: an approach to current-mode filtering, IEE Proceeding-G, Vol.140, 1993, pp.406-416

[62] M. T. Abuelma'atti and M. A. Al-Qahtani, Current-mode universal filters using unity-gain cells, Electronics Letters, Vol.32, No. 12, 1996, pp.1077-1078

APPENDIX A

Appendix A

It has been noticed that there are some differences between theory and measurements. To investigate the reasons behind these differences we will use the nonideal model of the current conveyor.

As an illustrative example consider the circuit shown in Fig. 3.1. Using the nonideal current conveyor model of Fig. 3.2, the equivalent circuit of Fig.3.1 is shown in Fig. A.1.

Analyzing the circuit shown in Fig. A.1, we have,

$$v_2 = \frac{\alpha_1 k_1 v_1}{R_{x\,1}} + k_1 I_1 \qquad (A.1)$$

Where,

$$k_1 = \frac{R_2}{S(C_1 + C_2)R_2 + 1} \qquad (A.2)$$

$$v_1 = -\frac{R_{x\,1}(R_3 + R_{x\,2})}{\alpha_1 \alpha_2 \beta_1 k_1 k_2} v_3 - \frac{R_{x\,1}}{\alpha_1} I_1 - \frac{R_{x\,1}(R_3 + R_{x\,2})}{\alpha_1 \alpha_2 \beta_1 k_1} I_2 \qquad (A.3)$$

Where,

$$k_2 = \frac{R_2 // R_4}{SC_2(R_2 // R_4) + 1}$$

$$v_4 = \frac{\alpha_3 \beta_2 k_3}{R_5 + R_{x\,3}} v_3 + k_3 I_3 \qquad (A.4)$$
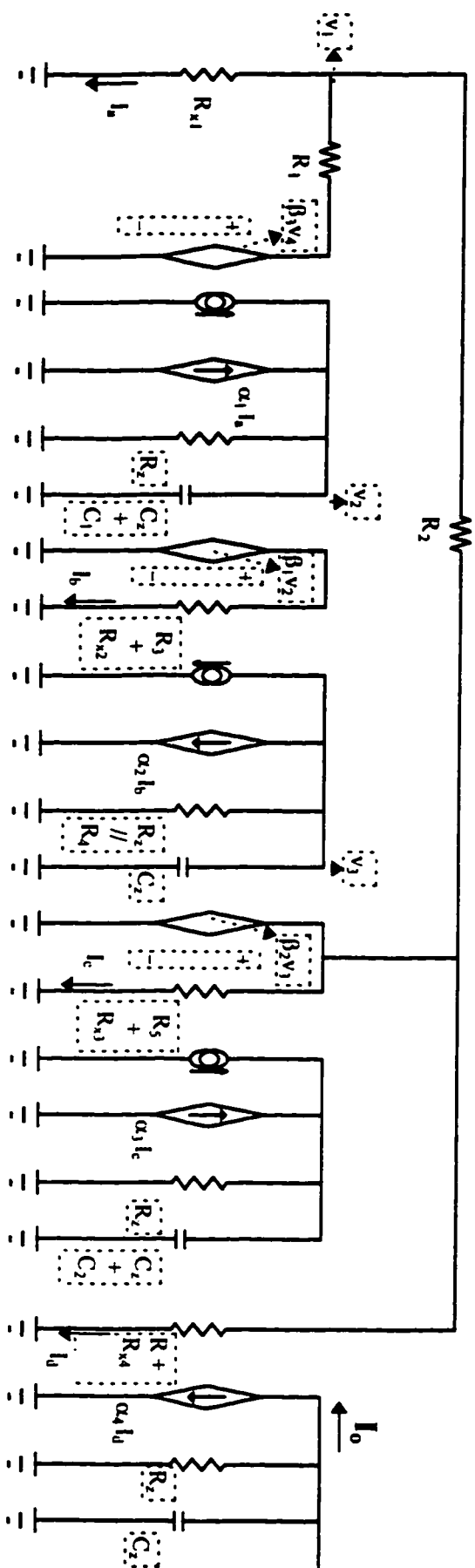
Where,

Fig A.1 Equivalent circuit of the universal filter of Fig 3.1 using Svaboda model

$$k_3 = \frac{R_2}{S(C_2 + C_2)R_2 + 1}$$

$$I_o = -\frac{\alpha_4 \beta_2 v_3}{R + R_{x\,4}}$$

(A.5)

Applying KCL at node (1) yields,

$$\frac{v_1 - \beta_2 v_3}{R_2} + \frac{v_1 - \beta_3 v_4}{R_1} + \frac{v_1}{R_{X\,1}} = 0$$

(A.6)

$$\frac{v_1}{R_1 // R_{X\,1} // R_2} = \frac{\beta_2 v_3}{R_2} + \frac{\beta_3 v_4}{R_1}$$

(A.7)

Substituting equations (A.1-A.4) in equation (A.7), we get

$$-\frac{R_{x\,1}(R_3 + R_{x\,2})}{(R_1 // R_{X\,1} // R_2)\alpha_1\alpha_2\beta_1 k_1 k_2} v_3 - \frac{R_{x\,1}}{(R_1 // R_{X\,1} // R_2)\alpha_1} I_1$$
$$-\frac{R_{x\,1}(R_3 + R_{x\,2})}{(R_1 // R_{X\,1} // R_2)\alpha_1\alpha_2\beta_1 k_1} I_2 = \frac{\beta_2 v_3}{R_2} + \frac{\alpha_3\beta_2\beta_3 k_3}{R_1(R_5 + R_{x\,3})} v_3 + \frac{\beta_3 k_3}{R_1} I_3$$

(A.8)

Rearranging equation (A.8) yields,

$$-\frac{R_{x\,1}}{(R_1 // R_{X\,1} // R_2)\alpha_1} I_1 - \frac{R_{x\,1}(R_3 + R_{x\,2})}{(R_1 // R_{X\,1} // R_2)\alpha_1\alpha_2\beta_1 k_1} I_2 - \frac{\beta_3 k_3}{R_1} I_3$$
$$= v_3 \left[\frac{\beta_2}{R_2} + \frac{\alpha_3\beta_2\beta_3 k_3}{R_1(R_5 + R_{x\,3})} + \frac{R_{x\,1}(R_3 + R_{x\,2})}{(R_1 // R_{X\,1} // R_2)\alpha_1\alpha_2\beta_1 k_1 k_2} \right]$$

(A.9)

$$-\frac{R_1 R_{x\,1}(R_3 + R_{x\,2})I_2 + R_1 R_{x\,1}\alpha_2\beta_1 k_1 I_1 + (R_1 // R_{X\,1} // R_2)\alpha_1\alpha_2\beta_1\beta_3 k_1 k_3 I_3}{R_1(R_1 // R_{X\,1} // R_2)\alpha_1\alpha_2\beta_1 k_1}$$
$$= v_3 \left[\frac{R_1 R_2 R_{x\,1}(R_3 + R_{x\,2})(R_5 + R_{x\,3}) + R_1(R_5 + R_{x\,3})(R_1 // R_{X\,1} // R_2)\alpha_1\alpha_2\beta_1\beta_2 k_1 k_2}{+ R_2(R_1 // R_{X\,1} // R_2)\alpha_1\alpha_2\alpha_3\beta_1\beta_2\beta_3 k_1 k_2 k_3} \right]$$
$$\overline{ R_1 R_2(R_5 + R_{x\,3})(R_1 // R_{X\,1} // R_2)\alpha_1\alpha_2\beta_1 k_1 k_2 }$$

(A.10)

$$v_3 = \left[\frac{R_2(R_5+R_{x3})k_2[R_1R_{x1}(R_3+R_{x2})I_2+R_1R_{x1}\alpha_2\beta_1k_1I_1+(R_1//R_{x1}//R_2)\alpha_1\alpha_2\beta_1\beta_3k_1k_3I_3]}{R_1R_2R_{x1}(R_3+R_{x2})(R_5+R_{x3})+R_1(R_5+R_{x3})(R_1//R_{x1}//R_2)\alpha_1\alpha_2\beta_1\beta_2k_1k_2 + R_2(R_1//R_{x1}//R_2)\alpha_1\alpha_2\alpha_3\beta_1\beta_2\beta_3k_1k_2k_3} \right] \quad (A.11)$$

Substituting equation (A.11) in equation (A.5), we get

$$I_o = \frac{R_2(R_5+R_{x3})\alpha_4\beta_2k_2}{R+R_{x4}} \left[\frac{[R_1R_{x1}(R_3+R_{x2})I_2+R_1R_{x1}\alpha_2\beta_1k_1I_1+(R_1//R_{x1}//R_2)\alpha_1\alpha_2\beta_1\beta_3k_1k_3I_3]}{R_1R_2R_{x1}(R_3+R_{x2})(R_5+R_{x3})+R_1(R_5+R_{x3})(R_1//R_{x1}//R_2)\alpha_1\alpha_2\beta_1\beta_2k_1k_2 + R_2(R_1//R_{x1}//R_2)\alpha_1\alpha_2\alpha_3\beta_1\beta_2\beta_3k_1k_2k_3} \right] \quad (A.12)$$

For bandpass response,

$$\frac{I_o}{I_i} = \frac{R_2(R_5+R_{x3})\alpha_4\beta_2k_2}{R+R_{x4}} \left[\frac{R_1R_{x1}\alpha_2\beta_1k_1}{R_1R_2R_{x1}(R_3+R_{x2})(R_5+R_{x3})+R_1(R_5+R_{x3})(R_1//R_{x1}//R_2)\alpha_1\alpha_2\beta_1\beta_2k_1k_2 + R_2(R_1//R_{x1}//R_2)\alpha_1\alpha_2\alpha_3\beta_1\beta_2\beta_3k_1k_2k_3} \right] \quad (A.13)$$

For ideal case,

$R_{x1}=C_z= 0$ and $R_z=\infty$

$$k_1 = \frac{R_z}{S(C_1+C_z)R_z+1} \approx \frac{1}{SC_1} \quad (A.14)$$

$$k_2 = \frac{R_z//R_4}{SC_z(R_z//R_4)+1} \approx R_4 \quad (A.15)$$

$$k_3 = \frac{R_z}{S(C_2+C_z)R_z+1} \approx \frac{1}{SC_2} \quad (A.16)$$

Substituting equation (A.14-A.16) in equation (A.13), we get

$$\frac{I_{out}}{I_{in}} = \alpha_2 \alpha_4 \beta_2 \frac{R_4}{R + R_{x4}} \frac{(s \dfrac{\beta_1}{C_1(R_3 + R_{x2})})}{s^2 + s \dfrac{\alpha_1 \alpha_2 \beta_1 \beta_2 R_4}{C_1 R_2 (R_3 + R_{x2})} + \dfrac{\alpha_1 \alpha_2 \alpha_3 \beta_1 \beta_2 \beta_3 R_4}{C_1 C_2 R_1 (R_3 + R_{x2})(R_5 + R_{x3})}} \qquad (A.17)$$

Fig. A.2 (a) and (b) show the experimental results and the calculated values using ideal equation (A.17) respectively.

Fig. A.2 (c) shows the calculated values using(A.13) including the effect of R_{x1} only. It appears that including the effect of R_{x1} only results in a reduced error between the calculated and the experimental results.

Fig. A.2 (d) shows the calculated values using (A.13) including the effect of the parasitic pole of the current conveyor only which results in small error between the calculated and the ideal values.

Fig. A.2 (e) shows the calculated values including the effect of both of the R_{x1} and the parasitic pole of the current conveyor. It appears that there is a small difference between Fig. A.2 (c) and (e). Therefore, it can be concluded that the deviation between ideal and experimental results is mainly due to the parasitic resistance R_{x1}.
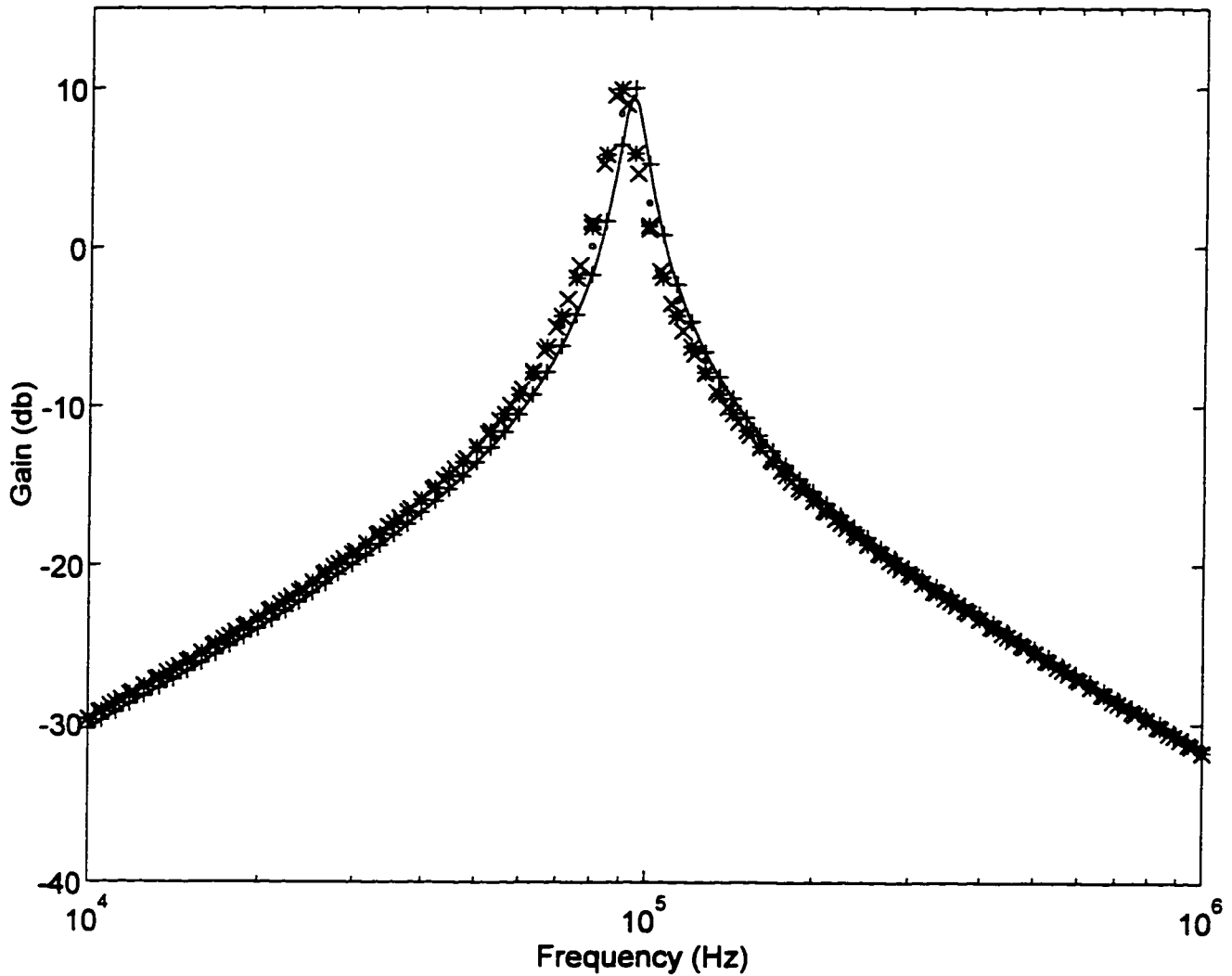
Fig. A.2 Comparison between experimental and calculated results for
the bandpass response of Fig A.1 with
$R_1= 1 k\Omega, R_3=R_4=R_5=2k\Omega, R_2=15 k\Omega, R=5k\Omega, R_{x2}=R_{x3}= R_{x4}=50$
$C_1=C_2=1.2nF$

a) [-] Ideal results using (A.17)

b) [o] Experimental results

c) [.] Simulated values (including the effect of R_{x1} only)

d) [+]Simulated values (including the effect of the finite pole of the CCII)

e) [x] Calculated values (including the effect of the R_{x1} and the finite pole of the CCII)

APPENDIX B

PUBLICATION

Current-mode universal filters using unity-gain cells

Muhammad Taher Abuelma'atti and
Muhammad Ali Al-Qahtani

Indexing terms: Current-mode circuits, Filters

Two new current-mode universal filters are presented. The proposed filters use unity gain current and voltage followers. The first filter has three inputs and one output and can realise lowpass, highpass and bandpass responses without any changes in the circuit topology. Realisation of notch and allpass responses can be easily achieved without adding any additional active elements. The second filter has three inputs and one output and can simultaneously realise lowpass, highpass and bandpass responses without any changes in the circuit topology. Realisation of notch and allpass responses can be easily achieved without adding any additional active elements. The proposed circuits enjoy low active and passive sensitivities

Introduction: Recently, there has been a growing interest in designing current-mode and voltage-mode continuous-time filters using unity gain current mirrors and/or voltage followers [1 - 4]. This is attributed to their low power dissipation and high frequency operation. While [1 - 3] report several specific application filters, [4] reports a universal filter structure which can implement all the basic second-order filter functions (lowpass, highpass, bandpass, notch and allpass). These five filters, however, cannot be realised without changing the circuit topology to achieve a specific filter function.

We present two new current-mode biquad filter structures using the unity-gain voltage follower and the two output unity gain current follower which can easily be obtained from the two output second generation current conveyor [5] by grounding its high input impedance terminal. The first circuit can realise second-order lowpass, highpass and bandpass filters without changing the circuit topology. The realisation of notch and allpass functions can be easily achieved without adding any additional active elements. The second circuit can simultaneously realise second order lowpass, highpass and bandpass filters. The realisation of notch and allpass functions can also be achieved by connecting the appropriate nodes. The proposed circuits enjoy the attractive feature of independent control of the parameters ω and ωQ.
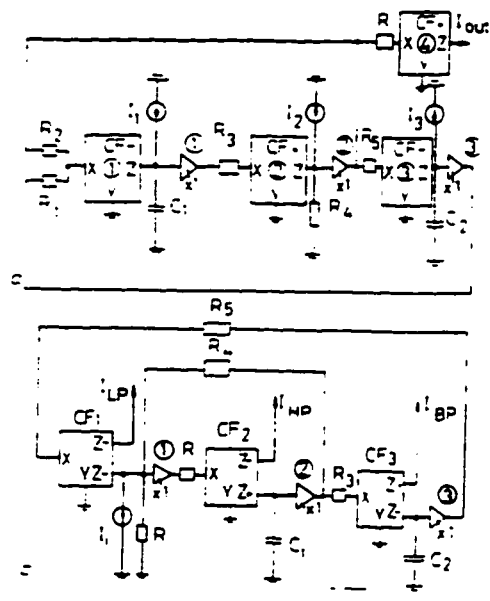

Fig. 1 *Proposed universal filters using unity gain current and voltage cells*

a With three inputs and one output
b With one input and three outputs

Proposed circuits: The first circuit is shown in Fig. 1a. Using standard notations, the two port current followers (I $\pm$) can be characterised by $i = \pm i$, $v = 1 - 4$ and the unity gain voltage

follower can be characterised by $v_{...} = \beta_i v_{...} n = 1 - 3$ where $\alpha = 1 - \epsilon$. $\epsilon \ll 1$ represents the current tracking error of the nth current follower and $\beta_i = 1 - \delta_i$. $\delta_i \ll 1$ represents the voltage tracking error of the mth voltage follower. Routine analysis yields the current transfer functions

$$I = \cdots \frac{R_i}{R} \frac{I_{...} - I_i(\cdots \frac{1}{r}) - I_i(\frac{\cdots}{\cdots r})}{\cdots - \cdots \frac{\cdots}{h_r r} - \frac{1}{h h h}} \qquad (1)$$

From eqn. 1 the parameters ω_i and ω_i, Q_i can be expressed as

$$-\frac{\cdot}{\cdot} = \frac{\cdots \cdot \cdot_1 \cdot_2 \cdot_3 R_4}{C_1 C_2 R_1 R_2 R_3} \qquad (2)$$

and

$$\frac{-}{Q_{..}} = \frac{\cdots \cdot_2 \cdot_3 R_4}{C_1 R_2 R_3} \qquad (3)$$

From eqn. 1 it can be seen that:
(i) the lowpass respone can be realised with $I_. = I_. = 0$.
(ii) the highpass respone can be realised with $I = I_. = 0$.
(iii) the bandpass response can be realised with $I_. = I_. = 0$.
(iv) the notch response can be realised with $I_. = 0$ and $I_. = I_i$ and
(v) the allpass response can be realised with $I_. = I_. = -I_.$ and $R_. = R$.

From eqn. 1 it can also be seen that the lowpass gain, the highpass gain and the bandpass gain at are approximately given by

$$G_{LP} \simeq \frac{R_3}{R} \qquad (4)$$

$$G_{HP} \simeq \frac{R_4}{R} \qquad (5)$$

and

$$G_{BP} \simeq \frac{R_2}{R} \qquad (6)$$

From eqns. 2 and 3 it can be seen that the parameter ω_i can be adjusted by controlling the resistors $R_. R.$ and/or the capacitor C_i without disturbing the parameter $\omega_i Q_{..}$ Moreover, the parameter $\omega_i Q$ can be adjusted by controlling the resistor R_i without disturbing the parameter $\omega_{..}$ However, controlling the resistance R_i and/or R will disturb the lowpass and the bandpass gains. A possible strategy for adjusting the parameters $\omega_i \omega_i Q_{..}$ the lowpass gain and the bandpass gain, is therefore as follows: first the resistor R is adjusted to control the parameter $\omega_i Q_{..}$ then the resistor R is adjusted to control the highpass gain or the bandpass gain: the resistor R is adjusted to control the lowpass gain, and finally the resistor R is adjusted to control the parameter $\omega_{..}$

From eqns. 2 and 3 it is easy to show that the active and passive sensitivities of the parameters ω_i and $Q_{..}$ are

$$S_{...} = S_{...} = S_{...} = S_{...} = S_{...} = -S_{..}^{...}$$

$$= -S_{...} = S_{R.} = -S_R^{...} = -S_{R.} = -S_R = \frac{1}{2}$$

$$S_{...} = S_{...} = -S_{...}^Q = S_{..}^Q = S_{...}^Q = -S_{..}^Q$$

$$= -S_R^Q = S_{..}^Q = S_R^Q = S_R^Q = S_C^Q = S_{..}^Q = -\frac{1}{2}$$

$$S_R^Q = 1. \quad S_R^{...} = S_R^Q = 0.$$

all of which are small.

The second circuit is shown in Fig. 1b. Using the standard notations of the two port current followers and the unity gain voltage follower, routine analysis yields the current transfer functions:

$$\frac{I_{HP}}{I} = \frac{- \cdot_1 \cdot_2}{\cdots - \cdots \frac{\cdots}{\cdots h_r} - \frac{\cdots}{h_r h}} \qquad (7)$$

$$\frac{I_{LP}}{I} = \frac{- \cdots}{\cdots - \cdots \frac{\cdots}{h_r} - \frac{\cdots}{\cdots h h}} \qquad (8)$$

and

$$\frac{I_{BP}}{I_i} = \frac{\cdots R_4}{\cdots + \cdots \frac{\cdots \cdots}{C_1 R_4} - \frac{\cdots \cdots \cdots}{C_1 C_2 R_1 R_2}} \qquad (9)$$

From eqns. 7 – 9 the parameters ω_i and $\omega_i/Q_{..}$ can be expressed

$$-\cdot = \frac{\cdots \cdots \cdots \cdot}{C_1 C_2 R_1 R_2} \qquad (10)$$

and

$$\frac{-\cdot}{Q_{..}} = \frac{\cdot_2 \cdot_1 \cdot_2}{C_1 R_2} \qquad (11)$$

From eqns. 7 – 9 it can be seen that the lowpass DC gain and the high frequency gain of the highpass are approximately equal to unity and the bandpass gain at ω equals

$$G_{BP} = \frac{R_4}{\cdot_2 R_1} \qquad (12)$$

From eqns. 10 – 12 it can be seen that the parameter ω_i can be adjusted by controlling the resistors $R_. R.$ and/or the capacitor C_i without disturbing the parameter $\omega_i Q_{..}$ Moreover, the parameter $\omega_i Q$ can be adjusted by controlling the resistor R. without disturbing the parameter $\omega_{..}$ However, controlling the resistances R and/or R_i will disturb the bandpass gain. A possible strategy for adjusting the parameters $\omega_i \omega_i Q_i$ and the bandpass gain, is therefore as follows: first the resistor R_i is adjusted to control the parameter $\omega_i Q_{..}$ then the resistor R_i is adjusted to control the bandpass gain: and finally the resistor R. is adjusted to control the parameter $\omega_{..}$

From eqns. 7 – 9 it can also be seen that an inverting notch response can be realised by connecting the I_{HP} and I_{LP} output terminals. An inverting allpass response can be obtained by connecting $I_{HP} I_{BP}$ and I_{LP} output terminals provided that $R_i = R_{..}$ Thus no additional current followers are required for realising notch and allpass responses.

From eqns. 10 and 11 it is easy to show that the active and passive sensitivities of the parameters ω_i and $Q_{..}$ of the circuit of Fig. 1b are

$$S_{...} = S_{...} = S_{...} = S_{...} = S_{...} = S_{..}$$

$$= -S_{C_1} = -S_{C_2} = -S_{R_1} = -S_{R_2} = \frac{1}{2}$$

$$S_{...}^Q = S_{..}^Q = S_{..}^Q = S_{C_1}^Q = -S_{..}^Q = -S_{..}^Q$$

$$= -S_{..}^Q = -S_{C_2}^Q = -S_{R_1}^Q = -S_{R_2}^Q = \frac{1}{2}$$

$$S_{R_4}^Q = 1. \quad S_R^{...} = S_R^Q = 0.$$

all of which are small.

Conclusion: Two new universal current-mode filters have been presented. The first circuit, shown in Fig. 1a, uses three inputs and one output and can realise lowpass, highpass and bandpass responses without changing the circuit topology. The circuit can also realise notch and allpass responses without using additional active elements. The second circuit, shown in Fig. 1b, uses one input and three outputs and can simultaneously realise lowpass, highpass and bandpass responses. The circuit can also realise notch and bandpass responses without using additional active elements. The proposed filter circuits enjoy the following advantages:
(i) employment of grounded capacitors which paves the way for high frequency operation.
(ii) independent tuning of the parameters ω_i and ω_i/Q_i
(iii) low active and passive sensitivities.

Muhammad Taher Abuelma'atti and Muhammad Ali Al-Qahtani (King Fahd University of Petroleum and Minerals, Box 203 Dhahran 31261, Saudi Arabia)

References

1 ZELE, R.H., ALLSTOT, D.J., and FIEZ, T.S.: 'Fully balanced CMOS current-mode circuits'. *IEEE J. Solid-State Circuits*, 1993, SSC-28, pp. 569–575

2 RAMIREZ-ANGULO, R., and SANCHEZ-SINENCIO, E.: 'Two approaches for current-mode filters using voltage follower and transconductance multipliers building blocks'. IEEE Int. Symp. Circuits and Syst., 1994, 5, pp. 669–672

3 TSIVIDIS, Y., and PAPANANOS, Y.: 'Continuous time filters using buffers with gain lower than unity'. *Electron. Lett.*, 1994, 30, pp. 629–630